Untargeted Metabolomics and Lipidomics

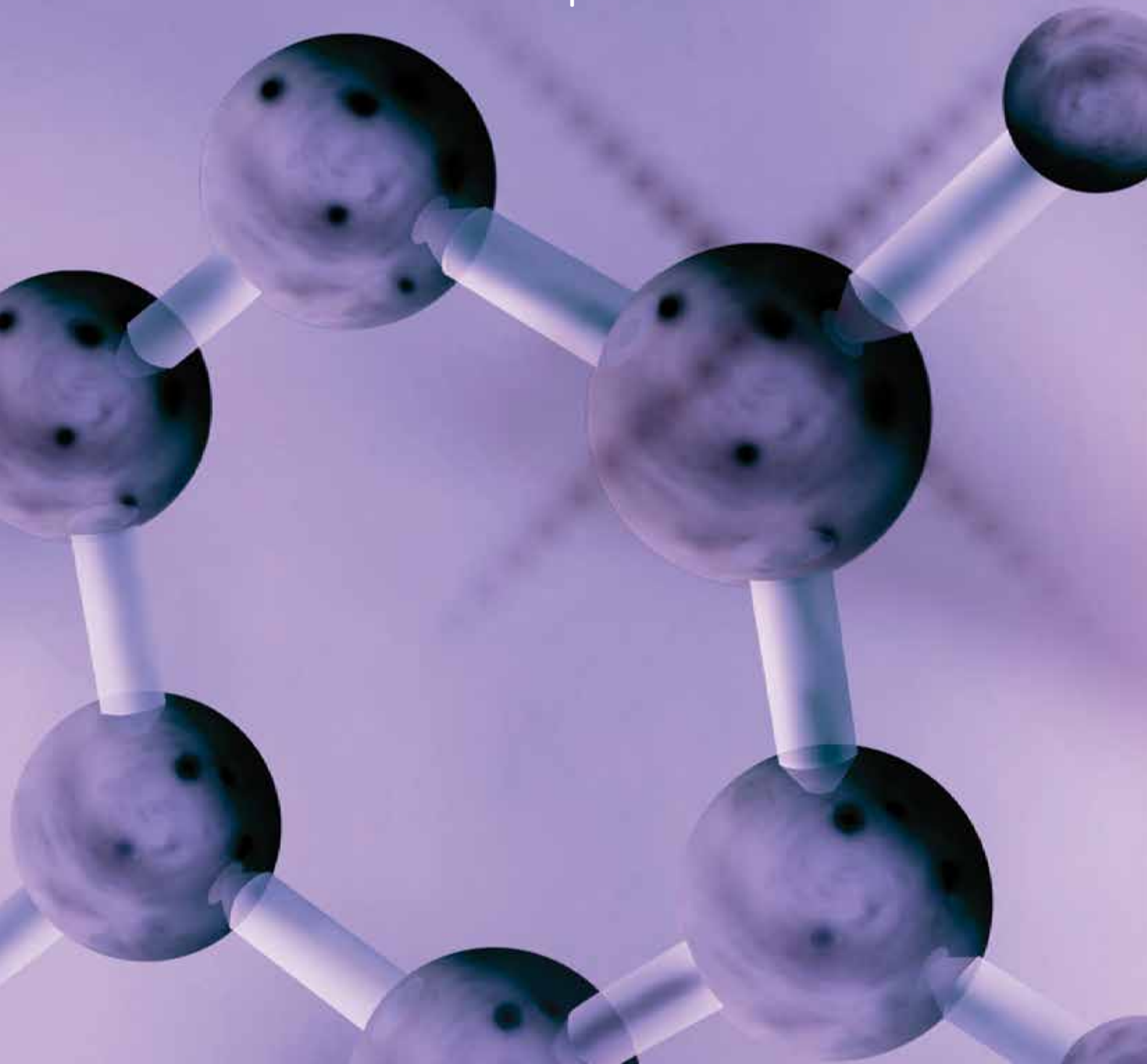

TABLE OF CONTENTS

UNTARGETED METABOLOMICS AND LIPIDOMICS

Untargeted metabolomics and lipidomics are hypothesis-generating and exploratory in nature, their purpose is to perform an unbiased screening of metabolites and lipids in biological samples. By comparing metabolite and lipid profiles, we can thus determine patterns of variations between different groups: healthy versus diseased, control versus treated, or wild-type versus genetically modified. Dealing with variations in thousands of molecular species, untargeted metabolomic and lipidomic strategies apply statistical tools, such as multivariate and pattern-recognition analyses to group and identify the observed changes in metabolite and lipid species.

Powerful LC-MS data analysis software is critical to the quantification and identification of metabolites and lipids that are significantly changing in biological samples. Progenesis® QI Software offers the capability to handle the large sample sets typical of today's experiments. With support for all common vendor data formats and a highly intuitive, visually guided workflow, Progenesis QI Software helps to rapidly, objectively, and reliably discover metabolites and lipids of interest using multi-group experimental designs. As well as conventional data-dependent analysis (DDA), Progenesis QI supports Waters MS^E and $HDMS^E$ DIA. Uniquely, the software also takes advantage of the additional dimension of resolution offered by ion-mobility separations to give improvements in the accuracy and precision of compound identification and quantification. Progenesis QI Software is developed by Nonlinear Dynamics, a Waters Company.

Central to Waters solutions for untargeted metabolomics and lipidomics are the use of novel and unique chromatographic tools, high-resolution exact mass time-of-flight (TOF) mass spectrometers and specialized software for statistical analysis.

- Advanced chromatographic separations of lipids and metabolites coupled to the widest range of ionization capabilities (UPLC, ionKey™, UPC^2, APGC)
- Powerful data dependant and data independent technology (MS^E) for both qualitative and quantitative routine applications
- Simple data processing and easy identification of statistically significant quantitative changes with Progenesis QI

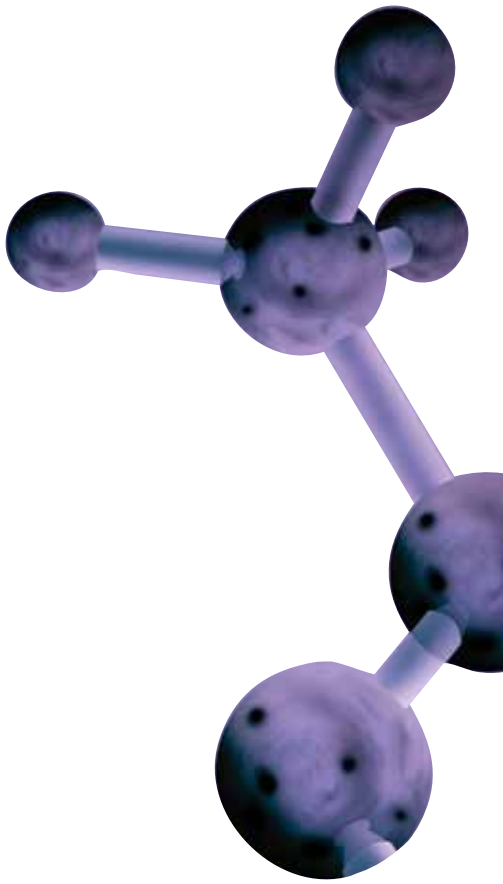

Waters
THE SCIENCE OF WHAT'S POSSIBLE.®

Development of a Metabolomic Assay for the Analysis of Polar Metabolites Using HILIC UPLC/QTof MS

Giuseppe Paglia,[1] James Langridge,[2] and Giuseppe Astarita[3]
[1]Center for Systems Biology, University of Iceland, Iceland; [2-3]Waters Corporation, Manchester, UK and Milford, MA, USA

APPLICATION BENEFITS

The combination of UPLC-based hydrophilic interaction liquid chromatography (HILIC) and a hybrid quadrupole time-of-flight (Q-Tof™) mass spectrometer allows the comprehensive analysis of small polar metabolites including sugars, phosphorylated compounds, purines and pyrimidines, nucleotides, nucleosides, acylcarnitines, organic acids, hydrophilic vitamins, and amino acids. Retention times and accurate masses of metabolites involved in key metabolic pathways were annotated for routine high-throughput screening in both untargeted and targeted metabolomics analyses.

WATERS SOLUTIONS

ACQUITY UPLC® System

ACQUITY UPLC BEH Amide Column

SYNAPT® G2 System

TransOmics™ Informatics

KEY WORDS

HILIC, UPLC®, small polar metabolites, QTof MS, metabolomics

INTRODUCTION

Metabolomics, a powerful tool in systems biology, aims to screen small metabolites present in biological samples. Differences in the species or amounts of metabolites can be used to characterize phenotypes and biological responses to perturbations (diseases, genetic modifications, or nutritional and pharmacological treatments).

Small metabolites can be mainly divided into hydrophilic and hydrophobic compounds. Because water is the major constituent of cells, a high number of hydrophilic metabolites are present in their intracellular content including sugars, phosphorylated compounds, nucleobases, nucleotides, nucleosides, acylcarnitines, organic acids, hydrophilic vitamins, and amino acids, as shown in Figure 1. Such polar metabolites are the building blocks of large macromolecules such as nucleic acids (DNA and RNA), proteins, and oligosaccharides. Furthermore, they are involved in central pathways (glycolysis, pentose-phosphate pathway and citric acid cycle), which are essential for energy metabolism.

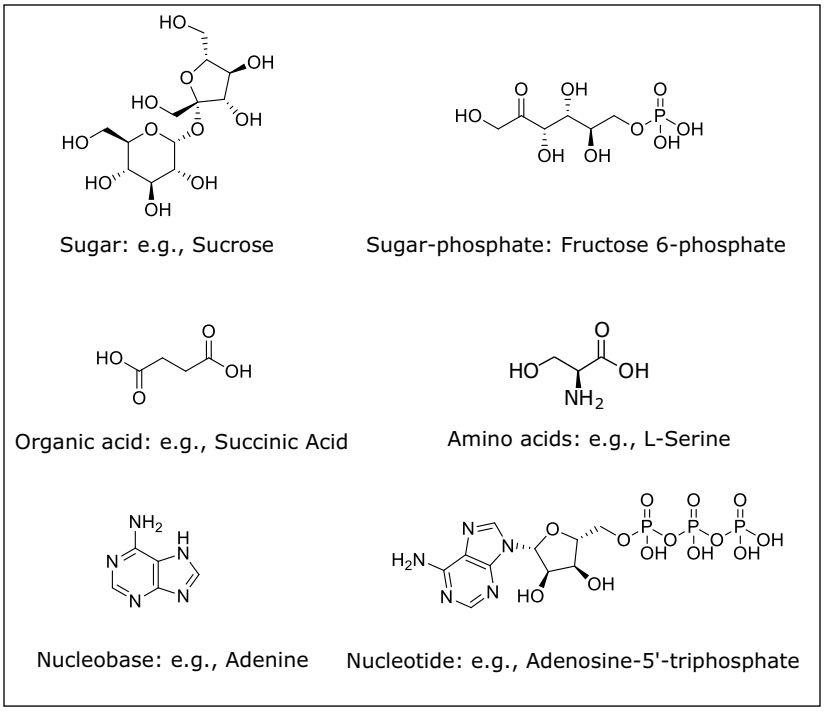

Figure 1. Representative classes of polar metabolites present in biological samples.

EXPERIMENTAL

LC conditions, acidic

System:	ACQUITY UPLC
Column:	BEH Amide 2.1 x 150 mm, 1.7 µm
Mobile phase A:	ACN + 0.1% formic acid
Mobile phase B:	H_2O + 0.1% formic acid
Flow rate:	0.4 mL/min
Column temp.:	45 °C
Injection volume:	3.5 µL
Sample loop option:	Partial loop with needle overfill
ESI mode:	Positive and negative

Elution gradient:	min	A%	B%	Curve
	0.0	99	1	
	0.1	99	1	6
	7.0	30	70	6
	7.1	99	1	6
	10.0	99	1	6

LC conditions, basic

System:	ACQUITY UPLC
Column:	BEH Amide 2.1 x 150 mm, 1.7 µm
Mobile phase A:	ACN 95% - ammonium bicarbonate 10 mM 5% (pH 9)
Mobile phase B:	ACN 5% - ammonium bicarbonate 10 mM 95% (pH 9)
Flow rate:	0.4 mL/min
Column temp.:	45 °C
Injection volume:	3.5 µL
Sample loop option:	Partial loop with needle overfill
ESI mode:	negative

Elution gradient:	min	A%	B%	Curve
	0.0	99	1	
	0.1	99	1	6
	6.0	30	70	6
	6.5	99	1	6
	10.0	99	1	6

MS conditions

Analytical column to ESI probe: PEEK Tubing, 1/16 inch (1.6 mm) O.D. x 0.005 inches (0.127 mm) I.D. x 5 ft (1.5 m) length , cut to 450 mm in length; (p/n WAT022995)

Mass spectrometer:	SYNAPT G2
Acquisition mode:	Sensitivity mode (centroid)
Capillary:	1.5 kV
Sampling cone:	30 V
Extraction cone:	5 V
Source temp.:	120 °C
Desolvation gas temp.:	500 °C
Desolvation gas flow:	800 L/h
Cone gas flow:	50 L/h
Lock spray:	Leukine enkephalin (3 ng/L) 556.2771 *m/z*
Scan range:	50 to 1000 *m/z*
Scan time:	0.3 s
Calibration:	Sodium formate

The analysis of hydrophilic compounds using traditional reversed-phase LC/MS presents some challenges due to the fact that these metabolites are poorly retained and usually eluted in the void volume.[1] On the other hand, it has been demonstrated that HILIC-MS methods easily resolve polar metabolites for better identification and quantification.[1,2] A HILIC-UPLC/MS strategy for the routine high-throughput screening of polar metabolites in biological samples is presented here. Such a strategy could be used for both targeted and untargeted metabolomics.

Sample description

All materials were purchased from Sigma-Aldrich (Germany). All chemicals and solvents were analytical grade or higher purity. Human platelets were obtained from the Blood Bank of Reykjavik.

Polar metabolites were extracted from platelets (0.5 mL of platelets concentrate) by adding 1 mL of 7:3 MeOH/H_2O containing a 30-µL mixture of chemical homologous internal standards, as shown in Table 1. Two freeze-and-thaw steps were applied, then samples were passed to vortex. After centrifugation (5 min 10,000 x g) the supernatant was recovered, filtered (cutoff: 0.2 µm), dried using speed vacuum, and reconstituted in 0.3 mL of 50:50 H_2O/CH_3CN. A typical sample list included water-based blank samples, quality control samples containing commercially available metabolites at two concentration levels, a five-point serial dilution of calibrators, and pooled quality control samples in which small aliquots of each biological sample are pooled and mixed together.

Metabolites	Molecular formula	MW	$[M+H]^+$	$[M-H]^-$	Retention time (min)			Concentration ng/L
					BASIC	NEG	POS	
Phenylalanine d_2	$C_9D_2H_9NO_2$	167.0915	168.0994	166.0837	3.15	3.7	3.7	50
Succinate d_4	$C_4D_4H_2O_4$	122.0517	123.0595	121.0439	2.5	2.3	–	50
Glucose $^{13}C_6$	$^{13}C_6H_{12}O_6$	186.0835	209.073	185.0757	–	4.2	4.2	2000
Carnitine d_9	$C_7D_9H_6NO_3$	170.1617	171.1695	169.1678	–	–	3.6	5
Glutamic Acid d_5	$C_5D_5H_4NO_4$	152.0845	153.0924	151.0767	3.2	4.4	4.4	40
AMP $^{13}C_{10}$, $^{15}N_5$	$^{13}C_{10}H_{14}{}^{15}N_5O_7P$	362.0818	363.0896	361.074	3.15	5.2	5.2	50
Octanoic Acid d_{15}	$C_8D_{15}H_1O_2$	159.2092	160.217	158.2014	1.2	1.2	–	180
Lysine d_4	$C_6D_4H_{10}N_2O_2$	150.1306	151.1385	149.1228	6.6	5.6	5.6	50

Table 1. Internal standard mixture.

Cleaning procedures

For practical consideration, to remove residues that can reduce column lifetime and instrument sensitivity, the samples were filtered before the UPLC/MS analysis (cutoff: 2 µm). Furthermore, a routine cleaning procedure was applied at the end of each analytical batch of approximately 80 samples, including both column and ion source cleaning. The column was flushed first with 50% of solvent A (acetonitrile) and 50% of solvent B (50:50 water/methanol) for 30 min at a flow rate of 0.25 mL/min, then for 20 min with 100% of solvent A at a flow rate of 0.25 mL/min. When a new column was used, at least 30 injections were required for system equilibration; whereas, 15 injections were sufficient after each cleaning procedure using the same column. The sample cone was sonicated in a 50:50 (vol/vol) methanol/water solution containing 1% (vol/vol) formic acid for 15 min, and dried with nitrogen b efore replacing.

RESULTS AND DISCUSSION

The primary focus of this work was to provide a high-throughput solution to screen for unknown metabolites and to simultaneously quantify selected polar metabolites in biological samples.

In order to optimize the separation conditions, the initial analysis focused on a mixture of commercially available polar metabolites, representative of the major cellular biochemical pathways including amino acids, sugars, acylcarnitines, organic acids, nucleobases, nucleotides, and nucleosides, as shown in Figure 1.

To allow a comprehensive separation of the different chemical classes of metabolites, two different HILIC-UPLC conditions (acidic and basic) were selected, as shown in Figure 2.

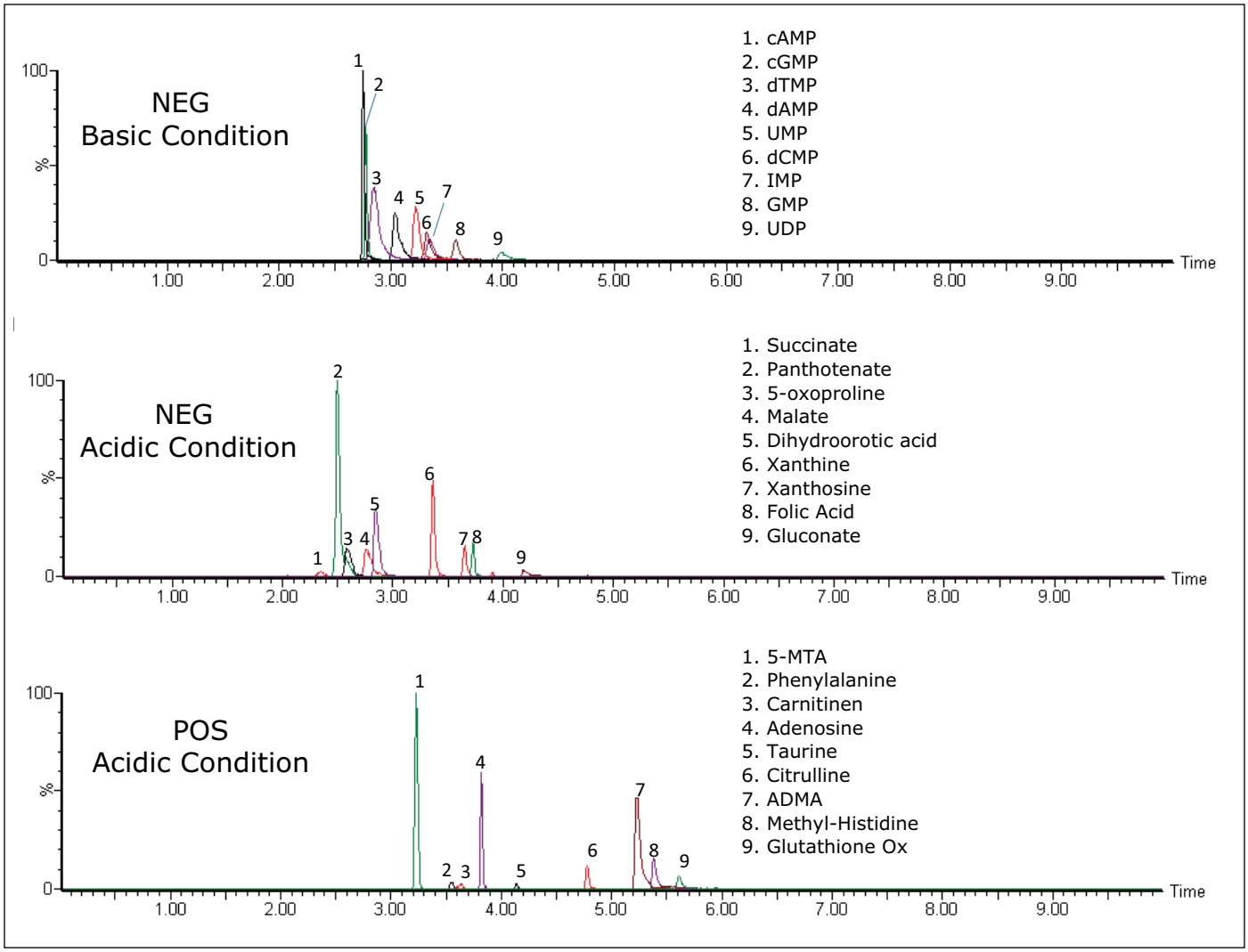

Figure 2. Representative UPLC/MS separation of selected polar metabolites using both basic and acidic chromatographic conditions.

In fact, the analysis of polar metabolites was strongly influenced by pH of the mobile phase, as shown in Figures 3A and 3B. In particular, many phosphorylated compounds, such as nucleotides, could be well separated using basic conditions; whereas, they were strongly retained using acidic conditions resulting in poor chromatographic peak shape, as shown in Figures 3A and 3B. Notably, the analysis of similar compounds using traditional reversed-phase LC/MS presented some challenges due to the fact that these metabolites were poorly retained and usually eluted in the void volume, as shown in Figure 3C.[1] Using HILIC conditions, the set of polar metabolites eluted in order of increasing polarity. Retention times were annotated, as well as with the accurate masses of precursor, adducts, and fragment ions using both ES^+ and ES^-, as shown in Table 2.

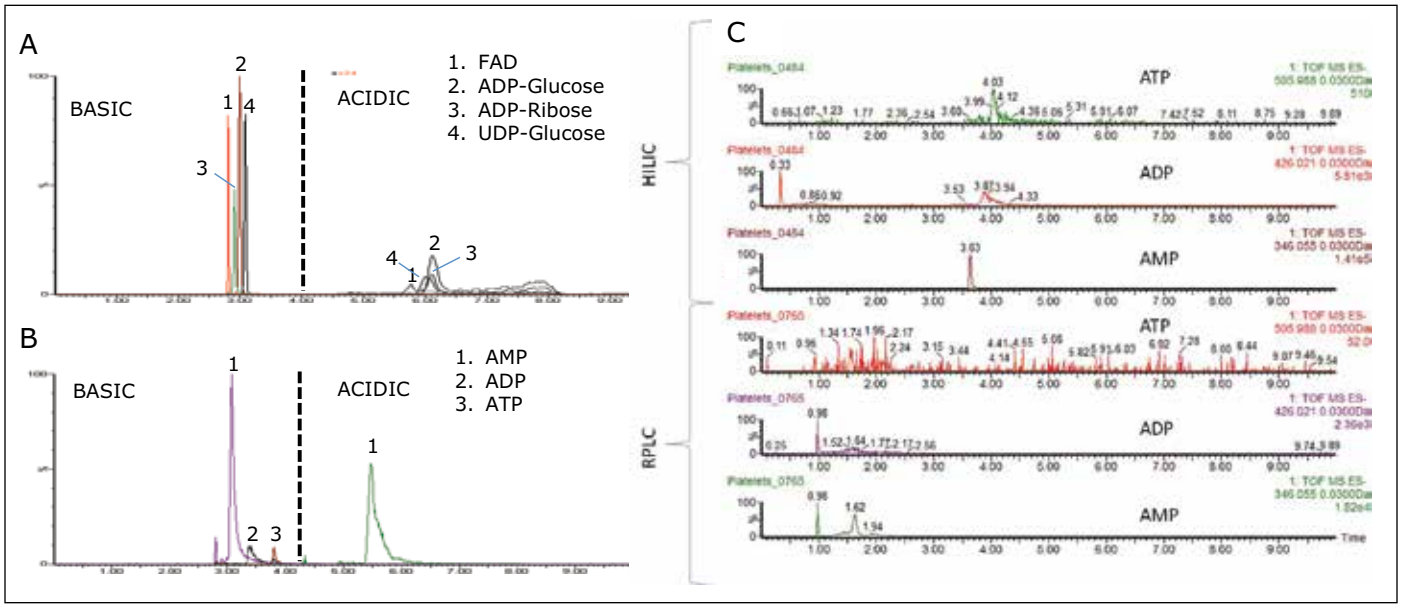

Figure 3. Basic chromatographic conditions allow for better separation of nucleoside phosphates compared to acidic conditions (Panels A and B); for method details please see Experimental section. Similarly, columns based on 150 mm HILIC amide chemistry improve the analysis of nucleoside phosphates compared to 150 mm reversed-phase HSS T3 C_{18} chemistry (Panel C; for method details please see reference 1).

	Class	HMDB ID	Metabolites	Molecular Formula	MW	[M+H]+	[M-H]-	Retention time (min)			Suggested Condition	Quantification Ions	Internal Standard
								BASIC	NEG	POS			
1	Aminoacid	HMDB00929	Tryptophan	C11H12N2O2	204.0899	205.0977	203.0821	3.2	3.6	3.6	ACID POS	205.098+188.070	Phenylalanine d2
2	Aminoacid	HMDB00517	Arginine	C6H14N4O2	174.1117	175.1195	173.1039	6.6	5.6	5.6	ACID POS	158.093+175.12	Lysine d4
3	Aminoacid	HMDB00904	Citrulline	C6H13N3O3	175.0957	176.1035	174.0879	4.2	4.8	4.8	ACID POS	176.104+159.076	Lysine d4
4	Aminoacid	HMDB00574	Cysteine	C3H7NO2S	121.0198	122.0276	120.0120	–	–	5.7	ACID POS	120.012	Lysine d4
5	Aminoacid	HMDB00177	Histidine	C6H9N3O2	155.0695	156.0773	154.0617	–	5.6	5.6	ACID POS	156.077+110.071	Lysine d4
6	Aminoacid	HMDB00182	Lysine	C6H14N2O2	146.1055	147.1133	145.0977	6.6	5.7	5.7	ACID POS	147.113+84.081	Lysine d4
7	Aminoacid	HMDB00159	Phenylalanine	C9H11NO2	165.0790	166.0868	164.0712	3.2	3.6	3.6	ACID POS	120.081+166.087	Phenylalanine d2
8	Aminoacid	HMDB00162	Proline	C5H9NO2	115.0633	116.0711	114.0555	3.7	4.1	4.1	ACID POS	116.071+160.035	Glutamic Acid d5
9	Aminoacid	HMDB00172	Isoleucine	C6H13NO2	131.0946	132.1024	130.0868	3.3	3.3	3.6	ACID POS	132.102+86.097	Phenylalanine d2
10	Aminoacid	HMDB00168	Asparagine	C4H8N2O3	132.0535	133.0613	131.0457	4.0	4.8	4.8	ACID POS	133.061	Phenylalanine d2
11	Aminoacid	HMDB00725	Hydroxyproline	C5H9NO3	131.0582	132.0660	130.0504	–	–	4.3	ACID POS	132.066+86.061	Glutamic Acid d5
12	Aminoacid	HMDB00696	Methionine	C5H11NO2S	149.0511	150.0589	148.0433	2.6	3.8	3.8	ACID POS	104.053+150.059	Phenylalanine d2
13	Aminoacid derivative	HMDB11745	Acetyl-methionine	C7H13NO3S	191.0616	192.0694	190.0538	2.6	-	2.2	ACID POS	192.069	Phenylalanine d2
14	Aminoacid derivative	HMDB03337	Glutathione Oxidized	C20H32N6O12S2	612.1520	613.1598	611.1442	3.9	5.6	5.6	ACID POS	613.16+355.073	Lysine d4
15	Aminoacid derivative	HMDB00125	Glutathione Reduced	C10H17N3O6S	307.0838	308.0916	306.0760	4.0	5.5	5.5	ACID POS	308.092+179.05	Lysine d4
16	Aminoacid derivative	HMDB00092	Dimethylglycine	C4H9NO2	103.0630	104.0708	102.0552	3.2	–	4.1	ACID POS	104.071	Glutamic Acid d5
17	Aminoacid derivative	HMDB01539	ADMA	C8H18N4O2	202.1430	203.1508	201.1352	–	–	5.2	ACID POS	203.150+158.129	Lysine d4
18	Aminoacid derivative	HMDB00192	Cystine	C6H12N2O4S2	240.0239	241.0317	239.0161	4.2	–	5.7	ACID POS	239.016	Lysine d4
19	Aminoacid derivative	HMDB00001	1-Methylhistidine	C7H11N3O2	169.0851	170.0929	168.0773	–	5.4	5.4	ACID POS	170.093+109.076	Lysine d4
20	Aminoacid derivative	HMDB00064	Creatine	C4H9N3O2	131.0690	132.0768	130.0612	3.9	4.1	4.1	ACID POS	90.056+132.077	Phenylalanine d2
21	Biogenic Amine	HMDB00259	Serotonin	C10H12N2O	176.0950	177.1028	175.0872	–	–	3.5	ACID POS	160.076+177.103	Phenylalanine d2
22	Biogenic Amine	HMDB00068	Epinephrine	C9H13NO3	183.0895	184.0973	182.0817	–	3.7	3.7	ACID POS	166.086+184.097	Phenylalanine d2
23	Carnitine	HMDB00201	Acetylcarnitine	C9H17NO4	203.1158	204.1236	202.1080	–	–	3.2	ACID POS	204.124+145.051	Carnitine d9
24	Carnitine	HMDB00062	Carnitine	C7H15NO3	161.1052	162.1130	160.0974	–	–	3.6	ACID POS	162.113+103.039	Carnitine d9
25	Carnitine	HMDB00222	Palmitoylcarnitine	C23H45NO4	399.3350	400.3428	398.3272	–	–	2.5	ACID POS	400.343	Carnitine d9
26	Nucleobase	HMDB00262	Thymine	C5H6N2O2	126.0429	127.0507	125.0351	1.8	2.4	2.4	ACID POS	127.051	Phenylalanine d2
27	Nucleobase	HMDB00034	Adenine	C5H5N5	135.0540	136.0618	134.0462	2.6	3.7	3.7	ACID POS	136.062	Phenylalanine d2
28	Nucleobase	HMDB00132	Guanine	C5H5N5O	151.0490	152.0568	150.0412	2.6	3.9	3.9	ACID POS	152.057+135.03	Phenylalanine d2
29	Nucleobase	HMDB00157	Hypoxanthine	C5H4N4O	136.0390	137.0468	135.0312	2.6	3.2	3.2	ACID POS	137.047+119.035	Phenylalanine d2
30	Nucleobase	HMDB00300	Uracil	C4H4N2O2	112.0273	113.0345	111.0195	–	–	3.2	ACID POS	113.035+96.008	Phenylalanine d2
31	Nucleoside	HMDB00050	Adenosine	C10H13N5O4	267.0970	268.1048	266.0892	–	–	3.8	ACID POS	136.062+268.105	Phenylalanine d2
32	Nucleoside	HMDB00089	Cytidine	C9H13N3O5	243.0855	244.0933	242.0777	3.2	4.1	4.1	ACID POS	244.093+266.075	Phenylalanine d2
33	Nucleoside derivative	HMDB01173	5-MTA	C11H15N5O3S	297.0896	298.0974	296.0818	-	-	3.2	ACID POS	298.097+136.062	Phenylalanine d2
34	Nucleoside derivative	HMDB00939	SAH	C14H20N6O5S	384.1216	385.1294	383.1138	4.1	5.2	5.2	ACID POS	134.027+385.129	Lysine d4
35	Nucleoside derivative	HMDB14266	SAMe	C15H22N6O5S	398.1372	399.1450	397.1294	–	–	6.0	ACID POS	298.094+399.145	Lysine d4
36	Nucleoside derivative	HMDB01517	AICAR	C9H14N4O5	258.0964	259.1042	257.0886	2.9	3.8	3.8	ACID POS	259.104+127.062	Phenylalanine d2
37	Phosphorilated compound	HMDB01565	Phosphorylcholine	C5H14NO4P	183.0660	184.0738	182.0582	Nd	–	5.1	ACID POS	184.074+124.999	AMP 13C10, 15N5
38	Sugar	HMDB00660	Fructose	C6H12O6	180.0634	181.0712	179.0556	–	–	4.0	ACID POS	203.054*	Glucose 13C6
39	Sugar	HMDB01514	Glucosamine	C6H13NO5	179.0794	180.0872	178.0716	–	–	4.5	ACID POS	180.087	Glucose 13C6
40	Sugar	HMDB00122	Glucose	C6H12O6	180.0634	181.0712	179.0556	–	4.2	4.2	ACID POS	203.054*	Glucose 13C6
41	Sugar	HMDB41627	Lactose	C12H22O11	342.1162	343.1240	341.1084	–	4.8	–	ACID POS	365.106*	Glucose 13C6
42	Sugar	HMDB00765	Mannitol	C6H14O6	182.0790	183.0868	181.0712	3.6	4.1	4.1	ACID POS	205.069*	Glucose 13C6
43	Sugar	HMDB00169	Mannose	C6H12O6	180.0634	181.0712	179.0556	–	4.0	4.0	ACID POS	203.054*	Glucose 13C6
44	Sugar	HMDB00215	Acetyl-Glucosamine	C8H15NO6	221.0899	222.0977	220.0821	–	–	3.8	ACID POS	222.098+204.086	Glucose 13C6
45	Sugar	HMDB00258	Sucrose	C12H22O11	342.1162	343.1240	341.1084	4.1	4.7	4.7	ACID POS	365.106*	Glucose 13C6
46	Sugar	HMDB03213	Raffinose	C18H32O16	504.1690	505.1768	503.1612	4.6	5.3	5.3	ACID POS	527.167*	Glucose 13C6
47	Vitamin	HMDB00121	Folic acid	C19H19N7O6	441.1397	442.1475	440.1319	2.9	3.7	3.7	ACID POS	442.148+295.094	Phenylalanine d2
48	Vitamin	HMDB01396	5-Me-THF	C20H25N7O6	459.1866	460.1944	458.1788	–	–	4.5	ACID POS	460.194+313.142	Glutamic Acid d5
49	Vitamin	HMDB01406	Niacinamide	C6H6N2O	122.0480	123.0558	121.0402	–	–	2.5	ACID POS	123.056	Carnitine d9
50	Vitamin	HMDB01488	Nicotinic acid	C6H5NO2	123.0320	124.0398	122.0242	–	–	2.3	ACID POS	124.04	Carnitine d9
51	Vitamin	HMDB01392	PABA	C7H7NO2	137.0480	138.0558	136.0402	–	–	1.4	ACID POS	138.056+94.065	Carnitine d9
52	Vitamin	HMDB00607	Vitamin B12	C63H88CoN14O14P	1354.5674	1355.5752	1353.5596	–	–	4.6	ACID POS	679.292**	Glutamic Acid d5
53	Vitamin	HMDB00030	Biotin	C10H16N2O3S	244.0882	245.0960	243.0803	–	2.6	2.6	ACID POS	245.096+227.085	Carnitine d9
54	Vitamin	HMDB00244	Riboflavin	C17H20N4O6	376.1383	377.1461	375.1305	–	3.4	3.4	ACID POS	377.146	Phenylalanine d2
55	Vitamin	HMDB00239	Pyridoxine	C8H11NO3	169.0739	170.0817	168.0661	–	3.5	3.5	ACID POS	170.0812	Phenylalanine d2
56	Vitamin	HMDB00235	Thiamine	C12H16N4OS	264.1045	263.0967	265.1123	–	–	5.2	ACID POS	265.112+122.071	Lysine d4
57	Vitamin	HMDB00097	Choline	C5H14NO	104.1075	104.1075	103.0997	–	–	2.7	ACID POS	104.107	Carnitine d9
58	Aminoacid	HMDB00191	Aspartic Acid	C4H7NO4	133.0375	134.0453	132.0297	3.3	4.6	4.6	ACID NEG	132.03	Glutamic Acid d5
59	Aminoacid	HMDB00641	Glutamine	C5H10N2O3	146.0691	147.0769	145.0613	4.1	4.7	4.7	ACID NEG	145.061+127.05	Glutamic Acid d5
60	Aminoacid	HMDB00187	Serine	C3H7NO3	105.0426	106.0504	104.0348	–	4.6	–	ACID NEG	104.035	Glutamic Acid d5
61	Aminoacid	HMDB00167	Threonine	C4H9NO3	119.0582	120.0660	118.0504	–	4.6	4.6	ACID NEG	118.051	Glutamic Acid d5
62	Aminoacid	HMDB00161	Alanine	C3H7NO2	89.0477	90.0555	88.0399	3.9	4.3	–	ACID NEG	88.04	Glutamic Acid d5
63	Aminoacid	HMDB00158	Tyrosine	C9H11NO3	181.0739	182.0817	180.0661	3.5	4.1	4.1	ACID NEG	180.066+163.04	Phenylalanine d2
64	Aminoacid	HMDB00883	Valine	C5H11NO2	117.0790	118.0868	116.0712	–	3.9	–	ACID NEG	116.071	Phenylalanine d2
65	Aminoacid derivative	HMDB00267	5-Oxoproline	C5H7NO3	129.0426	130.0504	128.0348	2.7	2.6	2.6	ACID NEG	128.035	Succinate d4
66	Nucleobase	HMDB00292	Xanthine	C5H4N4O2	152.0334	153.0412	151.0256	2.8	3.3	3.3	ACID NEG	151.026	Phenylalanine d2
67	Nucleobase	HMDB00289	Uric acid	C5H4N4O3	168.0283	169.0361	167.0205	2.7	4.0	4.0	ACID NEG	167.021	Phenylalanine d2
68	Nucleobase	HMDB00296	Uridine	C9H12N2O6	244.0695	245.0773	243.0617	2.6	3.1	3.1	ACID NEG	243.062+110.024	Phenylalanine d2
69	Nucleoside	HMDB00299	Xanthosine	C10H12N4O6	284.0757	285.0835	283.0679	2.8	3.7	3.6	ACID NEG	283.068	Phenylalanine d2
70	Nucleoside	HMDB00133	Guanosine	C10H13N5O5	283.0917	284.0995	282.0839	–	3.9	3.9	ACID NEG	282.084	Phenylalanine d2
71	Nucleoside	HMDB00195	Inosine	C10H12N4O5	268.0808	269.0886	267.0730	3.0	3.5	3.5	ACID NEG	267.073	Phenylalanine d2
72	Organic Acid	HMDB00072	Aconitic Acid	C6H6O6	174.0164	175.0242	173.0086	2.8	2.5	–	ACID NEG	173.009+85.029	Succinate d4
73	Organic Acid	HMDB03349	Dihydroorotic Acid	C5H6N2O4	158.0328	159.0406	157.0250	2.8	2.8	–	ACID NEG	157.025+113.036	Succinate d4
74	Organic Acid	HMDB00139	Glyceric Acid	C3H6O4	106.0270	107.0348	105.0192	2.7	2.7	–	ACID NEG	105.0192	Succinate d4
75	Organic Acid	HMDB00156	Malic Acid	C4H6O5	134.0215	135.0293	133.0137	3.1	2.8	–	ACID NEG	133.014+115.003	Succinate d4
76	Organic Acid	HMDB00134	Fumaric Acid	C4H4O4	116.0110	117.0188	115.0032	–	2.3	–	ACID NEG	115.003	Succinate d4
77	Organic Acid	HMDB00094	Citric Acid	C6H8O7	192.0270	193.0348	191.0192	4.0	3.7	–	ACID NEG	191.019	Phenylalanine d2
78	Organic Acid	HMDB00227	Mevalonic Acid	C6H12O4	148.0736	149.0814	147.0658	2.7	2.2	–	ACID NEG	147.066	Succinate d4
79	Organic Acid	HMDB00226	Orotic Acid	C5H4N2O4	156.0171	157.0249	155.0093	2.6	–	3.2	ACID NEG	155.009+111.0192	Succinate d4
80	Organic Acid	HMDB01895	Salicylic Acid	C7H6O3	138.0320	139.0398	137.0242	0.6	1.4	–	ACID NEG	137.024+93.035	Octanoic Acid d15
81	Organic Acid	HMDB00254	Succinic Acid	C4H6O4	118.0266	119.0344	117.0188	2.7	2.3	–	ACID NEG	117.019	Succinate d4
82	Sugar	HMDB00625	Gluconic Acid	C6H12O7	196.0583	197.0661	195.0505	2.9	4.2	4.2	ACID NEG	195.051	Glucose 13C6
83	Sugar	HMDB00127	Glucuronic Acid	C6H10O7	194.0426	195.0504	193.0348	3.0	4.2	–	ACID NEG	193.035	Glutamic Acid d5
84	Vitamin	HMDB00017	Pyridoxic Acid	C8H9NO4	183.0532	184.0610	182.0454	0.6	2.9	2.9	ACID NEG	138.055+182.045	Succinate d4
85	Vitamin	HMDB00044	Ascorbic Acid	C6H8O6	176.0321	177.0399	175.0243	–	3.0	–	ACID NEG	175.024	Succinate d4
86	Vitamin	–	Panthotenic Acid	C9H17NO5	219.1107	220.1185	218.1028	–	2.5	2.5	ACID NEG	146.082+218.103	Succinate d4
87	Aminoacid	HMDB00148	Glutamic Acid	C5H9NO4	147.0532	148.0610	146.0454	3.3	4.5	4.5	BASIC NEG	146.045+102.056	Glutamic Acid d5
88	Aminoacid derivative	HMDB00766	Acetylalanine	C5H9NO3	131.0582	132.0660	130.0504	2.7	2.5	–	BASIC NEG	130.05+88.04	Phenylalanine d2
89	Aminoacid derivative	HMDB00251	Taurine	C2H7NO3S	125.0147	126.0225	124.0069	3.4	4.2	4.2	BASIC NEG	79.957+124.007	Glutamic Acid d5
90	Coenzyme	HMDB01423	CoA	C21H36N7O16P3S	767.1152	768.1230	766.1074	3.7	–	–	BASIC NEG	766.107	"AMP 13C10, 15N5"
91	Coenzyme	HMDB00902	NAD	C21H27N7O14P2	663.1091	664.1169	662.1013	3.7	–	–	BASIC NEG	540.053+662.101	AMP 13C10, 15N5
92	Coenzyme	HMDB00217	NADP	C21H28N7O17P3	743.0755	744.0833	742.0676	3.8	–	–	BASIC NEG	620.023+742.068	AMP 13C10, 15N5
93	Coenzyme	HMDB01248	FAD	C27H33N9O15P2	785.1571	786.1649	784.1493	2.8	–	–	BASIC NEG	784.149+528.053	AMP 13C10, 15N5
94	dNucleotide	HMDB00058	cAMP	C10H12N5O6P	329.0525	330.0603	328.0447	2.7	–	–	BASIC NEG	328.045	AMP 13C10, 15N5
95	dNucleotide	HMDB01314	cGMP	C10H12N5O7P	345.0474	346.0552	344.0396	2.7	-	5.1	BASIC NEG	344.040	AMP 13C10, 15N5
96	dNucleotide	HMDB00905	dAMP	C10H14N5O6P	331.0682	332.0760	330.0604	3.0	5.2	–	BASIC NEG	330.060	AMP 13C10, 15N5
97	dNucleotide	HMDB01202	dCMP	C9H14N3O7P	307.0569	308.0647	306.0491	3.3	5.3	–	BASIC NEG	306.049	AMP 13C10, 15N5
98	dNucleotide	HMDB01227	dTMP	C10H15N2O8P	322.0566	323.0644	321.0488	2.9	–	–	BASIC NEG	321.049	AMP 13C10, 15N5
99	Nucleoside derivative	HMDB00536	Adenylosuccinic Acid	C14H18N5O11P	463.0740	464.0818	462.0662	3.6	–	–	BASIC NEG	462.066	Glutamic Acid d5
100	Nucleoside diphosphate	HMDB00295	UDP	C9H14N2O12P2	404.0022	405.0100	402.9944	4.0	–	–	BASIC NEG	402.994	AMP 13C10, 15N5
101	Nucleoside diP derivative	HMDB06557	ADP-Glucose	C16H25N5O15P2	589.0822	590.0900	588.0744	3.0	–	–	BASIC NEG	588.074	AMP 13C10, 15N5
102	Nucleoside diP derivative	HMDB01178	ADP-Ribose	C15H23N5O14P2	559.0717	560.0795	558.0639	2.9	–	–	BASIC NEG	558.064	AMP 13C10, 15N5
103	Nucleoside diP derivative	HMDB00286	UDP-Glucose	C15H24N2O17P2	566.0550	567.0628	565.0472	3.2	–	–	BASIC NEG	565.047	AMP 13C10, 15N5
104	Nucleoside diphosphate	HMDB01341	ADP	C10H15N5O10P2	427.0294	428.0372	426.0216	3.9	–	–	BASIC NEG	426.022	AMP 13C10, 15N5
105	Nucleoside diphosphate	HMDB01201	GDP	C10H15N5O11P2	443.0243	444.0321	442.0165	4.3	–	–	BASIC NEG	442.016	AMP 13C10, 15N5
106	Nucleoside Triphosphate	HMDB01273	GTP	C10H16N5O14P3	522.9907	523.9985	521.9829	4.3	–	–	BASIC NEG	521.983	AMP 13C10, 15N5
107	Nucleoside Triphosphate	HMDB00538	ATP	C10H16N5O13P3	506.9957	508.0036	505.9879	3.9	–	–	BASIC NEG	505.988+408.009	AMP 13C10, 15N5
108	Nucleotide	HMDB00045	AMP	C10H14N5O7P	347.0631	348.0709	346.0553	3.2	–	5.6	BASIC NEG	346.055	AMP 13C10, 15N5
109	Nucleotide	HMDB00095	CMP	C9H14N3O8P	323.0519	324.0597	322.0441	3.5	–	–	BASIC NEG	322.044	AMP 13C10, 15N5
110	Nucleotide	HMDB01397	GMP	C10H14N5O8P	363.0580	364.0658	362.0502	3.6	–	–	BASIC NEG	362.050	AMP 13C10, 15N5
111	Nucleotide	HMDB00175	IMP	C10H13N4O8P	348.0471	349.0549	347.0393	3.3	–	–	BASIC NEG	347.039	AMP 13C10, 15N5
112	Nucleotide	HMDB00288	UMP	C9H13N2O9P	324.0359	325.0437	323.0281	3.2	–	–	BASIC NEG	323.028	AMP 13C10, 15N5
113	Organic Acid	HMDB00357	3-Hydroxybutyric Acid	C4H8O3	104.0473	105.0551	103.0395	3.1	–	–	BASIC NEG	103.040	Phenylalanine d2
114	Organic Acid	-	4-Methyl-2-Oxopentanoic Acid	C6H10O3	130.0630	131.0708	129.0552	0.7	1.3	–	BASIC NEG	129.055	Octanoic Acid d15
115	Organic Acid	HMDB00190	Lactic acid	C3H6O3	90.0317	91.0395	89.0239	2.0	2.7	–	BASIC NEG	89.024	Succinate d4
116	Phosphorilated compound	HMDB00362	2-Phosphoglyceric Acid	C3H7O7P	185.9929	187.0007	184.9851	3.4	–	–	BASIC NEG	184.985	AMP 13C10, 15N5
117	Phosphorilated compound	-	Glycerol Monophosphate	C3H9O6P	172.0137	173.0215	171.0059	3.2	–	–	BASIC NEG	171.006	AMP 13C10, 15N5
118	Phosphorilated compound	HMDB01511	Phosphocreatine	C4H10N3O5P	211.0360	212.0438	210.0282	3.3	–	–	BASIC NEG	210.028	AMP 13C10, 15N5
119	Phosphorilated compound	HMDB00263	Phosphoenolpyruvic Acid	C3H5O6P	167.9820	168.9898	166.9742	3.4	–	–	BASIC NEG	166.974	AMP 13C10, 15N5
120	Phosphorilated Sugar	HMDB01316	6-Phosphogluconic Acid	C6H13O10P	276.0246	277.0324	275.0168	3.6	–	–	BASIC NEG	275.017+257.006	AMP 13C10, 15N5
121	Phosphorilated Sugar	HMDB00124	Fructose 6-Phosphate	C6H13O9P	260.0297	261.0375	259.0219	3.5	–	–	BASIC NEG	259.022	AMP 13C10, 15N5
122	Phosphorilated sugar	HMDB01058	"Fructose-1,6-Diphosphate"	C6H14O12P2	339.9961	341.0039	338.9883	4.1	–	–	BASIC NEG	338.988	"AMP 13C10, 15N5"
123	Phosphorilated Sugar	HMDB01254	Glucosamine-6-Phosphate	C6H14NO8P	259.0457	260.0535	258.0379	4.0	–	–	BASIC NEG	258.038	"AMP 13C10, 15N5"
124	Phosphorilated Sugar	HMDB01401	Glucose 6-Phosphate	C6H13O9P	260.0297	261.0375	259.0219	3.7	–	–	BASIC NEG	259.022	"AMP 13C10, 15N5"
125	Phosphorilated Sugar	HMDB01548	Ribose 5-Phosphate	C5H11O8P	230.0192	231.0270	229.0114	3.4	–	–	BASIC NEG	229.011	"AMP 13C10, 15N5"

* [M+Na]+

** [M+2H]2+

Calibration curves were obtained for various chemical classes of the metabolites, shown in Figure 4, which displayed a linear coefficient (Pearson's correlation, R^2) higher than 0.99. The LOD was lower than 100 ng/mL for most of the analytes reported in Table 2.

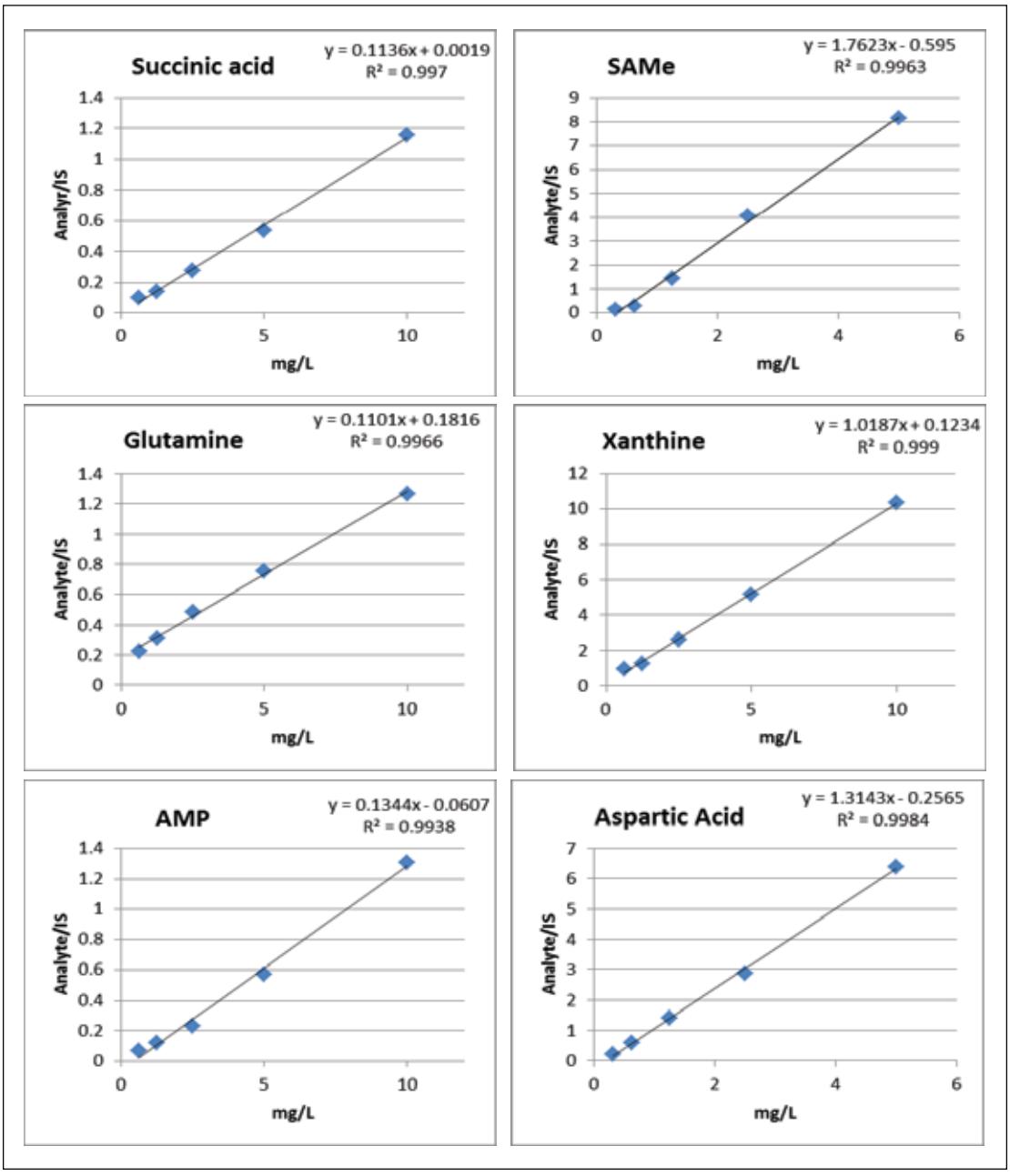

Figure 4. Calibration curves from selected small polar metabolites.

To test the applicability of this HILIC-UPLC/MS strategy in real biological samples, polar metabolites extracted from human platelets were analyzed. Polar metabolites were separated with excellent retention time reproducibility, shown in Figure 5, acquiring accurate mass information from *m/z* 50 to *m/z* 1000. As general workflow, untargeted analyses were performed on this dataset using TransOmics Informatics tools for the visualization, processing, and interpretation of MS data, allowing the discovery and identification of unexpected alterations among sample groups (data not shown).

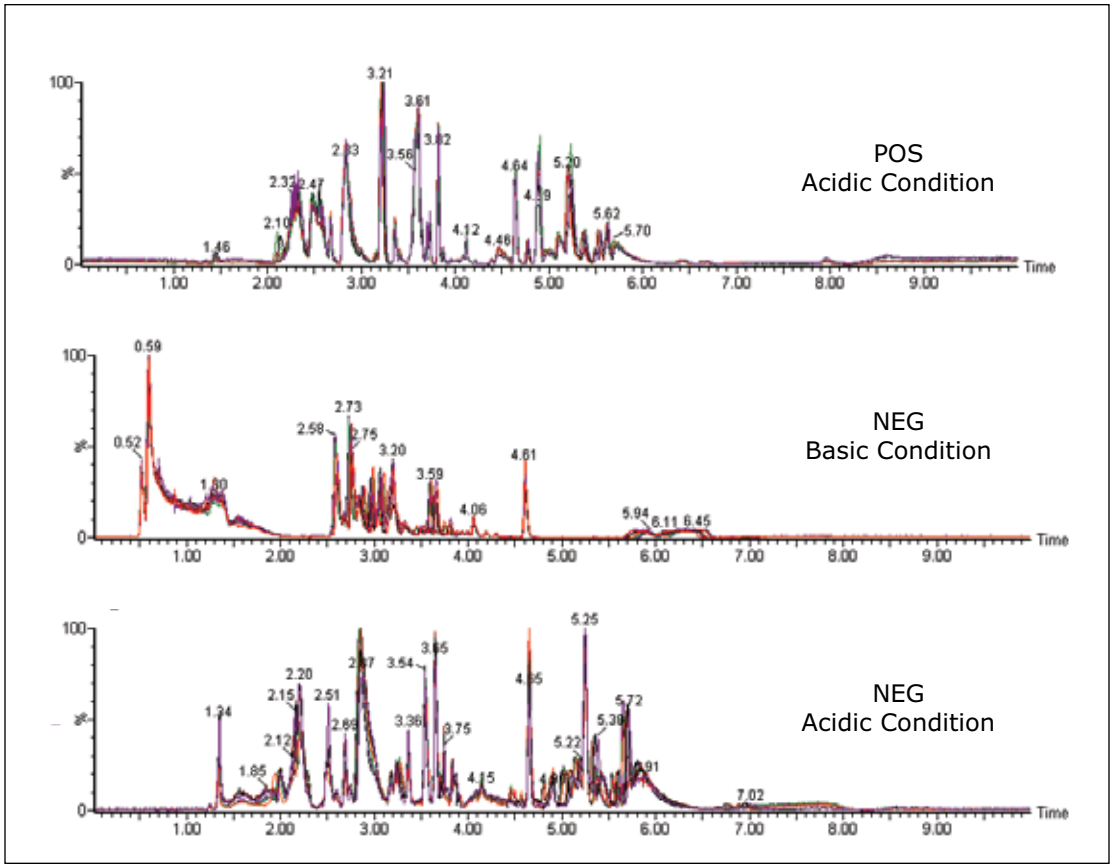

Figure 5. Overlaid chromatographic trace of multiple injections of polar metabolites exctracted from platelets. Each polar metabolite extract was injected eight times during two different batches (80 injections) in two different days of analysis.

Additionally, targeted analyses were conducted using the list of retention times and masses information reported in Table 2, allowing the identification and quantification of the most common metabolites present in biological samples, as shown in Figures 6A and 6B.

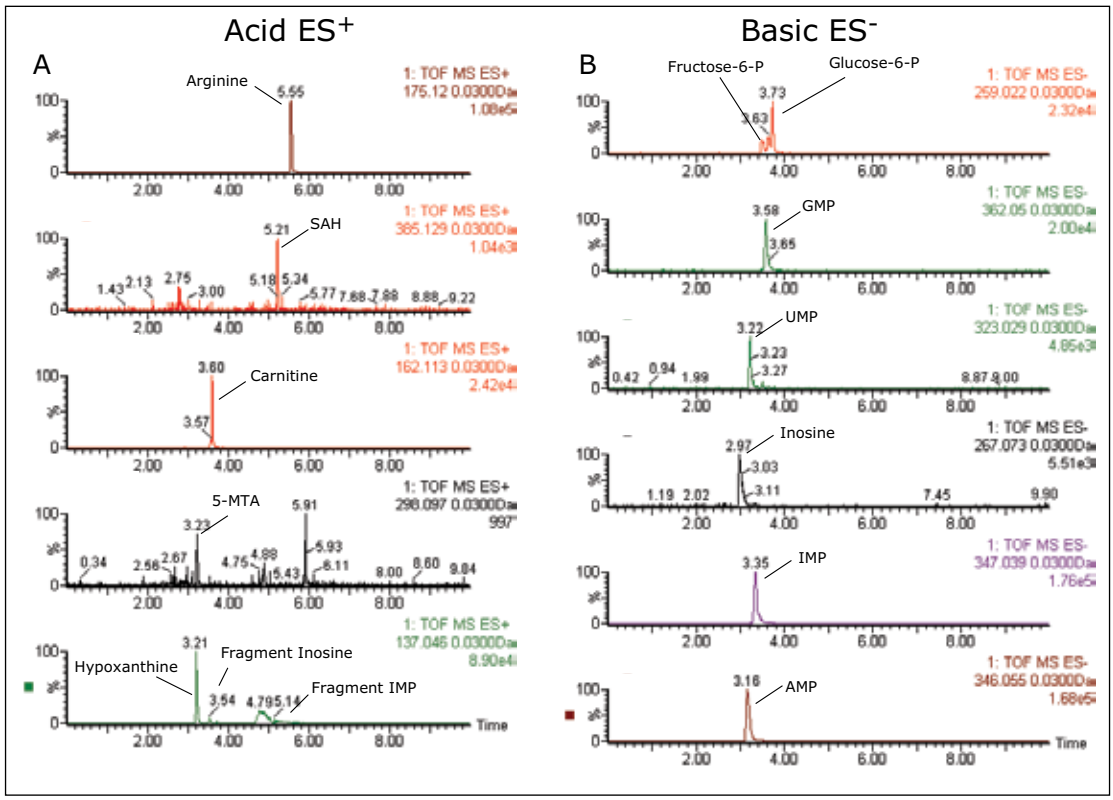

Figure 6. Representative UPLC/MS chromatograms of polar metabolites extracted from platelets and analyzed using acidic conditions for positive ES (A) and basic conditions for negative ES (B).

CONCLUSIONS

A HILIC UPLC/TOF-MS strategy was developed for the analysis of polar metabolites, which could not be easily analyzed using reversed-phase chromatography. Such a method is suitable for routine high-throughput screening of polar metabolites for both untargeted and targeted metabolomics applications.

References

1. Paglia G, Magnusdottir M, Thorlacius S, Sigurjonsson OE, Guethmundsson S, Palsson BO, Thiele I. Intracellular metabolite profiling of platelets: evaluation of extraction processes and chromatographic strategies. *J Chromatogr B Analyt Technol Biomed Life Sci.* 2012; 898:111-120. doi:10.1016/j.jchromb.2012.04.026.

2. Paglia G, Hrafnsdottir S, Magnusdottir M, Fleming RM, Thorlacius S, Palsson BO, Thiele I. Monitoring metabolites consumption and secretion in cultured cells using ultra-performance liquid chromatography quadrupole-time of flight mass spectrometry (UPLC-Q-ToF-MS). *Anal Bioanal Chem.* 2012;402(3):1183-1198. doi:10.1007/s00216-011-5556-4.

Waters

THE SCIENCE OF WHAT'S POSSIBLE.®

Waters Corporation
34 Maple Street
Milford, MA 01757 U.S.A.
T: 1 508 478 2000
F: 1 508 872 1990
www.waters.com

Waters
THE SCIENCE OF WHAT'S POSSIBLE.®

Lipid Separation using UPLC with Charged Surface Hybrid Technology

Giorgis Isaac, Stephen McDonald, and Giuseppe Astarita
Waters Corporation, Milford, MA, USA

APPLICATION BENEFITS

The chromatographic separation performed using Ultra Performance Liquid Chromatography (UPLC®) with Charged Surface Hybrid (CSH™) C_{18} Technology shows superior performance over traditional reversed-phase techniques to give fast, sensitive separation of lipids based upon their acyl chain length, and the number, position, and geometry of double bonds. The resolving power of the CSH C_{18} UPLC System provides an attractive solution for analyzing complex lipid mixtures in biological samples and comparative lipidomic analysis.

WATERS SOLUTIONS

ACQUITY UPLC®

UPLC

SYNAPT® G2 HDMS™

KEY WORDS

Separation of lipids, Charged Surface Hybrid, CSH, reversed-phase, lipids, time-of-flight mass spectrometry

INTRODUCTION

Lipids play key roles in human health. Alterations in lipid levels have been associated with the occurrence of various diseases, including cardiovascular diseases, diabetes, cancer, and neurodegenerative diseases.[1] Advances in LC/MS have allowed lipids to be studied with greater sensitivity and specificity, alleviating the effects of co-eluting compounds and isobaric interference, and allowing low abundance lipids to be more readily detected.[1]

Conventional mass spectrometric analysis of lipids is often performed by direct infusion, or reversed-phase (RP) / normal-phase (NP) HPLC.[2-5] However, each of these methods faces its own challenges.

With direct infusion, chromatographic separation of lipids is not performed prior to injection into the mass spectrometer. This method of sample introduction gives rise to ion suppression and it does not allow for separation of isobaric lipids, which can complicate the resultant analysis, necessitating deconvolution, and compromising the sensitivity of the method. In order to fully explore the lipidome, a technique of sample introduction into the mass spectrometer that minimizes these issues is needed.

NP chromatography allows separation of lipids by class but often suffers from long elution times, is difficult to handle due to the volatility and toxicity of the mobile phase, and proves challenging for ionization and introduction into mass spectrometry.[6] Recent work in HILIC chromatography overcomes many of these issues.[7]

Traditional RP methods similarly suffer from extensive elution times and the quality of the resulting chromatography is relatively poor. Peak capacity and resolution are compromised in a typical analysis and it is not unusual to see peaks widths > 30 seconds,[5] which ultimately results in poor sensitivity and difficulty in characterization.

In this application note, novel RP-UPLC separations are performed using a Waters® ACQUITY UPLC System with Charged Surface Hybrid (CSH™) C_{18} chemistry. The combination of sub-2-µm particle size with an optimized liquid chromatography system and novel chemistry allows for a significantly improved RP method that maximizes the performance of these particles and is optimized for the analysis of complex lipid mixtures.

EXPERIMENTAL

LC conditions

LC system:	ACQUITY UPLC
Column:	ACQUITY UPLC CSH C_{18} 2.1 x 100 mm, 1.7 µm
Column temp.:	55 °C
Flow rate:	400 µL/min
Mobile phase A:	Acetonitrile/water (60:40) with 10 mM ammonium formate and 0.1% formic acid
Mobile phase B:	Isopropanol/acetonitrile (90:10) with 10 mM ammonium formate and 0.1% formic acid
Injection volume:	5 µL

Gradient

Time (min)	% A	% B	Curve
Initial	60	40	Initial
2.0	57	43	6
2.1	50	50	1
12.0	46	54	6
12.1	30	70	1
18.0	1	99	6
18.1	60	40	6
20.0	60	40	1

MS conditions

Mass spectrometer:	SYNAPT G2 HDMS
Acquisition mode:	MS^E
Ionization mode:	ESI positive/negative
Capillary voltage:	2.0 KV (for positive) 1.0 KV (for negative)
Cone voltage:	30 V
Desolvation temp.:	550 °C
Desolvation gas:	900 L/Hr
Source temp.:	120 °C
Acquisition range:	100 to 2000 *m/z*

Sample preparation

Standard lipid mixtures

Lipid standards were purchased from Avanti Polar Lipids and Nu-Chek Prep. The standards were diluted prior to analysis in isopropanol/acetonitrile/water (2:1:1, 250 µL). The list of lipid standards analyzed and other detailed information is provided in Table 1.

Total liver extract

A total lipid extract from bovine liver was purchased from Avanti Polar Lipids. The extract was prepared by making a 5 mg/mL stock solution in chloroform/methanol (2:1). A working 0.1 mg/mL solution was then prepared by diluting the stock solution with isopropanol/acetonitrile/water (2:1:1).

Total plasma extract

Rat plasma (25 µL) from Equitech-Bio, Inc. was extracted with 100 µL of chloroform/methanol (2:1); this solution was then allowed to stand for 5 min at room temperature, followed by vortexing for 30 s. After centrifuging (12,000 g, for 5 min at 4 °C) the lower organic phase was collected in a new vial and evaporated to dryness under vacuum. Immediately prior to analysis the lipid extract was diluted with isopropanol/acetonitrile/water (2:1:1, 250 µL).

RESULTS AND DISCUSSION

The UPLC RP method employed for this analysis showed improved separation of both inter and intra class lipids over traditional HPLC RP methods. Figures 1 and 2 show the lipid classes based on Lipid MAPS classification and representative structures for major lipid categories respectively. Highlighted in yellow are the classes that are included in the standard mix, which reflect the most abundant lipids present in animal tissues.

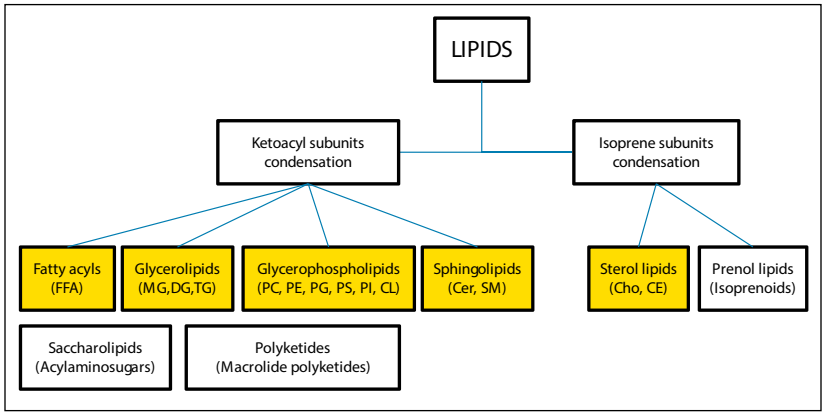

Figure 1. Lipid categories and examples of common lipids analyzed in this application. Abbreviations: FFA, free fatty acids; MG, monoacylglycerols; DG, diacylglycerols; TG, triacylglycerols; PC, phosphatidylcholines; PE, phosphatidylethanolamines; PG, phosphatidylglycerols; PS, phosphatidylserines; PI, phosphatidylinositols; CL, cardiolipins; Cer, ceramides; SM, sphingomyelins; Cho, cholesterol; CE, cholesterol esters.

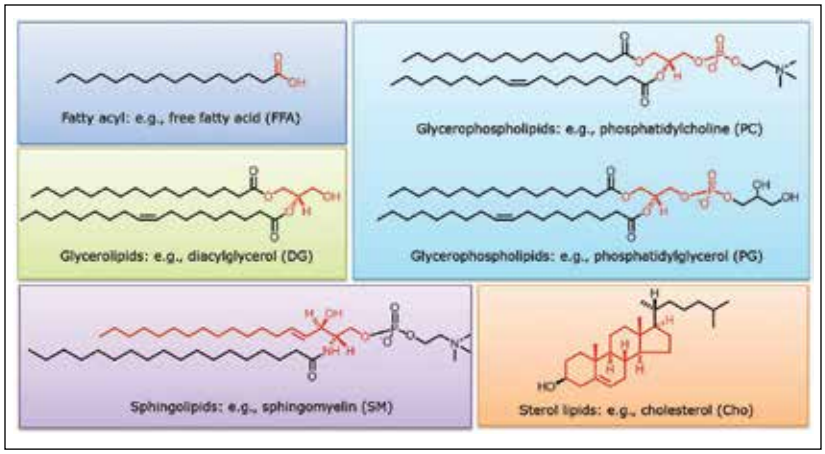

Figure 2. Representative structures for major lipid categories and examples of core structures in red.

The resolution, sensitivity, and speed of analysis were significantly increased compared with HPLC. The CSH chemistry's charged surface is believed to interact with the lipids on column in a unique manner. Due to the diverse chemical nature of lipids, from highly polar to highly non-polar, a different mechanism of retention from traditional RP columns was observed.

The additional speed allows for large sample sets to be analyzed efficiently, while the added resolution and sensitivity increase peak purity. This provides added confidence in the assignment of a lipid or class of lipids while allowing identification to be made at lower concentrations.

Our initial analysis focused on the separation of a mixture of 67 lipid standards, as shown in Table 1.

The resulting base peak intensity chromatogram can be seen in Figure 3.

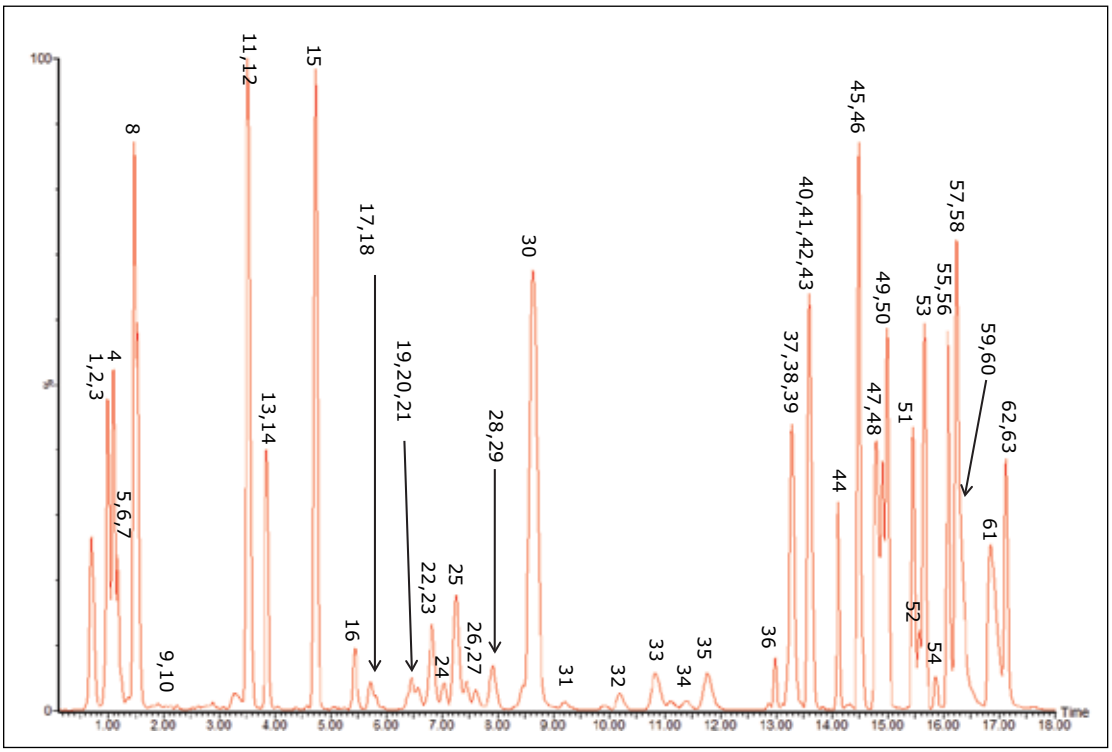

Figure 3. CSH C_{18} separation of 67 standard lipid mixtures.

As can be seen in Figure 3, several interesting observations were made during the course of developing this method. First, we have shown previously that the phophatidylcholines (PC) typically co-elute with sphingomyelins (SM) during a RP separation.[8] Using CSH Technology C_{18}, an enhanced separation of these classes was observed. This is especially useful when coupling with mass spectral detection as both classes fragment to give a phosphocholine ion at *m/z* 184.074, the common head group. Also, in complex biological matricies, SM are less abundant than PC species, leading to ion suppression effects that affect the efficiency of detection of minor species. Figures 4 and 5 show the analysis of total lipid extracts from bovine liver and rat plasma respectively.

Lipid sub class	Lipid molecular species	Concentration (pmol/uL)	Rt* (min)	Peak ID
FA	C13:1 (12Z)	4	1.24	**
	C17:1 (10Z)	4	2.3	**
	C23:1 (14Z)	4	5.44	**
MG	14:1 (9Z)	4	1.11	5
	17:1 (10Z)	4	1.7	9
	19:2 (10Z, 13Z)	4	1.87	10
D5-DG Mix I	1,3-14:0/14:0	2	7.6	27
	1,3-15:0/15:0	2	10.17	32
	1,3-16:0/16:0	2	12.98	36
	1,3-17:0/17:0	2	13.6	40
	1,3-19:0/19:0	2	14.55	46
	1,3-20:5 (5Z, 8Z, 11Z, 14Z, 17Z)/20:5 (5Z, 8Z,11Z, 14Z, 17Z)	2	5.41	16
	1,3-20:4 (5Z, 8Z, 11Z, 14Z)/20:4 (5Z, 8Z, 11Z, 14Z)	2	7.88	28
	1,3-20:2 (11Z, 14Z)/20:2 (11Z, 14Z)	2	13.23	38
	1,3-20:0/20:0	2	14.95	49
DG	19:1/19:1 (10Z)	4	13.65	42
	19:1/19:1 (10Z) 1,3 isomer	4	13.65	43
D5-TG Mix I	14:0/16:1 (9Z)/14:0	2	14.99	50
	15:0/18:1 (9Z)/15:0	2	15.65	53
	16:0/18:0/16:0	2	16.24	57
	19:0/12:0/19:0	2	16.24	58
	17:0/17:1 (10Z)/17:0	2	16.08	55
	20:4 (5Z, 8Z, 11Z, 14Z)/18:2 (9Z, 12Z)/20:4 (5Z, 8Z, 11Z, 14Z)	2	14.9	48
	20:2 (11Z, 14Z)/18:3 (6Z, 9Z, 12Z)/20:2 (11Z, 14Z)	2	15.46	51
	20:5 (5Z, 8Z, 11Z, 14Z, 17Z)/22:6 (4Z, 7Z, 10Z, 13Z, 16Z, 19Z)/20:5 (5Z , 8Z, 11Z, 14Z, 17Z)	2	14.1	44
	20:0/20:1 (11Z)/20:0	2	17.13	62
TG	19:2 (10Z, 13Z)/19:2 (10Z, 13Z)/19:2 (10Z, 13Z)	4	15.57	52
PC	17:0/20:4 (5Z, 8Z, 11Z, 14Z)	2.18	7.25	25
	18:1 (9Z)/18:0	4	10.84	33
	19:0/19:0	4	13.6	41
	21:0/22:6 (4Z, 7Z, 10Z, 13Z, 16Z, 19Z)	2.28	11.74	35
Lyso PC	17:0	4	1.5	8
PA	16:0/18:1	4	7.92	29
PE	15:0/15:0	4	6.46	20
	17:0/17:0	4	11.38	34
	18:0/18:0	4	13.2	37
Lyso PE	17:1 (10Z)	4	1.25	7
PS	16:0/18:1 (9Z)	4	6.38	19
	17:0/20:4 (5Z, 8Z, 11Z, 14Z)	2.61	5.7	17
	18:1 (9Z)/18:1 (9Z)	4	6.54	21
	21:0/22:6 (4Z, 7Z, 10Z, 13Z, 16Z, 19Z)	2.28	9.2	31
Lyso PS	17:1 (10Z)	4	1	2
PG	14:0/14:0	4	3.81	13
	17:0/17:0	4	8.36	30
	18:1 (9Z)/18:1 (9Z)	4	6.71	22
	18:1 (9E)/18:1 (9E)	4	7.36	26
	18:0/18:2 (9Z, 12Z)	4	6.97	24
Lyso PG	17:1 (10Z)	4	1	3
Lyso PI	17:1 (10Z)	25	1	1
CL Mix I	14:1 (9Z)/14:1 (9Z)/14:1 (9Z)/15:1 (10Z)	4	13.29	39
	15:0/15:0/15:0/16:1 (9Z)	4	14.82	47
	22:1 (13Z)/22:1(13Z)/22:1(13Z)/14:1 (9Z)	4	16.32	59
	24:1 (15Z)/24:1 (15Z)/24:1 (15Z)/14:1 (9Z)	4	16.89	61
Sphingolipid Mix	d17:1	5	1.08	4
	d17:0	5	1.16	6
	d18:1/12:0 SM	5	3.49	11
	d18:1/12:0 Cer	5	4.72	15
	d18:1/25:0 Cer	5	14.49	45
	d18:1/12:0 Glucosylceramide	5	3.84	14
	d18:1/12:0 Lactosylceramide	5	3.56	12
	d18:1/17:0 SM	4	6.83	23
Cho	Cho	4	5.84	18
CE	17:0	4	16.33	60
	18:2 (TT)	4	15.86	54
	18:1	4	16.16	56
	23:0	4	17.19	63

*Table 1. A list of analyzed 67 lipid standard mixtures with corresponding concentration (pmol/µL), retention time (min) and peak ID. For lipid abbreviation refer to the legend in Figure 1. *Rt, retention time in minutes;*
***Peak ID not shown in Figure 3. Retention time values are identified from negative mode.*

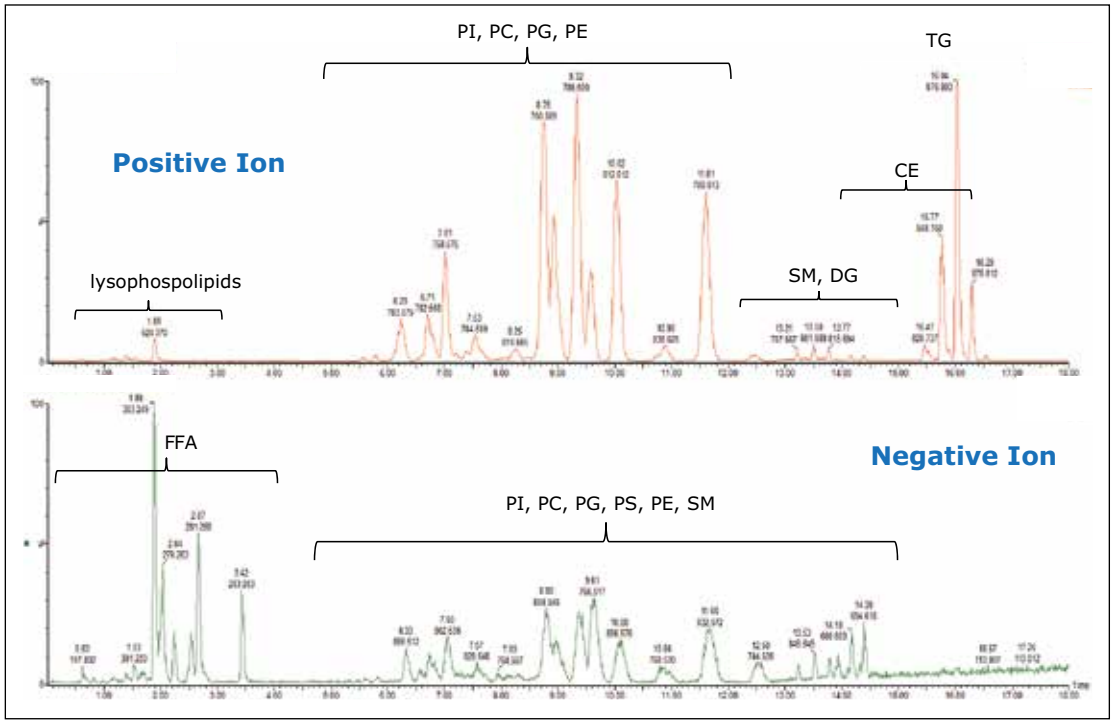

Figure 4. Total bovine liver lipid extract acquired in both positive and negative ionization modes. For lipid abbreviation refer to the legend in Figure 1.

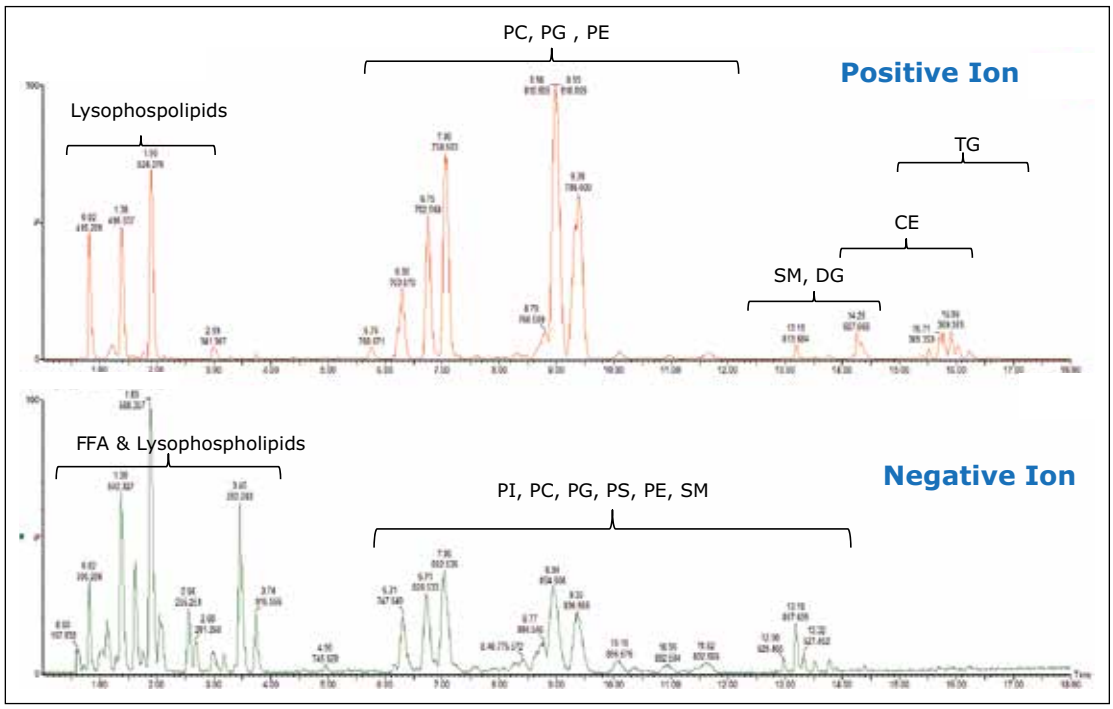

Figure 5. Total rat plasma lipid extract acquired in both positive and negative ionization modes. For lipid abbreviation refer to the legend in Figure 1.

In this analysis the ability of UPLC and CSH Technology to differentiate between structural cis (Z) and trans (E) isomers was also observed. The separation of cis and trans isobaric phosphatidylglycerol (PG) species, such as PG 18:1(9Z)/18:1(9Z) and PG 18:1(9E)/18:1(9E) were easily separated. In addition, structural isomers such as PG 18:1(9Z)/18:1(9Z) versus PG 18:0/18:2(9Z, 12Z) were resolved, as shown in Figure 6. This information would typically not be available using an infusion or traditional HPLC methods.

To test the applicability of this novel chromatographic method in real biological samples, we analyzed total lipid extracts from bovine liver and rat plasma. Using the CSH C_{18} ACQUITY UPLC System, we were able to separate the major lipid classes with high resolution and sensitivity, which improved the detection of low abundant lipid species, as shown in Figures 4 and 5. Notably, the CSH C_{18} ACQUITY UPLC System presented excellent retention time reproducibility from multiple injections of a bovine liver extract (%RSD < 0.136; n=20), as shown in Figure 7. This is especially useful for lipidomic analysis, which requires the comparison of a large number of LC/MS chromatograms deriving from multiple sample sets.

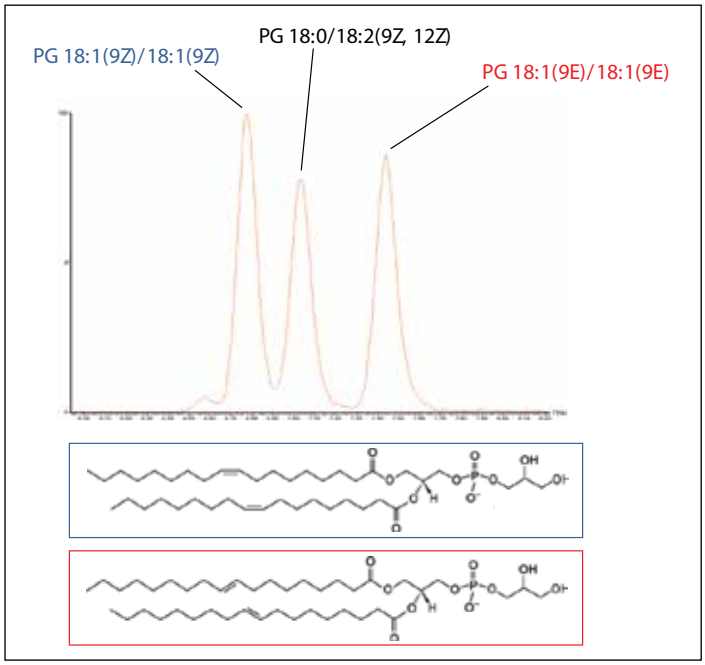

Figure 6. Separation of PG 18:1(9Z)/18:1(9Z) and PG 18:1(9E)/18:1(9E) as well as PG 18:0/18:2(9Z, 12Z).

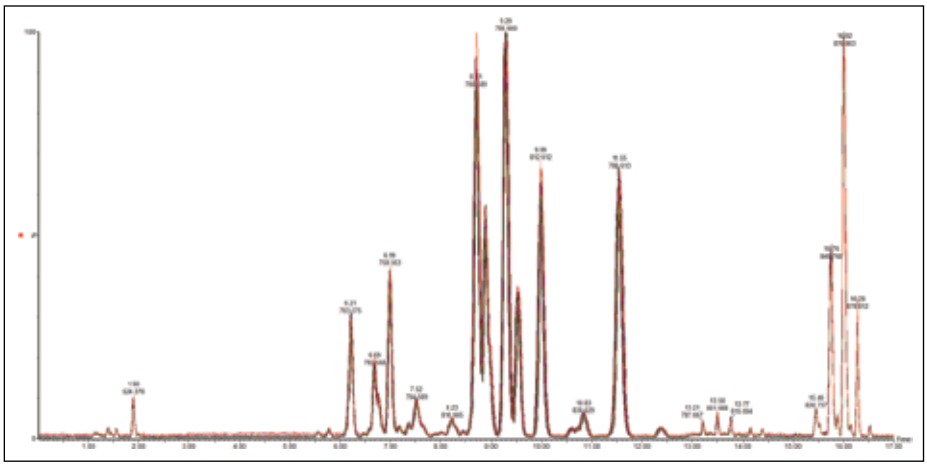

Figure 7. Overlaid chromatographic trace of 20 injections with < 0.136% RSD for retention time.

CONCLUSIONS

The use of UPLC with CSH C_{18} column described in this method provides clear improvements over other NP and RP traditional HPLC methods. It also marks an improvement over the UPLC methods highlighted in previous application notes for lipid analysis.[8] This method offers a robust and reliable approach for lipid analysis.

References

1. Shui G, *et. al.* Sensitive profiling of chemically diverse bioactive lipids. J. Lipid Res. 2007, 48; 1976-1984.
2. Han X, Gross RW. Shotgun lipidomics: electrospray ionization mass spectrometric analysis and quantitation of the cellular lipidomes directly from crude extracts of biological samples. Mass Spectr. Rev. 2005, 24; 367-412.
3. Sommer U, *et. al.* LC-MS based method for the qualitative and quantitative analysis of complex lipid mixtures. J. Lipid Res. 2006, 47; 804-814.
4. Castro-Perez JM, *et. al.* Comprehensive LC MS^E lipidomic analysis using a shotgun approach and its application to biomarker detection and identification in osteoarthritis patients. J. Proteome Res. 2010, 9; 2377-2389.
5. Camera E, *et. al.* Comprehensive analysis of the major lipid classes in serum by rapid resolution-high performance liquid chromatography and electrospray mass spectrometry. J. Lipid Res. 2010.
6. Henderson MA and McIndoe JS. Ionic liquids enable electrospray ionisation mass spectrometry in hexane. chem. Commun. 2006, 2872-2874.
7. Mal M and Wong S. A HILIC-based UPLC/MS method for the separation of lipid classes from plasma. 2011, 720004048en.
8. Shockor J, *et. al.* Analysis of intact lipids from biological Matrices by UPLC/High Definition MS. 2010, 720003349en.

Waters

THE SCIENCE OF WHAT'S POSSIBLE.®

September 2011 720004107en AG-PDF

Waters Corporation
34 Maple Street
Milford, MA 01757 U.S.A.
T: 1 508 478 2000
F: 1 508 872 1990
www.waters.com

Waters
THE SCIENCE OF WHAT'S POSSIBLE.®

High Resolution Separation of Phospholipids Using a Novel Orthogonal Two-Dimensional UPLC/QTof MS System Configuration

Jeremy Dietrich Netto, Stephen Wong, Mark Ritchie
Waters Pacific Private Limited, Singapore

APPLICATION BENEFITS

- Improved peak capacity by using multiple columns for better characterization of complex mixtures such as lipids
- Low abundance components are chromatographically separated from high abundance components allowing high confidence in identification and accurate quantification due to the removal of isotopic interferences
- Ability to use combinations of different chemistries, such as IEX and SEC, for truly orthogonal 2D LC separations

WATERS SOLUTIONS

ACQUITY UPLC® System with 2D Technology

Xevo® G2 QTof Mass Spectrometer

Ostro™ Sample Preparation Plates

KEY WORDS

2D UPLC®/MS, phospholipids, lipidomics, HILIC, CSH™ C_{18}, Ostro

INTRODUCTION

Lipids play many important roles in maintaining homeostasis of living organisms. These include energy storage, maintaining structural integrity of cell membranes, and acting as signaling molecules. Understanding these lipids may provide insights into mechanisms of disease, including the identification of biomarkers and potential drug targets. Lipids can be either hydrophobic or amphiphilic in nature, with phospholipids being the latter comprised of a hydrophilic phosphate head group and a lipophilic diglyceride tail.

The chemical behavior of amphiphilic lipids has led to the adoption of three main techniques for analysis by liquid chromatography including reversed phase, normal phase, and HILIC separation sciences. While reversed phase chromatography separates these lipids based on their lipophilicity (alkyl chain length and/or degree of saturation), it does not show class distinction especially between classes such as the phosphotidylcholines and sphingomyelins. Normal phase and HILIC chromatography, on the other hand, provide a separation based on the lipid's head group polarity but provides little separation within the given class.

In this application note, we present a novel configuration of the Waters® ACQUITY UPLC System with 2D Technology. This minimally modified system is able to utilize the advantages of both HILIC and reversed phase methods in tandem to provide a truly orthogonal and high resolution separation of amphiphilic lipids. We demonstrate the application of 2D UPLC/MS for the analysis of lipids in human plasma as this biofluid is a highly complex matrix with large lipid diversity covering many orders of concentration, thus presenting an analytical challenge when analyzed using traditional single-dimensional liquid chromatography.

EXPERIMENTAL

UPLC conditions

System: ACQUITY UPLC with 2D Technology

First dimension column: ACQUITY® BEH HILIC 2.1 x 100 mm, 1.7 µm

Second dimension column: ACQUITY CSH C_{18} 2.1 x 100 mm, 1.7 µm

Trap column: ACQUITY UPLC BEH C_8 VanGuard 130Å 2.1 x 5 mm, 1.7 µm

Alpha pump

Mobile phase A: 95% ACN 5% H_2O 10 mM NH_4Ac (pH 5.0)

Mobile phase B: 50% ACN 50% H_2O 10 mM NH_4Ac (pH 5.0)

UPLC flow rate: 0.5 mL/min

Gradient:

Time (min)	%A	%B
Initial	100	0
10.0	80	20
10.1	20	80
13.0	20	80
13.1	100	0
16.0	100	0

Beta pump

Mobile phase A: 40% ACN 60% H_2O 10 mM NH_4Ac (pH 5.0)

Mobile phase B: 10% ACN 90% IPA 10 mM NH_4Ac (pH 5.0)

UPLC flow rate: 0.5 mL/min

Gradient:

Time (min)	%A	%B
Initial	100	0
Fraction Elute (FE)*	100	0
FE + 0.10	60	40
FE + 20.0	0	100
FE + 23.0	0	100
FE + 23.1	100	0
FE + 25	100	0

*Fraction Elute (FE) time will vary according to the RT of the lipid class of interest.

Column Manager (CM-A)

First dimension column temp.: 30 °C

Second dimension column temp.: 65 °C

Valve Events Table:

Time (min)	Left valve	Right valve
0	Position 2	Position 2
Fraction Trap	Position 1	Position 1
Fraction Elute (FE)	Position 2	Position 2
FE + 25	Position 1	Position 1

MS conditions

Mass spectrometer: Waters Xevo G2 QTof

Acquisition mode: ESI +ve / -ve, MS^E

Capillary voltage: 2.0 kV (+ve) / 1.00 kV (-ve)

Sampling cone: 35.0 V

Extraction cone: 4.0 kV

MS collision energy: 4.0 V

MS^E energy ramp: 20 to 45 V

Source temp.: 120 °C

Desolvation temp.: 500 °C

Desolvation gas flow: 1000 L/h

Cone gas flow: 10 L/h

Acquisition range: *m/z* 50 to 1200

Lock mass (LeuEnk): +ve, *m/z* 556.2771 and 278.1141

-ve, *m/z* 554.2615 and 236.1035

Sample description

Lipids were extracted from human plasma using the Waters Ostro sample preparation method.[1]

2D UPLC flow diagram

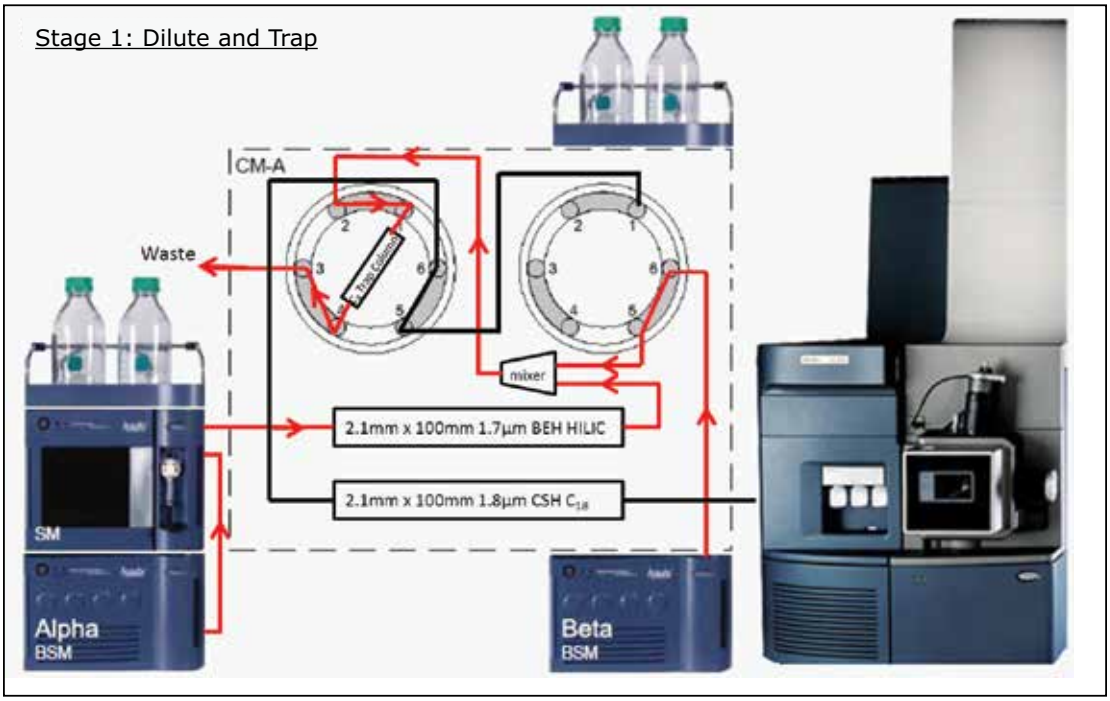

Figure 1. Flow diagram of the 2D UPLC/MS system showing stage 1 where the left and right valves are both in position 1, and trapping analytes eluting off the HILIC column is performed.

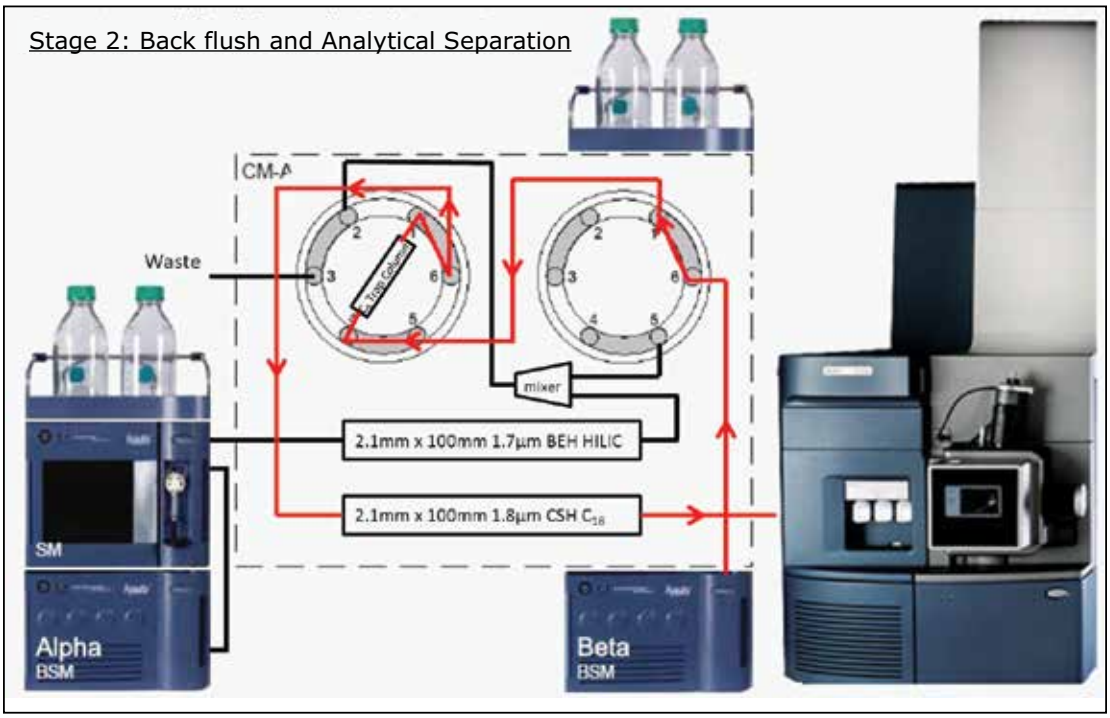

Figure 2. Flow diagram of the 2D UPLC/MS system showing stage 2 where the left and right valves are both in position 2 when the trapped analytes are back-flushed off the trapping column, and sent to the C_{18} column for reversed phase separation.

RESULTS AND DISCUSSION

Comparison of separation between 1D and 2D UPLC/MS

By combining the orthogonality of the HILIC and reversed phase separations into a single tandem 2D UPLC/MS method, we overcame the challenges of inter-class co-elution posed by reversed phase liquid chromatography, as shown in Figure 3, between the PC and SM classes. The coelution of these two classes are particularly problematic, as they have only a single dalton difference between them, and co-elution makes identification and accurate quantification difficult due to isotopic interferences.

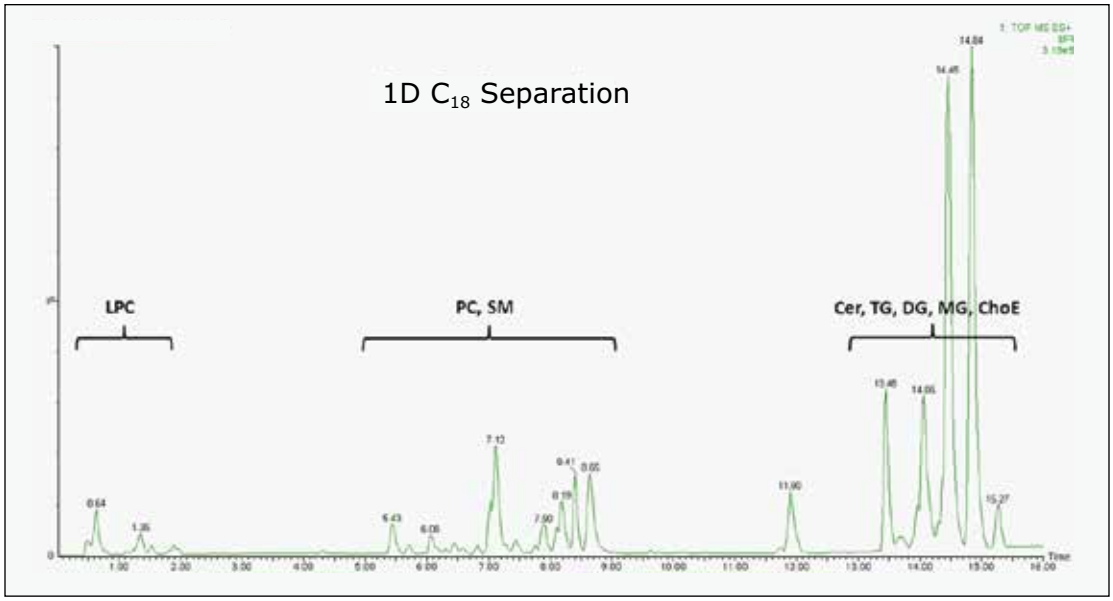

Figure 3. Chromatogram showing single-dimensional reversed phase separation of plasma lipids. SMs co-elute with PCs making identification and quantification difficult due to 1Da difference between species of the two classes.

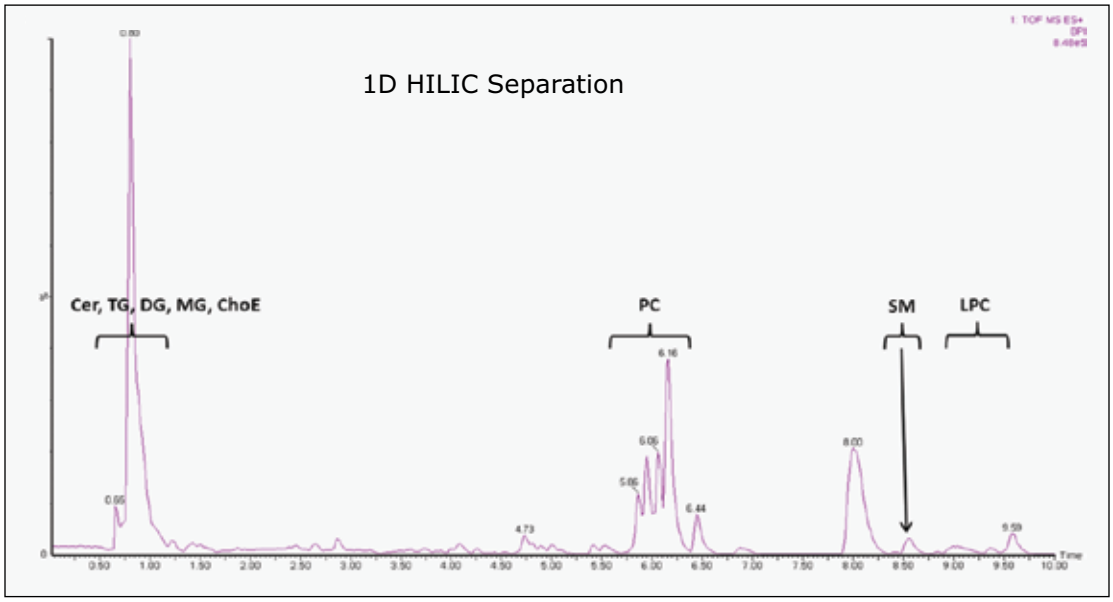

Figure 4. Chromatogram showing single-dimensional HILIC separation of plasma lipids. SMs are separated from PCs but individual species within each class co-elute, leading to poor resolution and dynamic range.

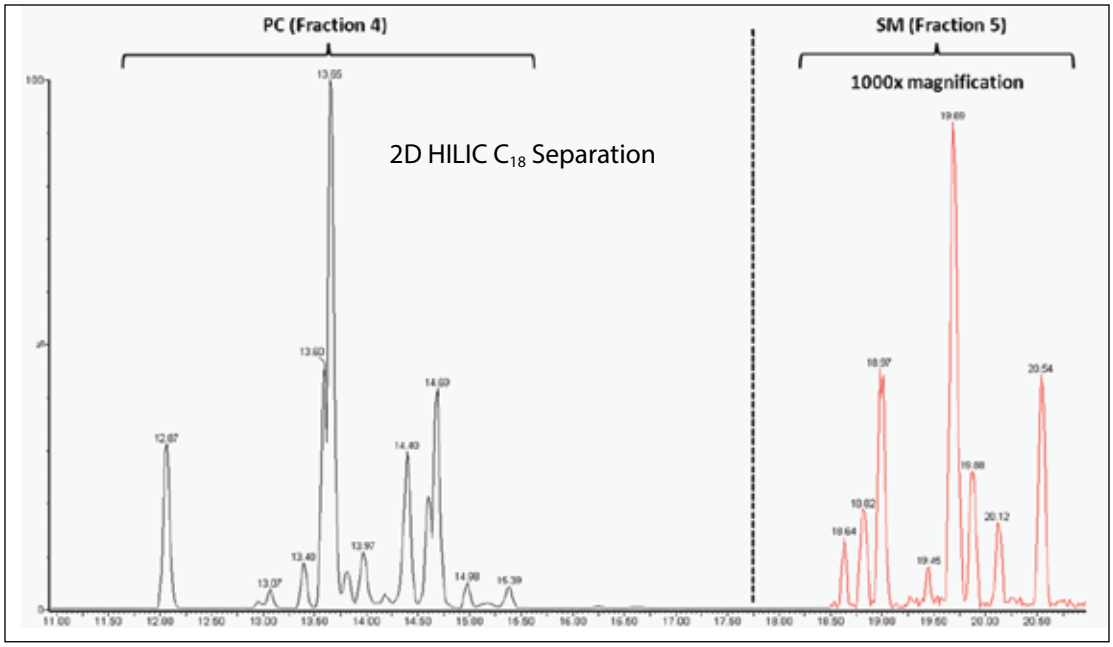

Figure 5. Overlay of fractions from two-dimensional separation of plasma lipids. SMs are now class separated from the PCs by HILIC, and the individual lipids within each class are separated further by reversed phase.

In the HILIC method, inter-class separation is eliminated, as shown in Figure 4, with the PCs and SMs well separated. However, there is now intra-class co-elution which affects the peak capacity and, hence, the sensitivity of the method. In the 2D UPLC/MS method there was improved resolution of the individual lipids of each class using the PC and SM classes as examples, as shown in Figure 5.

The increased peak capacity from the use of combined columns improved both the resolution, shown in Figure 5, as well as the dynamic range of the individual lipids within each class. Using the PC class as an example, the SimLipid (Premier Biosoft) lipid identification software was able to detect and identify 37% more PCs than the HILIC method, and 40% more PCs than the reversed phase C_{18} method. Generally, the ion intensities for the 2D UPLC/MS method were higher than the HILIC or C_{18} methods for the same samples run, which could be attributed to the removal of isotopic interferences.

Predictable separation of the 2D UPLC/MS method

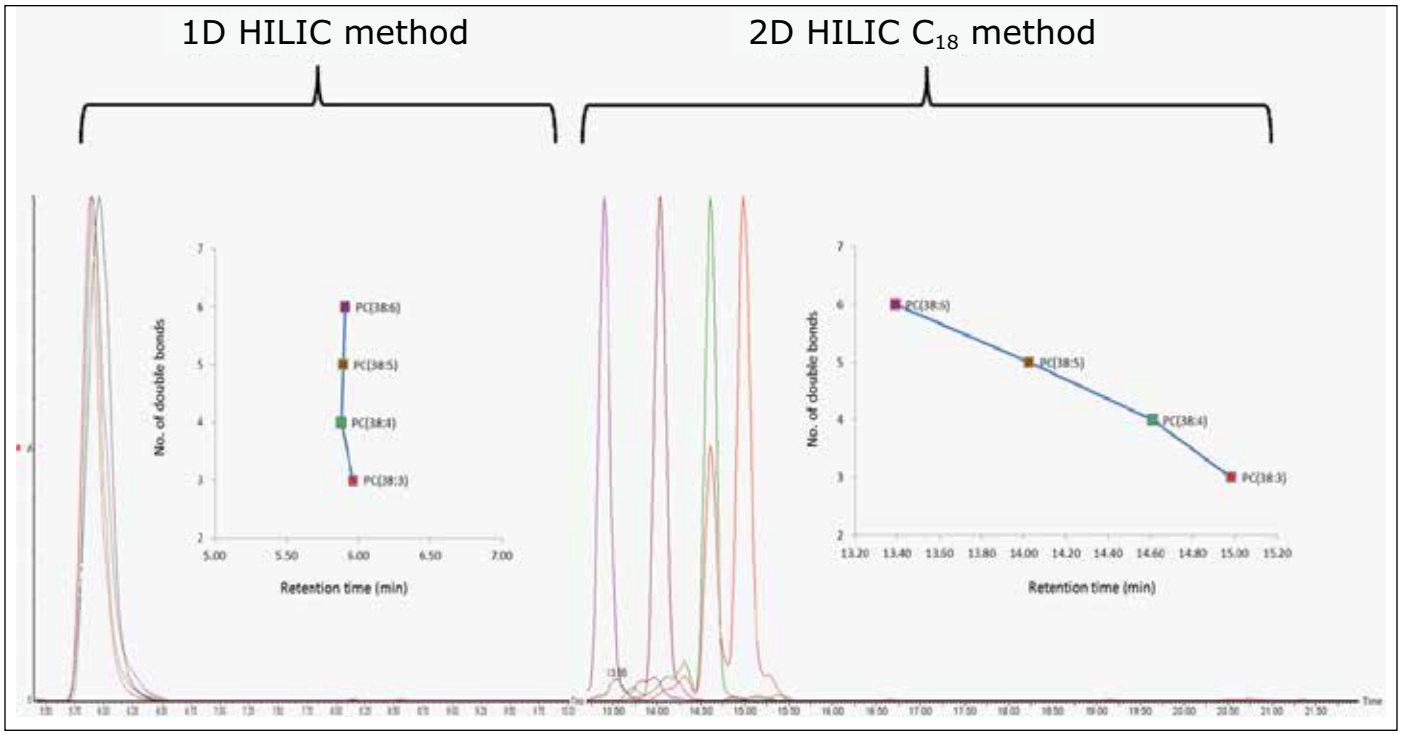

Figure 6. Comparison between 1D HILIC and 2D HILIC C_{18} of the degree of PC alkyl chain saturation (number of double bonds) against retention time.

Since the second dimension of separation is reversed phase, the lipids were able to be further separated chromatographically, according to their hydrophobicity (alkyl chain length and degree of saturation), as shown in Figure 6. This was more advantageous than the HILIC method; whereby, residual isotopic interferences due to the co-elution could affect the confidence level for positive identification and quantification of these lipids.

Improved specificity of the 2D UPLC/MS method

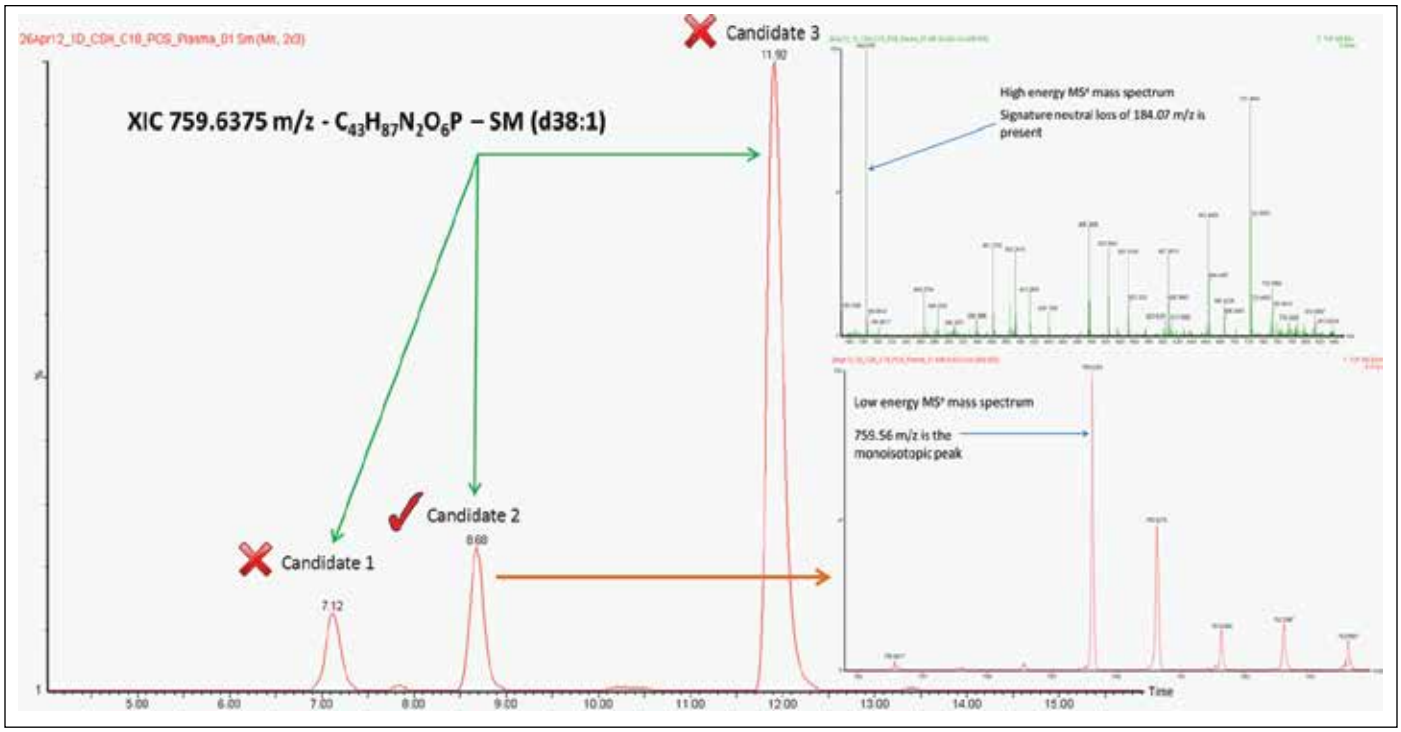

Figure 7. XIC of 759.6375 m/z from the 1D C_{18} TIC reveals three potential candidates for an SM. Further analysis of both the MS and MS^E data reveals candidate two to be the correct one.

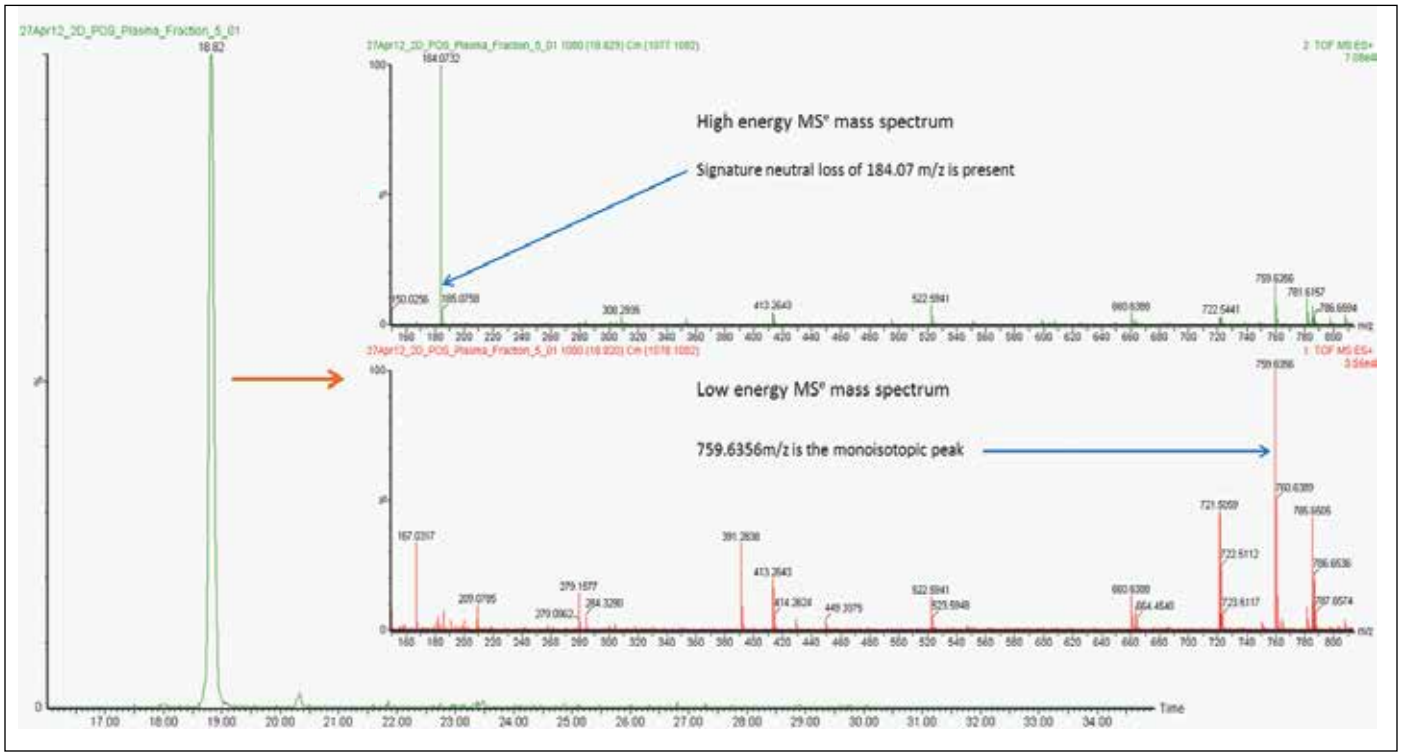

Figure 8. XIC of 759.6375 m/z from the 2D HILIC C_{18} TIC reveals only one potential candidate for the SM. Further analysis of both the MS and MS/MS data confirms this candidate is the correct one.

"Heart cutting" a pure fraction of each lipid class using the HILIC column as the first dimension, followed by further separation using reversed phase in the second dimension eliminates errors in identification due to isotopic interferences from co-eluting peaks. This is especially true for the PC and SM classes which differ by 1Da, as shown in Figures 7 and 8.

CONCLUSIONS

The limitations posed by traditional single-dimensional separations of HILIC or reversed phase were overcome by the introduction of this novel 2D UPLC/MS configured system which leverages the advantages of both types of methods. This resulted in improved chromatographic resolution, peak capacity, and specificity. In addition, the system is completely automated and UPLC technology provides the capability of high throughput, high resolution analyses compared to traditional HPLCs.

In this application note, we show the orthogonality of this system by pairing the HILIC and C_{18} chemistries; however, the system can also be easily adapted for other two-dimensional applications such as IEX-RP and SEC-RP. The 2D UPLC/MS system configuration described here uses commercially available components with little modification needed and can easily be switched to other UPLC with 2D technology modes, such as parallel column regeneration or conventional single-dimensional separation.

References

1. Ritchie M, Mal M, Wong S. Extraction of Phospholipids from Plasma using Ostro Sample Preparation. Waters Application Note 720004201en. 2012 Jan.
2. Mal M, Wong S. A HILIC-Based UPLC/MS Method for the Separation of Lipid Classes from Plasma. Waters Application Note 720004048en. 2011 July.
3. Ritchie M, Mal M, Wong S. UPLC BEH HILIC: The Preferred Separation Chemistry for Targeted Analysis of Phospholipids. Waters Application Note 720004219en. 2012 Jan.
4. Isaac G, McDonald S, Astarita G. Lipid Separation using UPLC with Charged Surface Hybrid Technology. Waters Application Note 720004107en. 2011 Sept.
5. Isaac G, McDonald S, Astarita G. Automated Lipid Identification Using UPLC/HDMS^E in Combination with SimLipid. Waters Application Note 720004169en. 2011 Dec.

Waters

THE SCIENCE OF WHAT'S POSSIBLE.®

Waters Corporation
34 Maple Street
Milford, MA 01757 U.S.A.
T: 1 508 478 2000
F: 1 508 872 1990
www.waters.com

Waters
THE SCIENCE OF WHAT'S POSSIBLE.®

A Multidimensional Lipidomics Method: HILIC Coupled with Ion Mobility Enabled Time-of-Flight Mass Spectrometry

Giuseppe Astarita,[1] Jeremy Netto,[2] Giorgis Isaac,[1] Marc V. Gorenstein,[1] Mark Ritchie,[2] James Langridge[3]
[1] Waters Corporation, Milford, MA, USA
[2] Waters Pacific, Singapore
[3] Waters Corporation, Manchester, UK

APPLICATION BENEFITS

Combining HILIC-UPLC® liquid phase separation with gas phase ion mobility mass spectrometry to achieve a multi-dimensional characterization of lipids in complex mixtures enhances profiling of lipids in biological samples.

WATERS SOLUTIONS

Omics Research Platform
with TransOmics™ Informatics

ACQUITY UPLC® System

SYNAPT® G2-S HDMS

KEY WORDS

Lipids, lipidome, metabolomics, lipidomics, ion mobility spectrometry, Hydrophilic interaction chromatography (HILIC), HDMS Compare, T-Wave™ Technology

INTRODUCTION

One of the main challenges for a global lipid analysis (lipidomics) is the separation of the wide array of lipid species present in biological samples (Figure 1). Such a separation is not achievable using a single chromatographic dimension such as reversed- or normal-phase separation methods.[1-5] Normal-phase UPLC separates lipid classes based on their polar head group, whereas reversed-phase separates lipids according to their acyl chain length and number of double bonds.[1-6] Hydrophilic interaction chromatography (HILIC) separation has been proposed as an alternative to normal-phase separation, offering better MS compatibility and using less toxic solvents.[4-6] Recently, a two-dimensional separation using HILIC and reversed-phase has been proposed to maximize the separation of the lipidome before MS detection.[5,6]

In addition to chromatography, ion mobility can be used to separate lipid ions in the gas phase according to their size and molecular shape.[7,8] In this study, we apply the Waters® Omics Research Platform with TransOmics Informatics. A HILIC-UPLC separation with ion mobility-Tof MS (SYNAPT G2-S HDMS) enables a multi-dimensional separation of complex biological mixtures, enhancing the information obtained from profiling lipids. HDMS Compare Software and TransOmics Informatics facilitate the comparison of the biological samples.

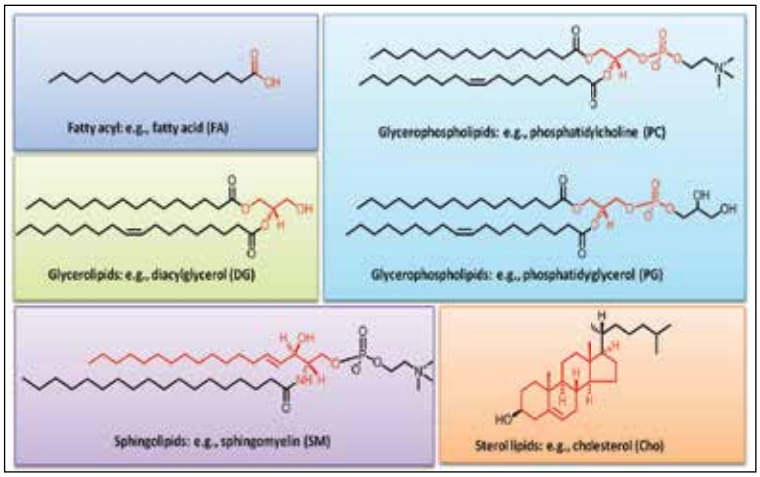

Figure 1. Lipid diversity. Lipids are divided into classes according to common structural moieties (in red), which may give rise to different chromatographic behaviors during HILIC.

EXPERIMENTAL

Sample description

Lipid standards and total lipid extracts from bovine brain, heart, and liver were purchased from Avanti Polar Lipids. Non-natural lipids were spiked in the biological extracts and used as internal standards (Table 2).

UPLC conditions

System:	ACQUITY UPLC
Column:	ACQUITY UPLC BEH HILIC 2.1 x 100 mm
Column temp.:	30 °C
Mobile phase A:	10 mM ammonium acetate (pH 8.0) in 95% ACN
Mobile phase B:	10 mM ammonium acetate (pH 8.0) in 50% ACN

Gradient:

Time/min	%A	%B
0.00	99.9	0.1
10.00	80.0	20.0
13.00	20.0	80.0
13.01	99.9	0.1
16.00	99.9	0.1

Flow rate:	0.5 mL/min
Injection volume:	5 µL

MS conditions

MS analyses were performed on a SYNAPT G2-S HDMS (Figure 2) with a conventional ESI source in LC/HDMS^E mode. Capillary voltages were optimized separately for positive (2.8 kV) and negative (1.9 kV) ion modes. Data were collected in two channels all of the time; low collision energy (6.0 V) for the molecular ions and high collision energy (20 to 35 V) for product ions. IMS gas: nitrogen; IMS T-Wave velocity: 900 m/s; IMS T-Wave height: 40 V.

Data acquisition and processing

TransOmics Informatics and HDMS Compare Software

RESULTS AND DISCUSSION

To separate lipids, we used hydrophilic interaction chromatography (HILIC) with an ACQUITY UPLC BEH HILIC 2.1 x 100 mm, 1.7 µm Column, and a reversed-phase solvent system (organic/aqueous) characterized by high organic mobile phase (>80% acetonitrile). This UPLC method was highly compatible with ESI, and separated lipids by classes, according to their polar properties (Figure 3 and Table 1).

In addition to HILIC chromatography, the ion mobility capability of the SYNAPT G2-S HDMS Mass Spectrometer (Figures 2A-C and 3) was used to further discriminate lipid classes into their constituent components, based upon the different size and shape, that is, the ions collision cross section (Ω).[7,8] Lipid ions with different degrees of unsaturation and acyl length migrate with characteristic mobility times, due to their unique shape in the gas phase as they migrate through the ion mobility cell, which is filled with nitrogen gas at relatively high pressure (Figures 3 and 5). Ion mobility separations occur in the millisecond timeframe, making it ideal for situating between LC and MS, where LC separations upstream typically work in the second timeframe and Tof MS downstream works in the nanosecond timeframe (Figures 2A and 3). The addition of ion mobility to the LC/MS provides enhanced peak capacity and improved signal-to-noise ratio (Figure 3).

To gain more structural information, we analyzed lipids employing LC/MS^E, which uses an alternating low and elevated collision energy in separate scans to acquire both precursor and product ion information in a single analytical run (Figures 2B and 4A). Ion mobility separation coupled with LC/MS^E (HDMS^E) improves the specificity for coeluting lipids by fragmenting ions after IMS separation (Figures 2C and 4B). Due to the complexity of the lipidome, the addition of ion mobility drift time as an orthogonal measurement to retention times provides complementary information regarding the lipid species, adding further specificity to lipid identification and data interpretation (Figure 4B).

Using this novel technological approach, multidimensional molecular maps of lipids present in various animal tissues were generated. In these maps, each lipid is characterized by a combination of molecular coordinates including retention time, drift time, exact mass, fragment ions, and intensity (Figure 5). Such features highlighted the capacity of ion mobility to separate isobaric lipid species (i.e., species with the same mass). The molecular landscape visualized using multidimensional molecular maps also allows the detection of lipid species that could otherwise go unnoticed (Figures 3 and 5).

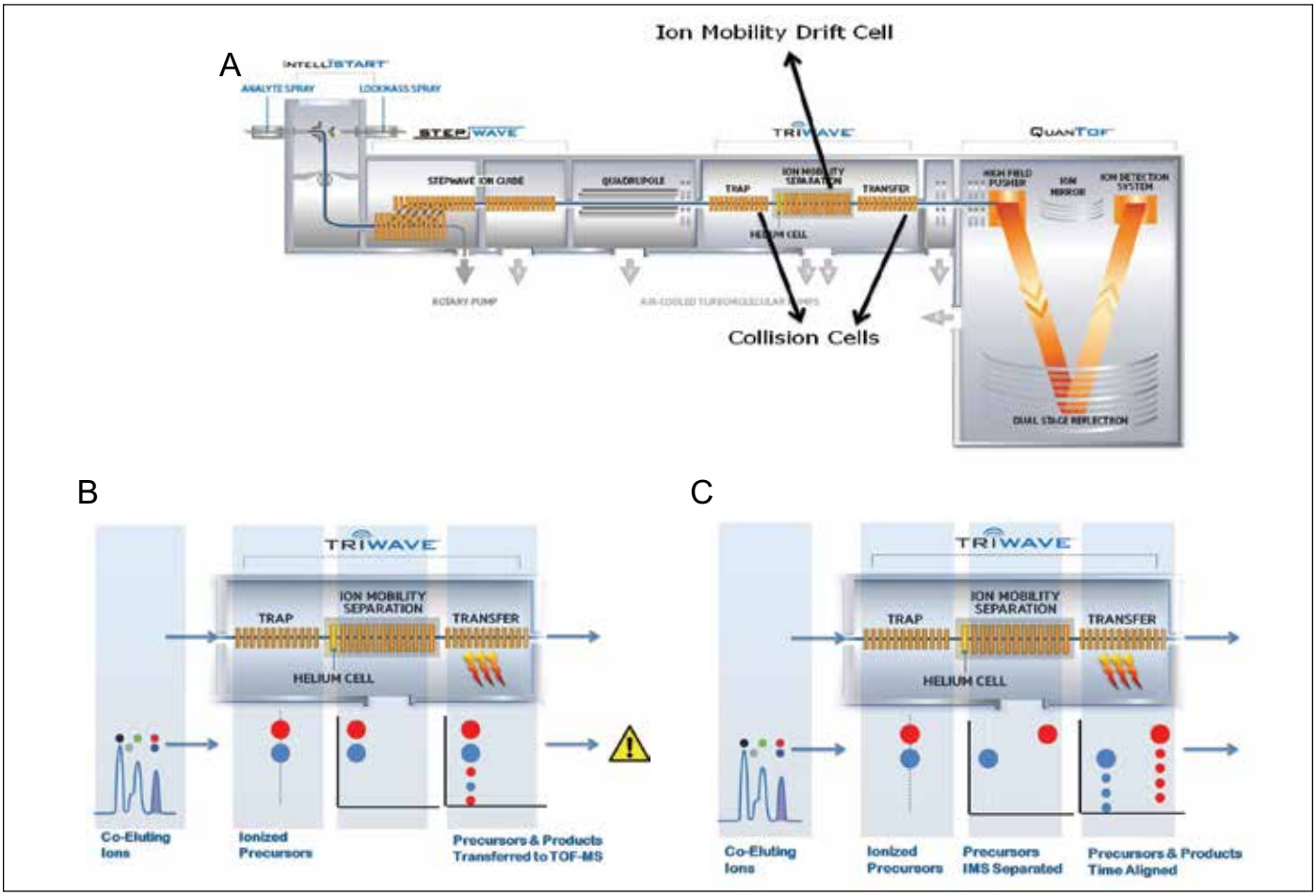

Figure 2. Ion mobility separation and fragmentation. A) Schematic of the SYNAPT G2-S HDMS System. B) MS^E can be extremely useful by itself, however when we consider a complex mixture of metabolites present in biological samples, they often co-elute. By fragmenting them, we only obtain a mixture of fragments which derive from various co-eluting precursors in this example. C) Ions can be separated in the ion mobility cell and subsequently fragmented in the transfer collision cell. The product ions generated in the collision cell have the same mobility drift time as their parent ions. Using this acquisition condition namely high-definition MS^E (HDMS^E), product ions can be aligned with their parent ions on the basis of mobility drift time as well as chromatographic retention time using the Waters® proprietary Apex4D algorithm.

Lipid class	ES polarity	RT window
FA	Neg	0-1
Cer	Pos	0-2
HexCer	Neg	0-2
ST	Neg	0-2
DiHexCer	Neg	2-4
PG	Neg	1-3
PE	Neg/Pos	5-7
PI	Neg	3-5
PS	Neg	4-6
PC	Pos	5-7
LPE	Neg/Pos	6-8
SM	Pos	7-9
LPC	Pos	8-10

Abbreviations: FA, fatty acids; Cer, ceramides; HeXCer, HexosylCeramides; ST, sulfatides; DiHexCer, DihexosylCeramides; PG, phosphatidylglycerols; PE, phosphatidylethanolamines; PI, phosphatidylinositols; PS, phosphatidylserines; PC, phosphatidylcholines; LPE, lysophosphatidylethanolamines; SM, sphingomyelins; LPC, lysophosphatidylcholines.

Table 1. Lipid classes are separated by retention time (RT) windows in HILIC conditions.

The comparison of molecular maps is facilitated by the use of HDMS Compare and TransOmics (Figures 6 and 7). HDMS Compare Software was used for a rapid comparison of different drift versus *m/z* plots at selected windows of retention times (Table 1). The drift time and spectral information associated with the components responsible for the differentiation can be extracted from the dataset and further analyzed (Figure 6). The use of TransOmics Informatics allows feature detection, alignment, and comparions across multiple samples using multivariate statistical approaches (PCA, dendrogram analysis) and database searching of discriminating features for the identification of the lipids alternating between samples. TransOmics uses ion mobility information to separate co-eluting isobaric lipids in the drift time dimension, increasing the specificity of identification and quantification (Figure 7). Lipid quantification was performed using appropriate internal standards for each lipid class (Table 2).

Lipid class	Internal standard	Abbreviation	Vendor	Catalog #
Sphigolipids				
Ceramides	N-Lauroyl-D-erythro-sphingosine	Cer(d18:1/12:0)	Avanti Polar Lipids	860512P
Sphingomyelin	N-(dodecanoyl)-sphing-4-enine-1-phosphocholine	SM (d18:1/12:0)	Avanti Polar Lipids	860583P
Glycerophospholipids				
Phosphatidylethanolamines	1,2- Dimyristoyl-sn-glycero-3-phosphoethanolamine	PE (14:0-14:0)	Avanti Polar Lipids	850745
	Avanti Polar Lipids			
Phosphatidylcholines	1,2- Dimyristoyl-sn-glycero-3-phosphocholine	PC (14:0/14:0)	Avanti Polar Lipids	850345
	Avanti Polar Lipids			
Phosphatidylserine	1,2- Dimyristoyl-sn-glycero-3-phosphoserine	PS (14:0/14:0)	Avanti Polar Lipids	840033
	Avanti Polar Lipids			
Phosphatidylglycerol	1,2- Dimyristoyl-sn-glycero-3-phosphoglycerol	PG (14:0/14:0)	Avanti Polar Lipids	840445
	Avanti Polar Lipids			
Phosphatidylinositol	1,2-DiHexanoyl-sn-glycero-3-phospho-(1'-myo-inositol)	16:0 PI	Avanti Polar Lipids	850141
	Avanti Polar Lipids			
Lysophosphatidylcholine	1-Heptadecenoyl-2-hydroxy-sn-glycero-3-phosphocholine	LPC (17:1)	Avanti Polar Lipids	LM-1601
Fatty acyl				
Fatty acids	10-heptadecenoic acid	FA (17:1)	Nu-Chek Prep	U-42-A

Table 2. List of lipids used as internal standards for selected lipid classes.

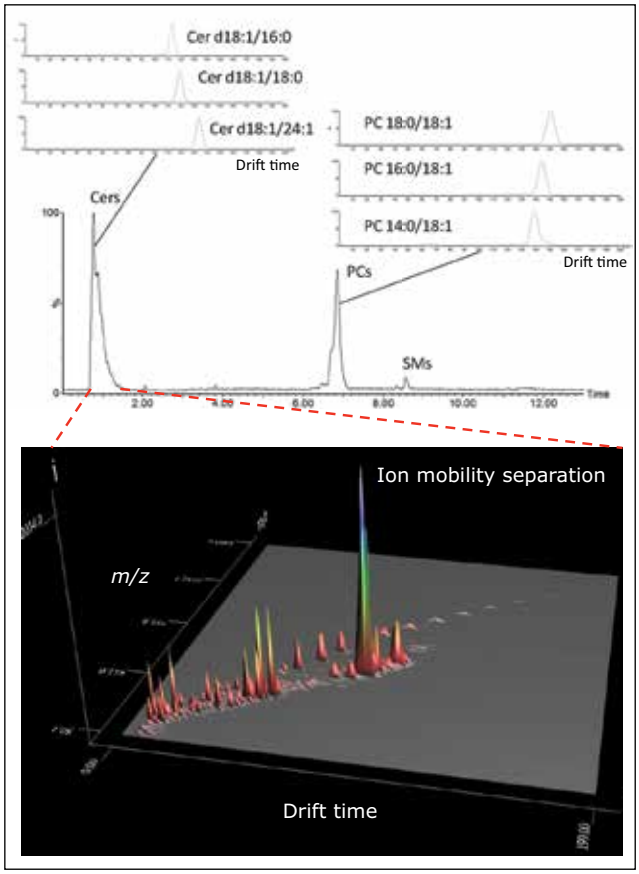

Figure 3. 2D separation by HILIC-ion mobility. Representative analysis of lipid standards using a combination of HILIC separation and ion mobility (IM) separation (inserts) in positive ion mode. HILIC-IM analysis provides an additional degree of separation beyond chromatography, which is ideal for the analysis of complex lipid mixtures extracted from biological samples. After HILIC separation, ion mobility further separates ceramide species according to their molecular shapes. The molecular landscape visualized using an unbiased 3D representation (drift time, m/z, intensity) of a selected interval of retention time (0.5 to 1.5 minutes) allows the detection of many isobaric ceramide species. Such an approach highlights the power of ion mobility for the discovery of many low abundance molecular species that could otherwise be undetected.

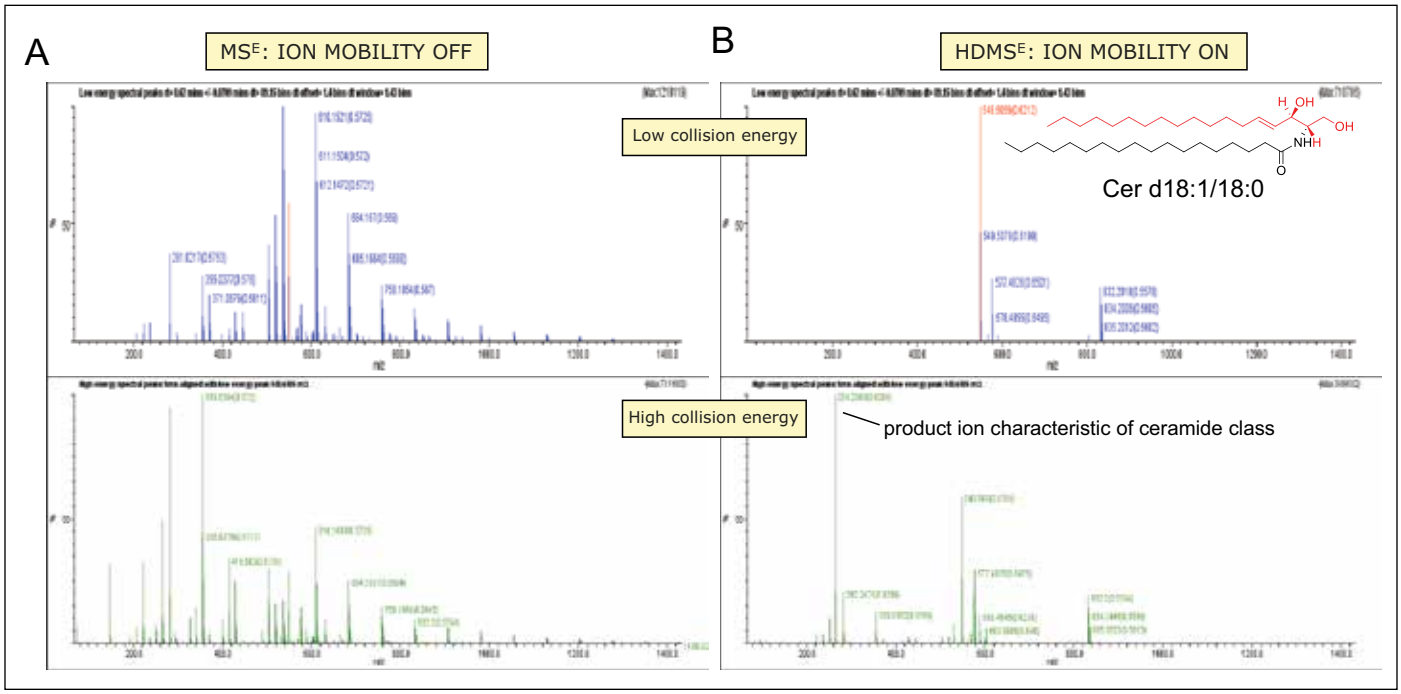

Figure 4. Structural characterization of lipid classes. Lipid classes generate characteristic fragments (product ions) upon collision-induced dissociation (CID). In positive ionization mode, ceramides are usually detected as dehydrated molecular ions using low collision energy; however, high collision energy generates all ceramide species with a common characteristic product ion. A) Waters instruments enable alternating low and high collision energy (MS^E), allowing to acquire precursor and product ion information in a single chromatographic run. The presence of co-eluting lipids, however, makes the interpretation of the high collision energy spectra difficult. B) By applying ion mobility separation, co-eluting lipids are separated based on their molecular size and shape before fragmentation in the transfer cell. This mode of acquisition ($HDMS^E$) results in cleaner fragmentation spectra and a more confident identification of lipid classes.

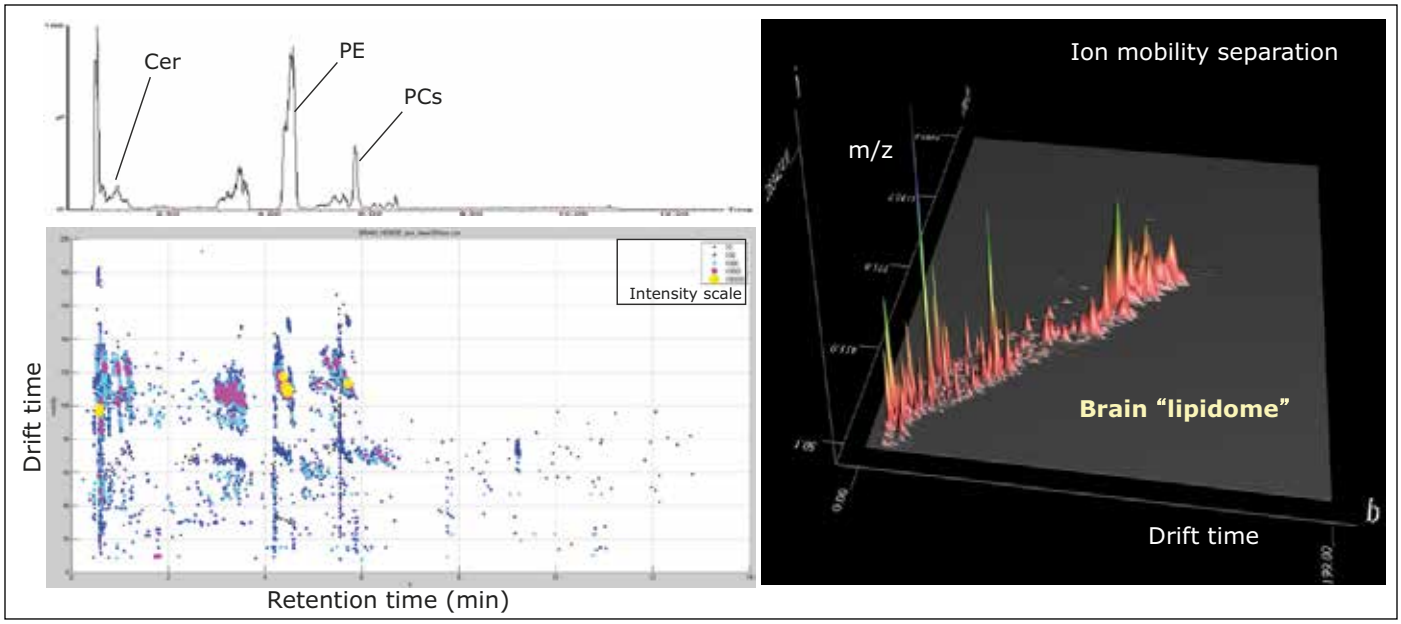

Figure 5. Mapping the brain lipidome using HILIC-ion mobility. Representative HILIC-ion mobility Tof analysis of total lipid extract from bovine brain. Lipids are separated by both retention time and mobility time (drift time). A multi-dimensional molecular map could be generated using unique coordinates such as retention times, mobility times, accurate masses, and intensities.

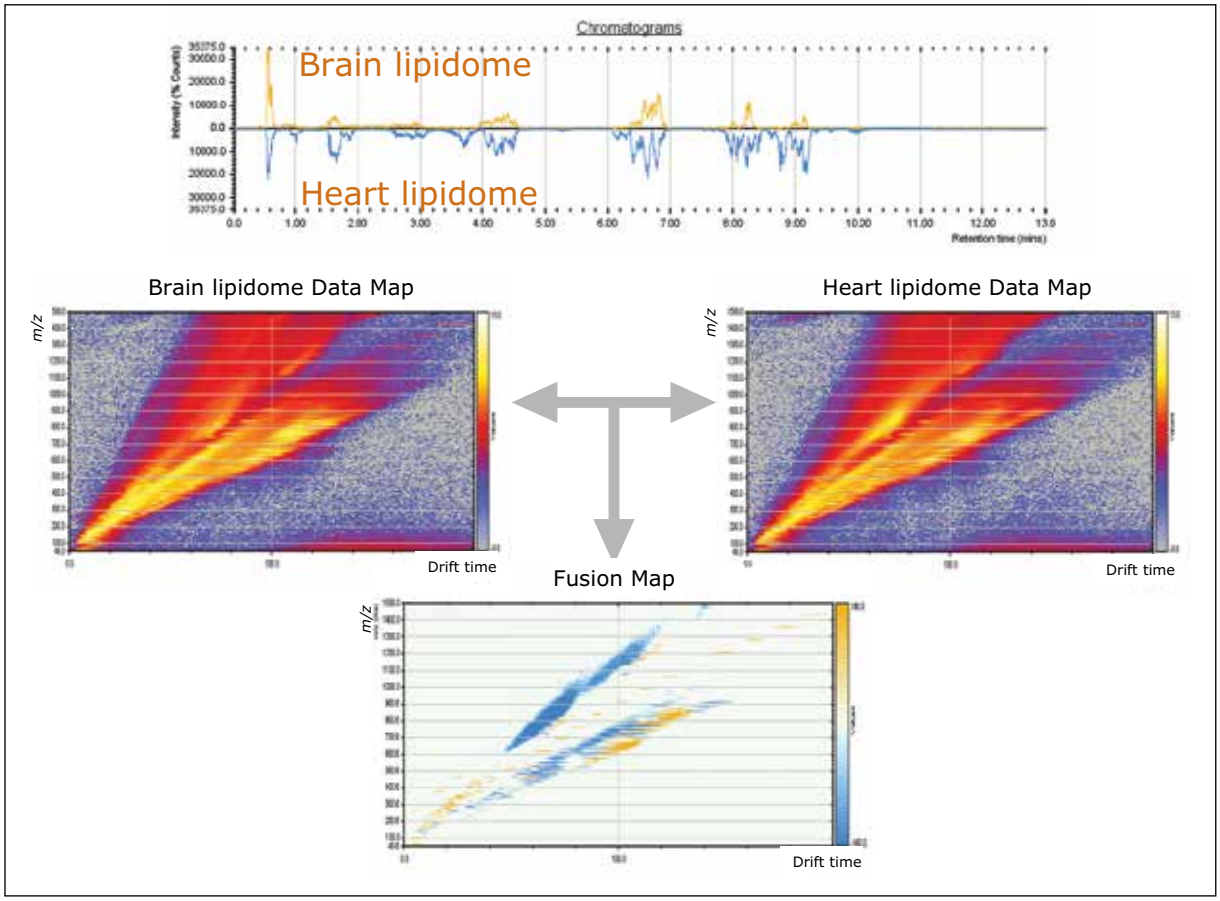

Figure 6. HDMS Compare Software for the comparison of lipid extracted from brain and heart tissues. HDMS Compare Software was used to overlay tissue-specific molecular maps. Key areas of significant differences between two samples were clearly visualized and identified with two different colors. Retention times, drift time, and mass information can be used for database searches and further identification of such molecular differences.

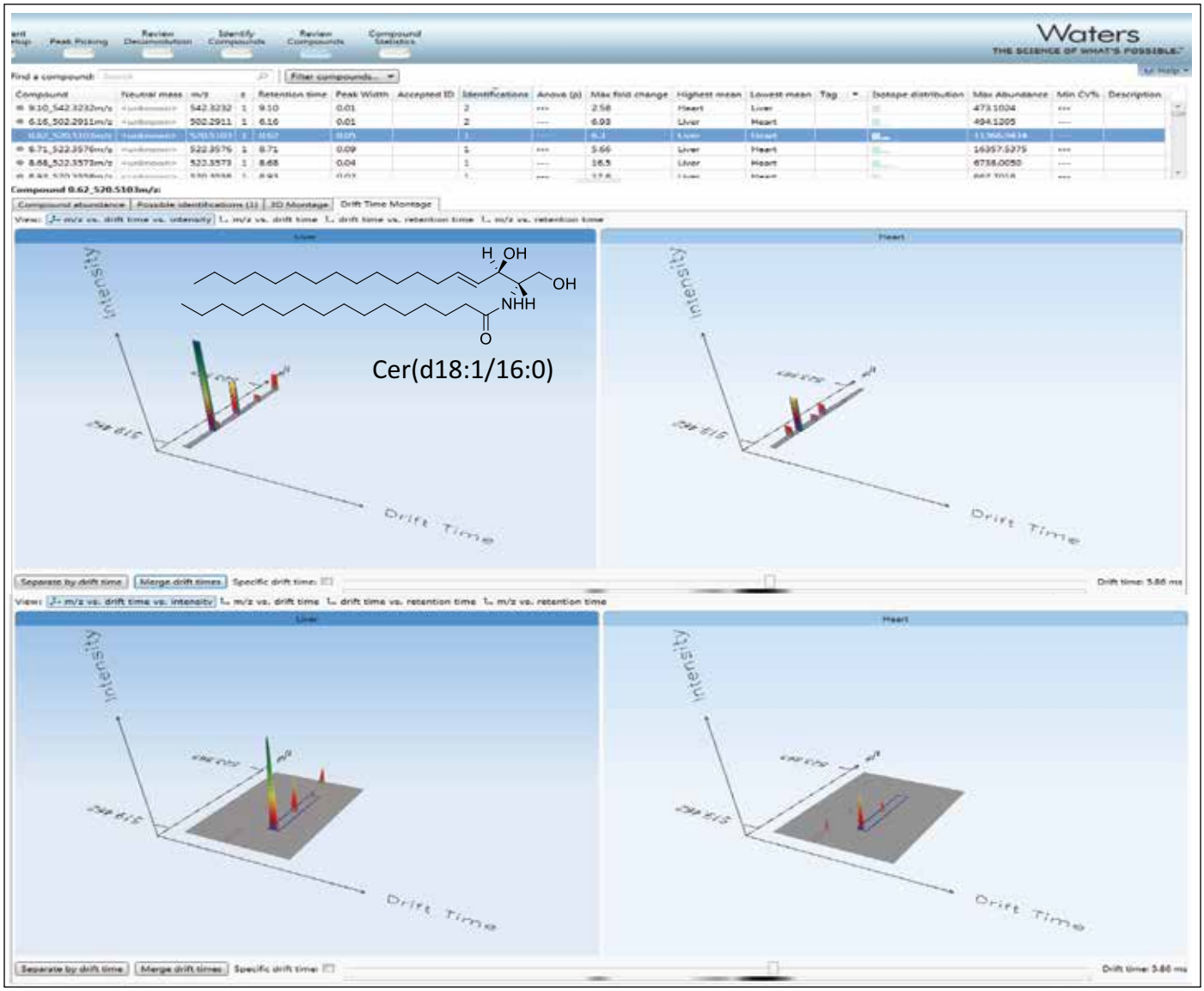

Figure 7. TransOmics for the comparison of lipid extracted from heart and liver tissues. TransOmics uses ion mobility information to separate co-eluting isobaric lipids in the drift time dimension, increasing the specificity of identification and quantification.

CONCLUSIONS

The combination of liquid chromatography, ion mobility, and oa-Tof mass spectrometry is a multidimensional separation strategy capable of analyzing complex biological mixtures to a depth not previously possible, enhancing the detail obtained from lipidomic profiling.

- HILIC separates lipid classes according to their polarity, providing stable retention time coordinates.
- Ion mobility separates lipids according to their difference in size and molecular shapes, providing Ω values (drift time coordinates).
- LC/MS^E coupled with ion mobility separation (HDMS^E) allows the simultaneous collection of exact mass precursor and fragment ion information, providing structural information and improving the experimental specificity.
- HILIC coupled with LC/HDMS^E generates molecular maps with unique coordinates, including retention times, drift times, accurate precursor and fragment ion masses, as well as intensities.
- HDMS Compare and TransOmics provide informatics solutions to compare large numbers of molecular maps in a scalable fashion using multi-variate statistical approaches, adding further specificity and confidence to lipid identification and biological interpretation.

References

1. Rainville PD, Stumpf CL, Shockcor JP, Plumb RS, Nicholson JK. Novel Application of Reversed-Phase UPLC-oaTOF-MS for Lipid Analysis in Complex Biological Mixtures: A New Tool for Lipidomics. *J Proteome Res.* 2007 Feb; 6(2):552-8.
2. Lísa M, Cífková E, Holčapek M. Lipidomic profiling of biological tissues using off-line two-dimensional high-performance liquid chromatography-mass spectrometry. *J Chromatogr A.* 2011 Aug 5; 1218(31):5146-56. Epub 2011 May 30.
3. Isaac G, McDonald S, Astarita G. Lipid Separation: UPLC System for the Separation of Complex Biological Total Lipid Extracts. Waters Application Note 720004107en. 2011 Sept.
4. Netto J, Wong S, Ritchie M, Torta F, Narayanaswamy P. A Definitive Lipidomics Workflow for Human Plasma Utilizing Off-line Enrichment and Class Specific Separation of Phospholipids. Waters Application Note 720004521en. 2012 Dec.
5. Nie H, Liu R, Yang Y, Bai Y, Guan Y, Qian D, Wang T, Liu H. Lipid profiling of rat peritoneal surface layers by online normal- and reversed-phase 2D LC QToF-MS. *J Lipid Res.* 2010 Sep; 51(9):2833-44.
6. Netto JD, Wong S, Ritchie M. High Resolution Separation of Phospholipids Using a Novel Orthogonal Two-Dimensional UPLC/QTof MS System Configuration. Waters Application Note 720004546en. 2013 Jan.
7. Shvartsburg AA, Isaac G, Leveque N, Smith RD, Metz TO. Separation and classification of lipids using differential ion mobility spectrometry. *J Am Soc Mass Spectrom.* 2011 Jul;22(7):1146-55. Epub 2011 Apr 12. Erratum in: *J Am Soc Mass Spectrom.* 2011 Jul; 22(7):1156.
8. Kliman M, May JC, McLean JA. Lipid analysis and lipidomics by structurally selective ion mobility-mass spectrometry. *Biochim Biophys Acta.* 2011 Nov; 1811(11):935-45.

Waters

THE SCIENCE OF WHAT'S POSSIBLE.®

Waters Corporation
34 Maple Street
Milford, MA 01757 U.S.A.
T: 1 508 478 2000
F: 1 508 872 1990
www.waters.com

Waters
THE SCIENCE OF WHAT'S POSSIBLE.®

Lipid Class Separation Using UPC²/MS

Michael D. Jones,[1,3] Giorgis Isaac,[1] Giuseppe Astarita,[1] Andrew Aubin,[1] John Shockcor,[1] Vladimir Shulaev,[2]
Cristina Legido-Quigley,[3] and Norman Smith[3]
[1]Waters Corporation, Milford, MA, USA
[2]Department of Biological Sciences, Center for Plant Lipid Research, University of North Texas, Denton, Texas, USA
[3]Pharmaceutical Science Division, School of Biomedical and Health Sciences, King's College, London, UK

APPLICATION BENEFITS

- Provides ACQUITY UPC²™ methodology conditions for comprehensive lipid intra- and inter-class analysis
- Highlights the method parameters that aid as method development tools for comprehensive lipid profiling
- Provides a single separation technique and a single instrumentation approach for rapid lipids analyses

WATERS SOLUTIONS

ACQUITY UPC² System with MS detection

Empower 3® Software

ACQUITY UPC² columns

KEY WORDS

UPC², MS, UPC²/MS^E, lipidomics, metabolomics, method development, convergence chromatography

INTRODUCTION

The analysis of complex lipids has historically been a challenging task and may require a variety of analytical techniques. Lipids are generally recognized as hydrophobic compounds, but the properties of complex lipids containing phosphorus, sulfur, sugar, and nitrogen have a wide polarity range. Developing separation-based methodology utilizing a single technique is recognized as a common challenge for scientists researching lipidomic and metabolomic applications.

Recent advances in technology have revived the exploration of supercritical fluid chromatography (SFC) as a viable analytical technique. Research and development focused on improvements of SFC instrumentation has provided a holistically designed chromatographic system that utilizes liquid CO_2 as a mobile phase to leverage the chromatographic principles and selectivity of normal phase chromatography while providing the ease-of-use of reversed phase LC (RPLC). This new separation technique is referred to as UltraPerformance Convergence Chromatography™ (UPC²™).

In this application note, UPC² technology is implemented for the analysis of lipid class separation. Method variables influencing the peak integrity and chromatographic separation for a mixture of lipids with different degrees of polarity are explored. The experiments were designed to understand the chromatographic behavior of lipids in a controlled setting using a variety of lipid extracts. Acyl chain length and a number of double bond influences were investigated using single moiety standards. The methodology parameters were tested using lipid extracts composed of intra-class components. The method conditions are applied to biological lipid extracts, whereas method adjustments are investigated to manipulate the chromatography based on the goal of the analyst. Insights from these method variable manipulations help to scope the development of targeted lipid profiling and screening protocols.

EXPERIMENTAL

Lipid abbreviations

CER	Ceramides
SM	Sphingomyelin
PG	Phosphatidylglycerol
PE	Phosphatidylethanolamine
PC	Phosphatidylcholine
LPC	Lyso-Phosphatidylcholine
LPE	Lyso-Phosphatidylethanolamine

Sample description

Samples and standards were purchased from Avanti Polar Lipids. Mix 1 and Mix 2 were brain (porcine) extracts except LPC and PG which were egg (chicken) extracts. Stocks were prepared in 50:50 chloroform/methanol. Working lipid mixtures were prepared to the specified concentration.

Mix 1:	Ceramide, SM, (0.05 mg/mL) PG, PE, PC, (0.1 mg/mL)
Mix 2:	LPC, LPE, (0.05 mg/mL)
Mix 3:	1:1 of [mix 1] and [mix 2]

UPC^2 conditions

System:	ACQUITY UPC^2
Columns:	ACQUITY UPC^2 BEH and HSS C_{18} SB
Column temp.:	60 °C
Sample temp.:	10 °C
Injection volume:	1 µL
Flow rate:	1.85 mL/min
Back pressure:	1500 psi
Mobile phase A:	CO_2
Mobile phase B:	50:50 methanol/acetonitrile with 1 g/L ammonium formate
Gradient:	Refer to figures for detailed information

MS conditions

Mass spectrometers:	ACQUITY® SQD and SYNAPT® G2 MS
Ionization mode:	ESI positive
Acquisition range :	100 to 1500 Da
Capillary voltage :	3.5 kV
Cone voltage :	30 V
Informatics:	Empower 3 and MassLynx® Software

RESULTS AND DISCUSSION

MS optimization

The ACQUITY UPC^2 System was configured with an ACQUITY single quadrupole detector (SQD) for this preliminary investigation of chromatographic parameters. Injections of [Mix 3] were screened with different cone and capillary voltages to determine the best operating conditions. Based on the cone voltage screening results, 30 V was chosen for controlling overall in-source fragmentation of the optimal signal for the spectra of L-α-phosphatidylglycerol (egg PG) to provide precursor ion and valuable fragmentation information, as shown in Figure 1A. The optimal capillary voltage observed for all the peaks in the [Mix 3] was 3.5 to 4.0 kV, as shown in Figure 1B. The final MS conditions used 3.5 kV capillary voltage and 30 V cone voltage.

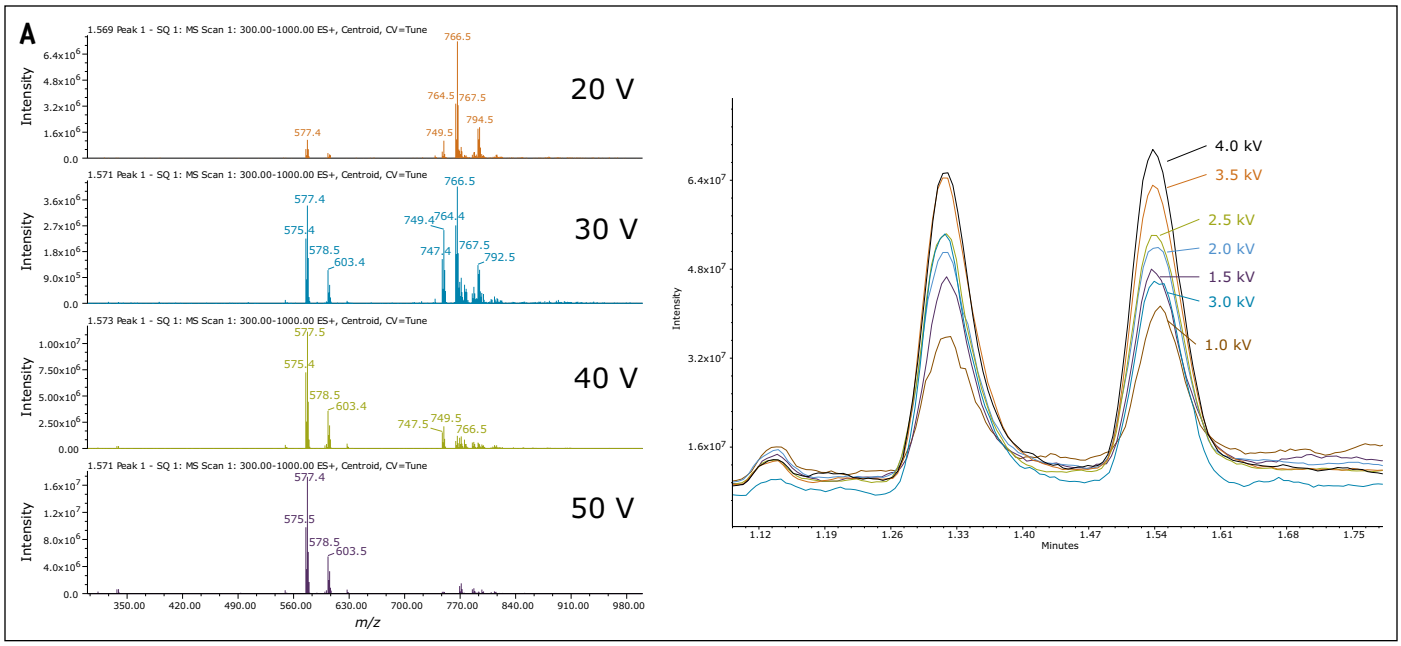

Figure 1. (A) Cone voltage screening results for L-α-phosphatidylglycerol; and (B) capillary voltage screening results for L-α-phosphatidylglycerol.

Chromatographic method development

The sample preparation workflow was very convenient for use with the ACQUITY UPC^2 System. The chloroform/methanol diluent provided good solubility without any noticeable adverse effects on peak shape. In a typical RPLC lipid analysis, the organic extract containing the lipids would have to be evaporated and re-constituted in a more compatible solvent. When using UPC^2, however, the organic extract containing the lipids can be directly injected onto the system, thereby saving time and costs when analyzing hundreds of biological samples. Screening different column stationary phases typically changes selectivity during method development. Therefore, our initial approach was to screen three stationary phases including UPC^2 CSH Flouro-Phenyl, UPC^2 BEH 2-EP, and UPC^2 BEH. Optimal peak shape and selectivity was achieved on the UPC^2 BEH stationary phase for the inter-class separation of the lipid mixture, as shown in Figure 2.

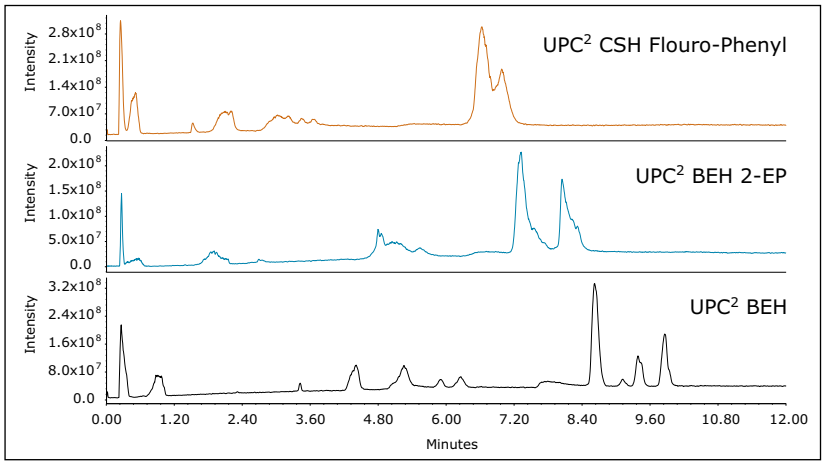

Figure 2. Column screening of the [metdev] mixture of neutral and polar lipids. A 12-minute 10% to 50% B screening method was used. Due to less retentivity of the BEH 2-EP and CSH Flouro-Phenyl columns, the gradients were modified (10% to 30% B) to adjust for comparative use of the separation space. The mobile phase co-solvent was 1 g/L ammonium formate in MeOH derived from previously published reports.[1]

Method development screening columns and modifier indicated the bridged ethylene hybrid (BEH) silica columns provided the best selectivity and peak shape. The lipid classes were identified by MS ESI+ utilizing the parameters determined by the MS optimization experiments. Injections of the individual lipid mixtures verified current peak assignments. The method used for screening the columns was optimized to focus on the inter-class separation of analytes in [Mix 3]. The previous 12-minute method was reduced and completed in 5 minutes, as shown in Figure 3.

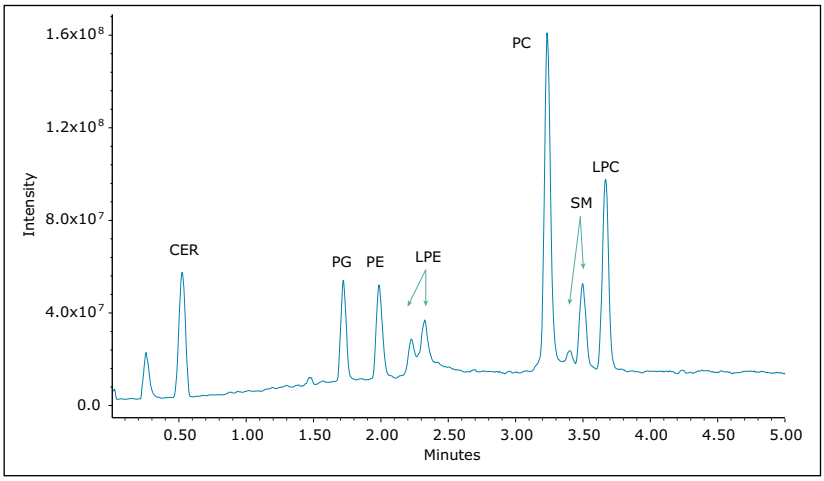

Figure 3. Injection of [Mix 3] mixture using the ACQUITY UPC^2 BEH column. The original gradient was 5% to 50% at 1.85 mL/min over 10 min with a 2 min hold at 50% B and 1-min re-equilibration at initial conditions before the next injection. The gradient was modified to 15% to 50% B at 1.85 mL/min over 3 min, held at 50% B for 2 min. The column was re-equilibrated at initial conditions before the next injection.

The lipid extracts purchased from Avanti provide documentation indicating various ratios of lipid intra-class constituents present within a respective standard extract. This was further confirmed when evaluating the mass spectral data for the two LPE peaks observed in chromatographic trace, as shown in Figure 4. It was found that the elution order of the molecular species within each lipid class depended on the number of double bonds on the acyl chain. Thus, the more saturated the acyl chain, the shorter the retention time. The acyl chain length has no effect on the elution order with each lipid class. Interestingly, the intra-class separation of LPE and SM standard extracts is observed when using the UPC^2 BEH stationary phase. The other stationary phases that provided broader peaks may offer a better intra-class separation of the Avanti extract standards. This hypothesis will be explored in future studies.

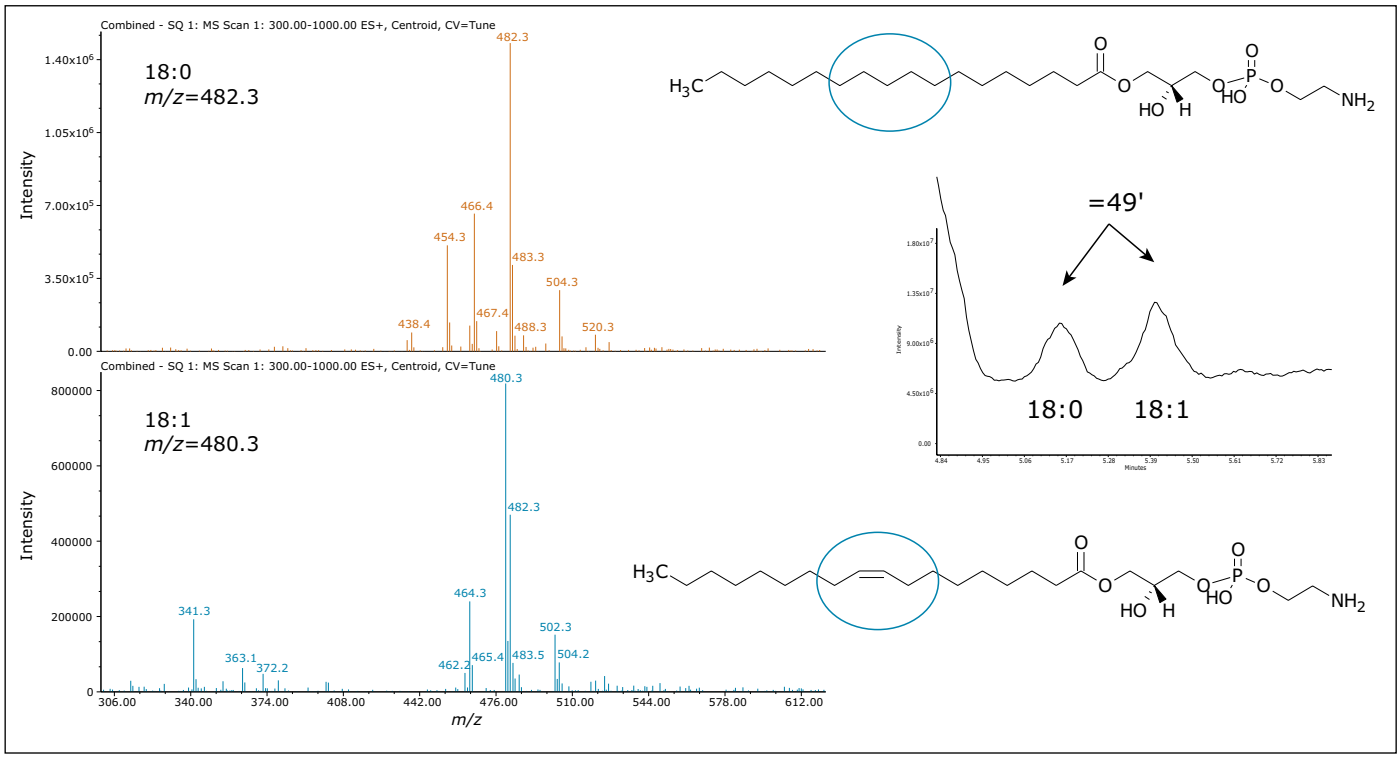

Figure 4. Interrogation of MS spectra for the two LPE peaks.

Manipulating retentivity

The method development process explored changes in gradient slope; however, changes in resolution were not significant. Experiments to manipulate retentivity were investigated. The variable which resulted in the greatest retentivity changes included the addition of a less polar solvent, such as acetonitrile, to the modifier. Two experiments were performed. The first was conducted with the original modifier composition of 100% methanol. The second experiment was conducted with modifier composition of 80% methanol and 20% acetonitrile. Both modifiers were doped with 1 g/L ammonium formate. In general, using acetonitrile in the modifier improved resolution, as shown in Table 1.

Peak ID	100% MeOH (RS)	80:20 MeOH:ACN (RS)	% Difference
PG	–	–	–
PE	2.69	3.54	+31.6
LPE 1	1.96	2.74	+39.8
LPE 2	1.67	2.17	+29.9
PC	10.81	8.56	-20.8
SM (1)	2.24	2.07	-7.6
SM (2)	1.10	1.06	+45.5
LPC	1.33	1.05	+12.8

Table 1. Impact of modifier composition on lipid resolution. Ceramide was excluded due to the large amount of resolution from the other peaks of interest.

Analysis of biological samples

The methodology was used to investigate two biological samples, each for distinctly different purposes. The first example examines a mouse heart extract using the six-minute method for the rapid inter-class targeted screening of lipids with different polarity. The objective was to determine if the methodology could detect the presence of specific lipids within the hundreds of samples collected from the diabetic treatment study. This proof of concept approach will be used for further studies utilizing MS/MS quantification assessing increases of phospholipids and sphingolipids during treatment. As seen in Figure 5, many of the phospholipids and sphingolipids were easily identified in the mouse heart extract by using this targeted UPC^2/MS method.

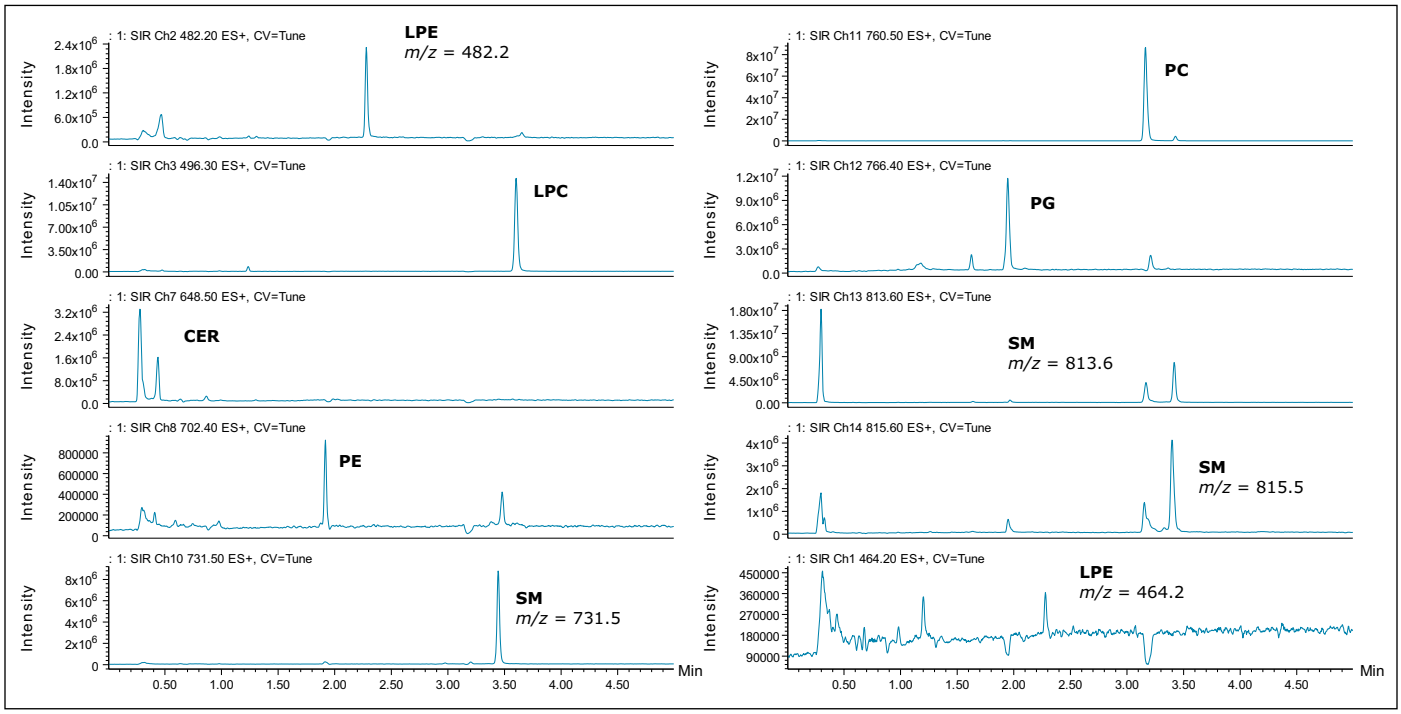

Figure 5. Targeted SIR analysis of a mouse heart extract. The gradient was 15% to 50% B at 1.85 mL/min over 3 min, held at 50% B for 2 min. The column was re-equilibrated at initial conditions for 1 min before the next injection.

Neutral lipids, such as acylglyceride and cholesterol esters, are characteristically non-polar. Typically, plant metabolomic profiling distinguishes heterogeneous distribution of neutral lipids, such as triacylglycerols and diacylgylcerols[2] at different conditions. The example in Figure 6 investigates lipids present in a cotton seed oil extract. The data was collected using MS^E on a SYNAPT G2 Mass Spectrometer allowing for the characterization of the neutral lipids by precursor and product ion alignment. During the method development process, many neutral lipids eluted near the chromatographic void when starting the compositional gradient above 5% modifier using methanol (or methanol/acetonitrile). In this example, the UPC[2]/MS method was modified to retain the neutral lipids by reducing the starting percentage of modifier. The modifier was ramped to elute the polar lipids, known to be present as membrane lipid classes in cotton embryos.[2] By using this approach, the chromatography can be altered to provide greater retention, and often greater specificity for the neutral lipids. From an analytical technique perspective, the elution mechanisms are conceptually similar to performing a mobile phase gradient elution profile by liquid chromatography.

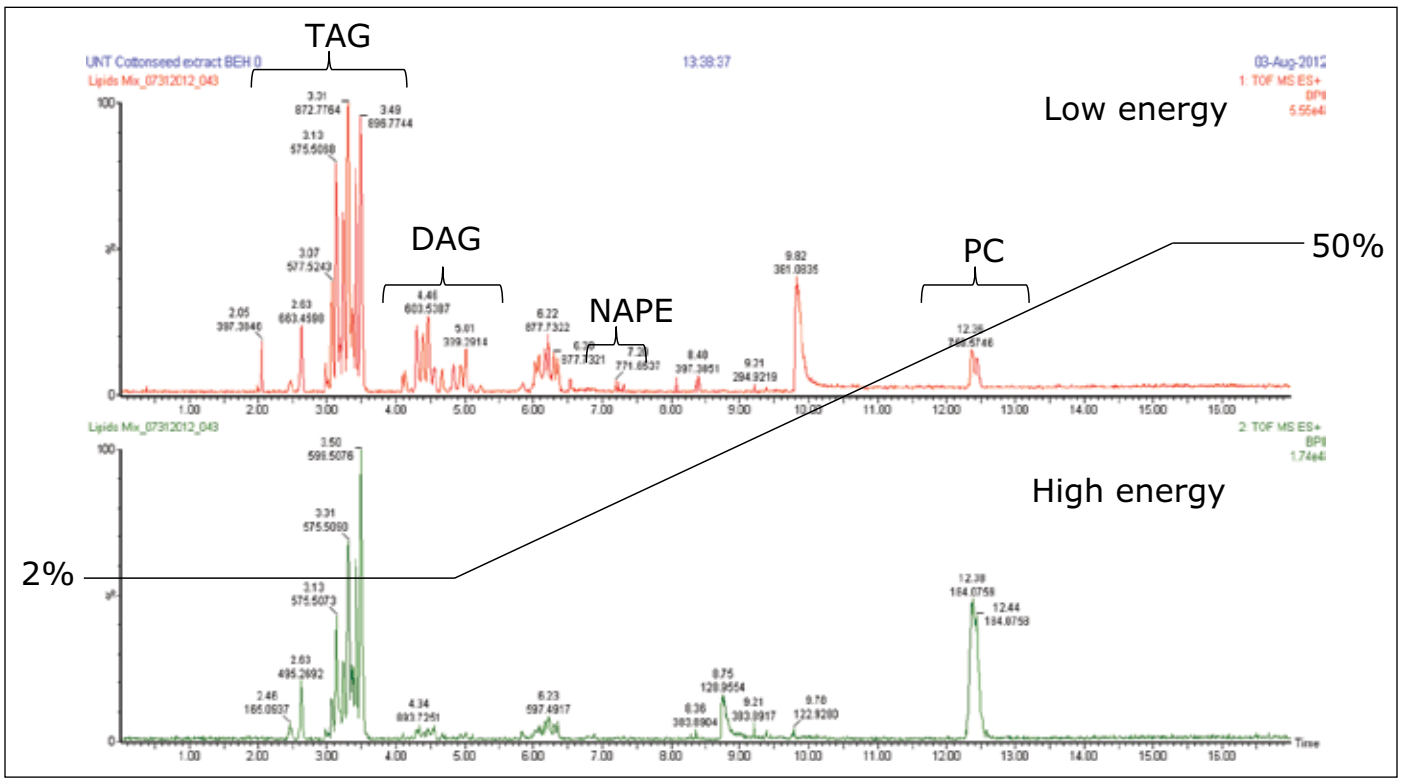

Figure 6. Comprehensive profiling of a cotton seed oil extract. The gradient was 2% to 5% B over 5 min, increased to 50% B over 10 min, and held at 50% B for 2 min using a flow rate of 1.85 mL/min. The column was re-equilibrated at initial conditions for 1 min before the next injection.

CONCLUSIONS

A flexible universal method was developed for the analysis of inter-class separations of neutral and amphipathetic lipids. Since the goal of the experiment was to achieve flexible parameters providing the separation of lipids by class, the core methodology using the ACQUITY UPC^2 BEH column, methanol/acetonitrile modifier with ammonium formate as an additive provided the best results. The gradient methodology and run time was adjustable to focus on rapid screening or comprehensive profiling of lipids in biological samples. The lipid sample preparation workflow is suitable for UPC^2. The organic phase of the biological lipid extract can be directly injected onto the ACQUITY UPC^2 System with MS detection, thereby saving time and operating costs.

The rapid inter-class screening provided an analysis within seven minutes including re-equilibration. The MS spectral information confirmed instances of intra-class separation by distinguishing between the degrees of saturation, as demonstrated for the Lyso- Phosphatidylethanolamine separation on the ACQUITY UPC^2 BEH column. Resolution can be increased within the chromatographic space by the addition of acetonitrile. For this methodology, an increase of 30% to 40% resolution can be observed between lipid classes for the majority of the analytes. The method development knowledge gained from these experiments build a foundation for the applicability of lipid analysis by convergence chromatography.

References

1. Bamba T, Shimonishi N, *et al.* High throughput and exhaustive analysis of diverse lipids by using supercritical fluid chromatography-mass spectrometry for metabolomics. *J Biosci Bioengin.* 2008 May; 105(5): 460-469.

2. Horn PJ, Korte AR, Neogi PB, *et al.* Spatial Mapping of Lipids at Cellular Resolution in Embryos of Cotton. *Plant Cell.* 2012 Feb; 24(2): 622-636.

Waters

THE SCIENCE OF WHAT'S POSSIBLE.®

Waters Corporation
34 Maple Street
Milford, MA 01757 U.S.A.
T: 1 508 478 2000
F: 1 508 872 1990
www.waters.com

Waters
THE SCIENCE OF WHAT'S POSSIBLE.®

A Facile Database Search Engine for Metabolite Identification and Biomarker Discovery in Metabolomics

Panagiotis Arapitsas,[1] James Langridge,[2] Fulvio Mattivi,[1] Giuseppe Astarita[2]
[1]Department of Food Quality and Nutrition, Research and Innovation Centre, Fondazione Edmund Mach, San Michele all'Adige, Italy
[2]Waters Corporation, Milford, MA, USA

APPLICATION BENEFITS

Progenesis™ QI Informatics simplifies the process of metabolite identification and biomarker discovery. Potential biomarkers can be searched in both publicly available and in-house databases for accurate mass, retention time, collision cross section, and fragmentation information. Such an approach is fast and it increases the confidence of metabolite identification in metabolomics experiments.

WATERS SOLUTIONS

SYNAPT HDMS® System

ACQUITY UPLC® System

Progenesis QI Informatics

KEY WORDS

Metabolomics, lipidomics, natural products, food, nutrition, wine

INTRODUCTION

Metabolomics experiments offer a promising strategy for biomarker discovery. In a metabolomics workflow, however, the major bottleneck still remains metabolite identification. Currently, there are four levels of annotation for metabolite identification: 1) Confidently identified compound (two orthogonal properties based in authentic chemical standard analysis under the same condition); 2) Putative identified compounds (one or two orthogonal properties based in public database); 3) Putative identified compound class; and 4) Unknown compound.[1] A typical database search that relies only on one property *(i.e.*, accurate mass) usually leads to an extensive number of false positive and negative identifications. To increase the confidence of identification, a search engine should be able to use of in-house databases containing orthogonal molecular descriptors for each metabolite.[2]

Progenesis QI Informatics is a novel software platform that is able to perform alignment, peak-picking, and mining of metabolomics data to quantify and then identify significant molecular alterations between groups of samples. The software uses a search engine (MetaScope) for metabolite identification, with user-definable search parameters to probe both in-house and publicly available databases. With an easy-to-use interface, the user can combine information for metabolite identification, including accurate mass, retention time, collision cross section, and theoretical and/or experimental fragment ions. These physiochemical properties can increase the confidence of metabolite identification while concurrently decreasing the number of false positives.

In this study, we show the Progenesis QI workflow for metabolite identification using, as an example, a study on the effect of different bottling conditions on the nutritional composition of Italian wines.

EXPERIMENTAL

UPLC conditions

System:	ACQUITY UPLC
Column:	ACQUITY UPLC HSS C_{18} SB 1.8 µm 2.1 x 150 mm (p/n 186004120)
Pre column:	ACQUITY UPLC HSS T3 VanGuard™ 1.8 µm, 2.1 x 5 mm (p/n 186003976)
Mobile phase A:	Water + 0.1% formic acid
Mobile phase B:	Methanol + 0.1% formic acid
Flow rate:	0.28 mL/min
Column temp.:	40 °C
Injection volume:	10.0 µL

Elution gradient:

Min	A%	B%	Curve
Initial	100.0	0.0	Initial
1.0	100.0	0.0	6.0
3.0	90.0	10.0	6.0
18.0	60.0	40.0	6.0
21.0	0.0	100.0	6.0
25.5	0.0	100.0	6.0
25.6	100.0	0.0	6.0
28.0	100.0	0.0	6.0

MS conditions

MS system:	SYNAPT HDMS
Mode of operation:	Tof MS^E
Ionization:	ESI +/-
Capillary voltage:	2.5 kV (+) and 2.5 kV (-)
Cone voltage:	25 V
Transfer CE:	Ramp 15 to 45 V
Source temp.:	150.0 °C
Desolvation gas flow:	1000 L/h
Desolvation temp.:	500.0 °C
Cone gas:	50 L/h
MS gas:	Nitrogen
Acquisition range:	50 to 1200

Data processing and mining:

Progenesis QI Informatics

Sample collection and preparation

Mezzacorona winery (Trentino, Italy) provided the wines, which were bottled in typical 750-mL wine bottles with the filling industrial machine of the winery. The sample set included two types of wines bottled with nitrogen addition (N_2) and without nitrogen addition (O_2). Under nitrogen atmosphere, every wine was uncorked, 2 mL were transferred into a 5-mL amber vial, 2 mL Milli-Q water was added, and finally each sample was filtrated with 0.2-µm PTFE filters into a 2-mL Waters LCMS Certified Amber Glass Vial prior to LC/MS analysis.[3]

RESULTS AND DISCUSSION

Wine is one of the most complex foods as far as its metabolomic profile is concerned, since grapes, yeasts, bacteria, fungi, exogenous antioxidants, fining agents, and other oenological materials, packaging, and aging are involved in its preparation. This great number of different primary and secondary metabolites, most of which are unknowns, highly affects wine quality and the important role it plays in human diet, health, and enjoyment. Different bottling and storage conditions may affect the molecular composition of wines, and thus value and quality.

In this study, we used Progenesis QI to identify the metabolites that were altered between wines bottled under two different levels of oxygen: high level (O_2) versus low level (N_2). Data were acquired in LC/MS^E mode (Figure 1A) and pre-processed using retention time alignment and peak picking (Figure 1B). A composite ion map was built, which contained more than 3,000 compounds after isotopic and adduct deconvolution (Figure 1B). Metabolites of interest were filtered according to the ANOVA P value <0.01 and fold change >2, which decreased the number of metabolites of interest (markers) to less than 200 (Figure 2A). This data reduction strategy allowed us to focus on the metabolites that clearly discriminate the two groups of samples as shown by principal component analysis (Figure 2B).

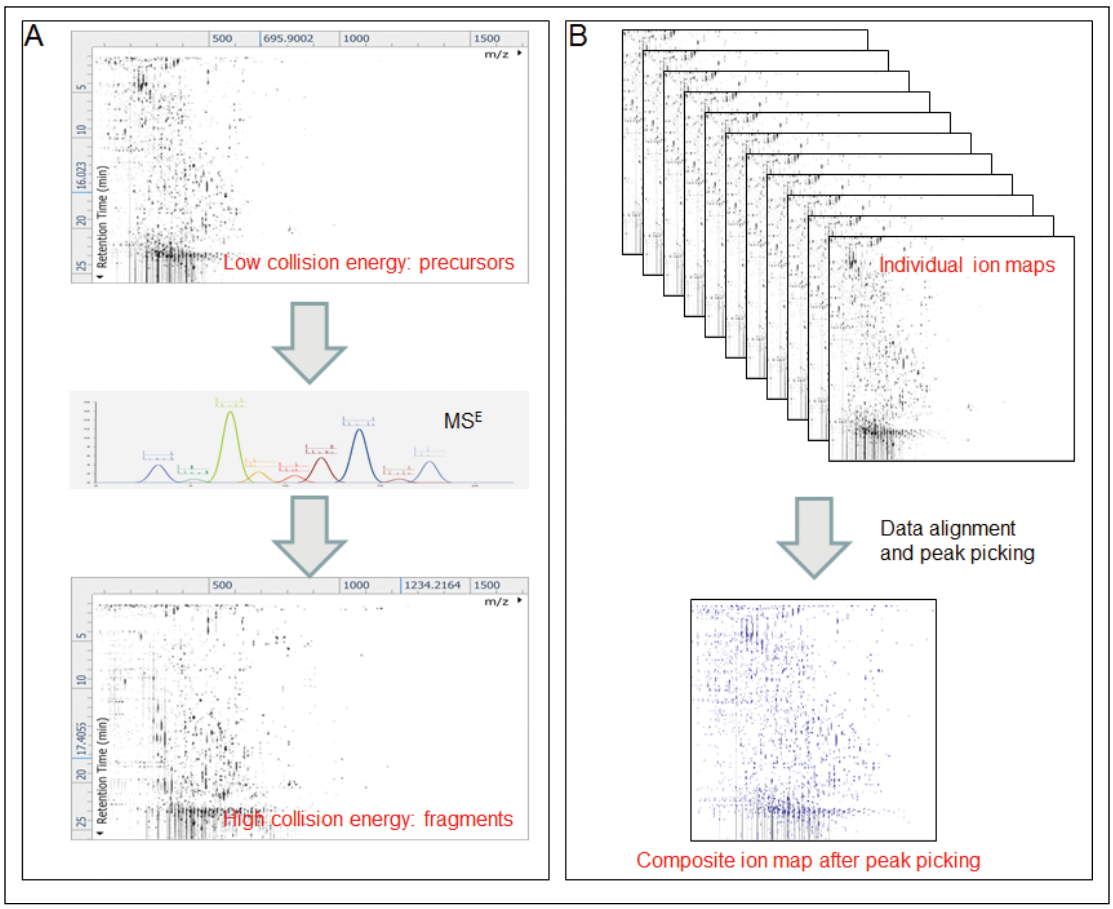

Figure 1. A: Samples were acquired using data independent analysis (MS^E), which provided information for both the intact precursor ions (at low collision energy, upper panel) and the fragment ions (high collision energy, bottom panel). B: From the aligned runs, Progenesis QI produces an aggregate run that is representative of the compounds in all samples, and uses this aggregate run for peak picking. The peak picking from this aggregate is then propagated to all runs, so that the same ions are detected in every run.

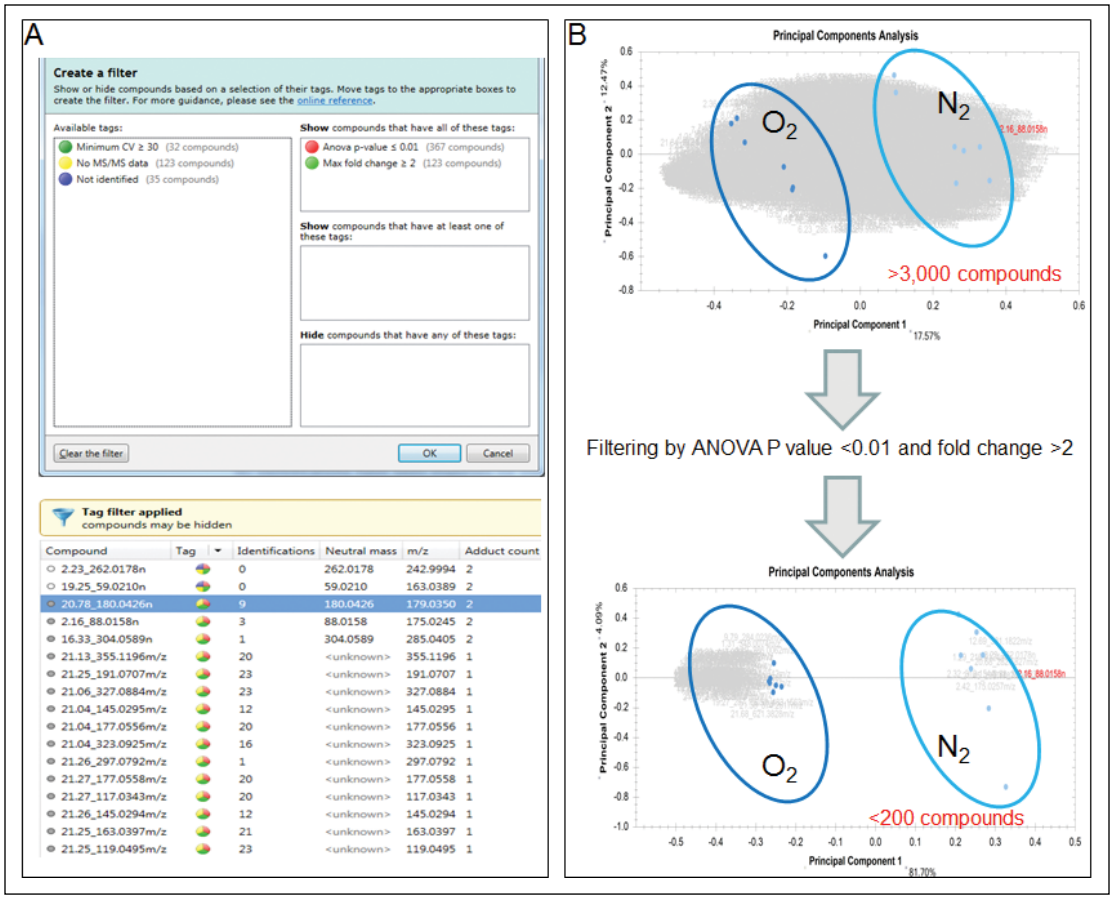

Figure 2. A: Progenesis QI allows tagging data according to various criteria, including ANOVA P values and fold changes. B: Principal component analysis (PCA) containing the entire dataset showed that the wines samples clustered according to the different amount of oxygen in which they were stored, suggesting that the two groups of wine contained a diverse set of metabolites (upper panel). After data reduction, PCA showed the discriminatory power of the selected compounds by filtering only those compounds that had ANOVA p values <0.01 and fold changes >2 (bottom panel).

Initial identification of metabolites was performed using the Human Metabolome Database (HMDB), leading to multiple ambiguous identifications for each compound of interest (Figure 3A and 3B). To decrease the number of false positives, we used in-house metabolite databases, which contain accurate mass, retention time, and fragment information.[2] (Figure 3A-C). We customized the search engine parameters for these orthogonal measures (Figure 3A), allowing a more balanced set of tolerance criteria, which significantly decreased the number of false positives and false negatives (Figure 3B). Experimental fragments were matched against those derived from theoretical fragmentation to further increase the confidence in metabolite identification (Figure 3C). The entire metabolomics workflow for data processing, mining, and identification was completed in just a few hours.

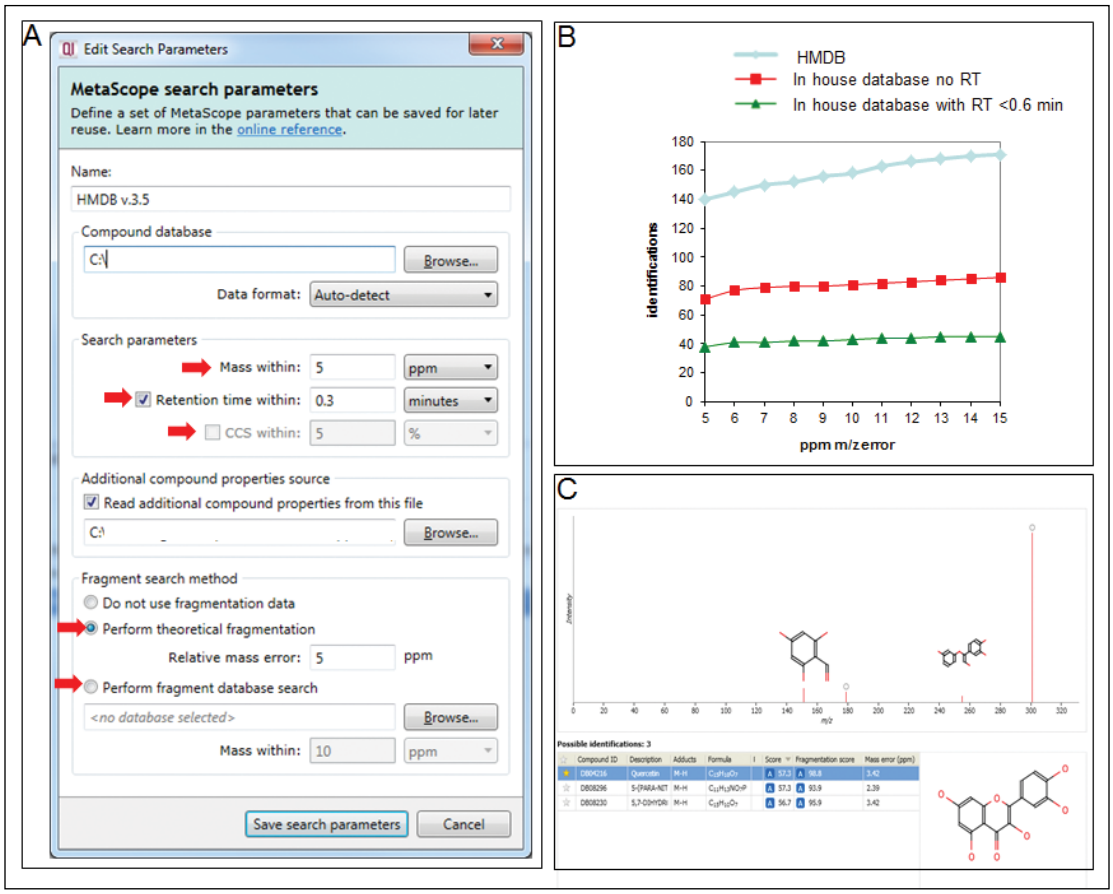

Figure 3. A: The Progenesis QI search engine allows users to query both publicly available databases (e.g., HMDB) and in-house databases, customizing the search parameters for the metabolite identification according to multiple orthogonal measures: mass accuracy, retention time, collision cross section and fragmentation matching. B: Metabolite identification using in-house database allows to filter the results by mass accuracy and retention time tolerance reducing significantly the number of false positives. C: Representative identification of the metabolite Quercetin using mass accuracy, retention time, isotopic distribution and four MS^E fragments, which were matched against theoretically-generated fragments.

CONCLUSIONS

Progenesis QI effectively streamlines and simplifies complicated metabolomics workflows and makes metabolite identification faster, easier, and more robust. User-definable search parameters dramatically decrease the number of false positive and false negative results in the identification workflow, improving the confidence of identification.

References

1. Dunn WB, Erban A, Weber RJM, Creek DJ, *et al.* Mass appeal: metabolite identification in mass spectrometry-focused untargeted metabolomics. *Metabolomics*. 2013 March; 9 (1 Supplement): 44-66. doi:10.1007/s11306-012-0434-4.
2. Shahaf N, Franceschi P, Arapitsas P, Rogachev I, Vrhovsek U, Wehrens R. Constructing a mass measurement error surface to improve automatic annotations in liquid chromatography/mass spectrometry based metabolomics. *Rapid Commun Mass Spectrom.* 2013 Nov 15;27(21):2425-31. doi: 10.1002/rcm.6705.
3. Arapitsas P, Speri G, Angeli A, Perenzoni D, Mattivi F. (2014). The influence of storage on the "chemical age" of red wine. *Metabolomics*. 2014 February; online. doi: 10.1007/s11306-014-0638-x.

Waters

THE SCIENCE OF WHAT'S POSSIBLE.®

Waters Corporation
34 Maple Street
Milford, MA 01757 U.S.A.
T: 1 508 478 2000
F: 1 508 872 1990
www.waters.com

Waters
THE SCIENCE OF WHAT'S POSSIBLE.®

Xevo G2-S QTof and TransOmics: A Multi-Omics System for the Differential LC/MS Analysis of Proteins, Metabolites, and Lipids

Ian Edwards, Jayne Kirk, and Joanne Williams
Waters Corporation, Manchester, UK

APPLICATION BENEFITS

- Simplified workflow, validation, and data interpretation
- Designed for large-scale metabolomics and proteomics data sets
- Integrated Omics platform for versatile and comprehensive qualitative and quantitative profiling
- Statistically validated results across Omics sample sets

WATERS SOLUTIONS

Omics Research Platform Solutions with TransOmics™ Informatics

ACQUITY UPLC® I-Class System

nanoACQUITY® UPLC® System

Xevo® G2-S QTof

TransOmics Informatics

MassPREP™ Protein Digestion Standard

KEY WORDS

Omics, metabolomics, lipidomics, proteomics, MS^E, principal components analysis, label-free LC/MS

INTRODUCTION

Recent advances in omics technologies, including LC/MS-based metabolomics, lipidomics, and proteomics instrumentation, enable the quantitative monitoring of the abundance of various biological molecules in a high-throughput manner, thus allowing for determination of their variation between different biological states.

The ultimate aim is to improve the understanding of biological processes, leading to improved disease treatment efficacy, more efficient drug development, or maintaining optimal agricultural growth conditions for crop growth while minimizing infection and other negative effects. In this regard, the results provided from different analytical disciplines are often seen as complementary since they afford orthogonal insights.

The development and application of flexible informatics solutions that are capable of integrating the results from multiple discovery areas is of key importance. This study describes a multi-omics solution for the large-scale analysis of MS data from metabolomics and proteomics data sets. The Waters® Omics Research Platform Solutions with TransOmics Informatics, featuring the Xevo G2-S QTof System, was utilized in a study comprised of both technical and biological replicates.

RESULTS AND DISCUSSION

A metabolomics experiment was conducted involving the identification of low- and high-dosed samples versus a control/pool sample. According to the experimental design, the samples should be classified into three different groups and the marker ions responsible for the group separation identified. The TransOmics for metabolomics and lipidomics (TOIML) procedure involves the following steps:

1. Importing the raw MS^E continuum data set (six technical replicates/group)
2. Peak alignment to correct retention time drift between analytical runs
3. Chromatographic peak normalization to allow comparison across different sample runs
4. Chromatographic peak detection (peak picking)
5. Ion deconvolution to group ions by compound
6. Compound identification against an available custom built database
7. Perform data analysis to find the ions (features) responsible for the separation of the groups into QC (pool), blank (matrix), and analyte (high dose)

The matrix background comprised System Evaluation Matrix to which Analgesic Standard Mixture A was differentially added, creating a low- (QC) and high-dose (blank) sample. A pool sample (QC) was created by combing equal volumes of the low- and high-dose sample.

The metabolites were separated and analyzed using the ACQUITY UPLC I-Class System coupled with a Xevo G2-S QTof, operated in positive electrospray mode at a mass resolution of >30k FWHM. Data were acquired in LC/MS^E mode, an unbiased Tof acquisition method in which the mass spectrometer switches between low and elevated energy on alternate scans. Processing, searching, and quantification were conducted with TOIML using a compound database.

Steps one, two, and three of the TOMIL procedure are detailed elsewhere (TransOmics Informatics Powered by Nonlinear Dynamics). The grouping by means of principal component analysis (PCA) of the detected ions prior to identification, as shown in Figure 1, represents a composite scores and loadings plot. Primary clustering at the technical replicate level and clear separation of the samples were achieved.

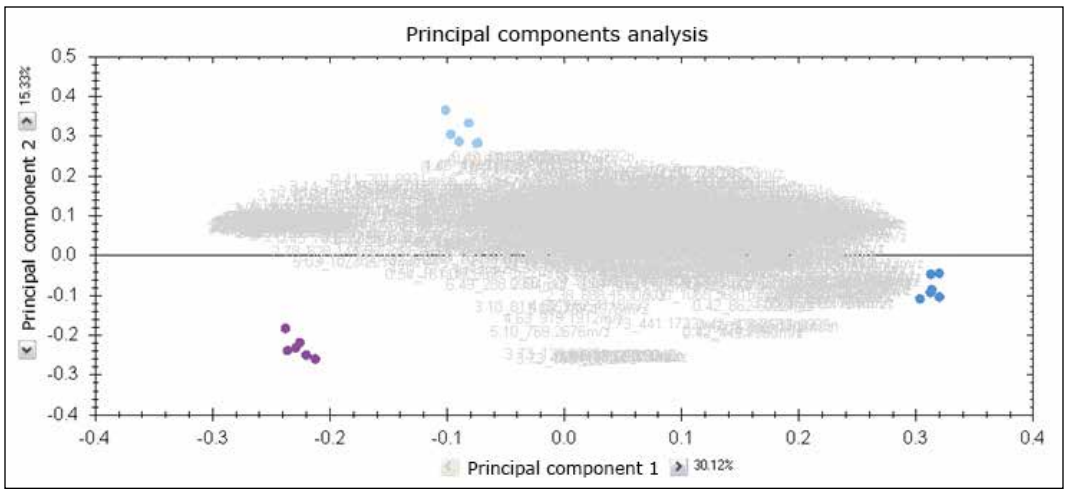

Figure 1. Principal component analysis of analyte (Analgesic Standard Mixture A high dose; purple), Blank (System Evaluation Matrix; light blue) and QC (pooled sample; dark blue).

Next, compound identification was conducted using an integrated search tool, leading to the correct identification of the four Analgesic Standard Mixture standards that can be detected in positive ion electrospray mode. An overview of the TOIML compound search results page is shown in Figure 2, highlighting the identification of caffeine based on accurate mass, retention time (optional), and theoretical isotopic pattern distribution.

In addition to the previously described PCA, additional multivariate statistical tools are integrated within TOIML, including correlation and trend analysis. An example is shown in Figure 3, representing normalized trend plots for the four spiked standards, illustrating good agreement between the six technical replicates of each of the standards, as well as relative abundances that are in agreement with the experimental design.

Moreover, TOIML enables the scientist to link the analysis results with other omics data or provide input into separate statistical software packages such as EZinfo. Results from downstream bioinformatics (i.e., Umetrics software) can be imported back into an analyzed experiment, combining all compound data into a single table to review or share.

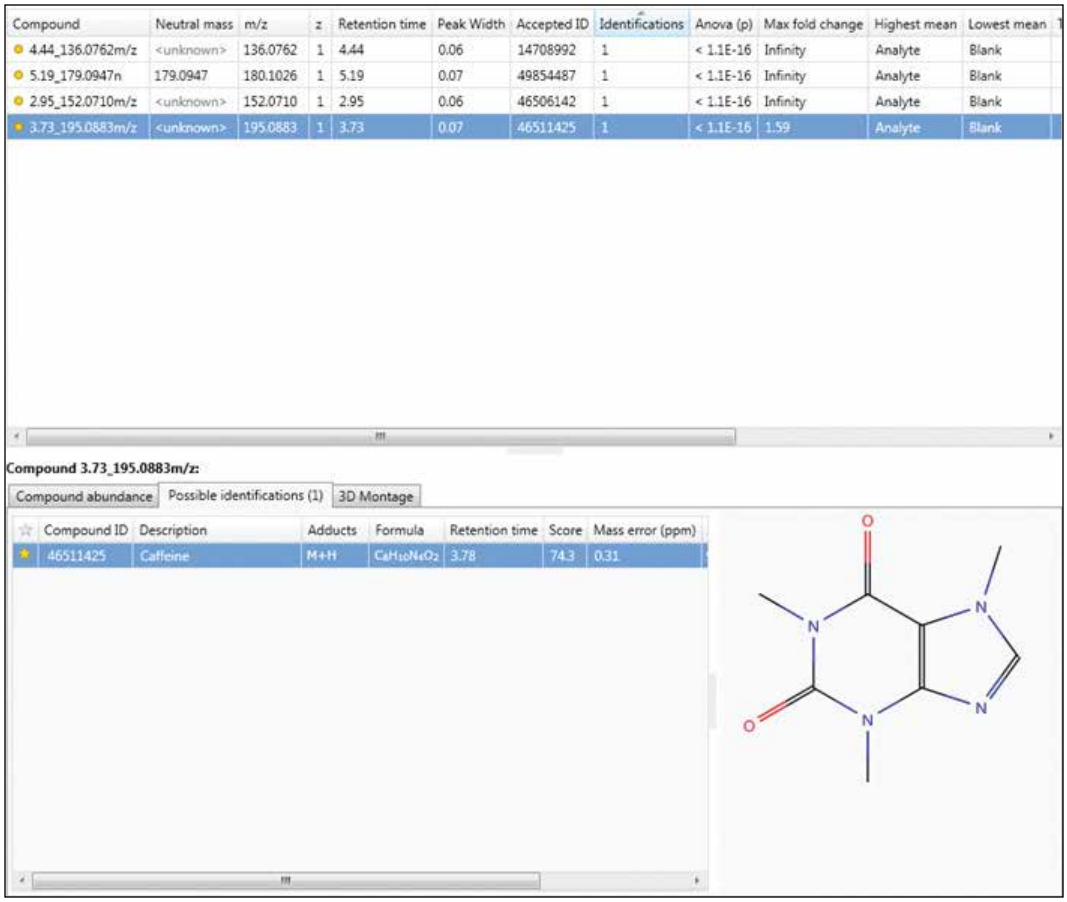

Figure 2. Compound identification page TOIML.

Figure 3. Normalized abundance profiles analgesic standards.

For the proteomics experiment, three replicates of two 10-ng *E.coli* samples differentially spiked with bovine serum albumin (BSA), alcohol dehydrogenase (ADH), enolase, and glycogen phosphorylase B were analyzed. The injected on-column amounts for the spiked protein in the first sample (Mixture 1) were one femtomoles each and 8, 1, 2, and 0.5 femtomoles for the second sample (Mixture 2), respectively. The nominal expected ratios (Mixture 2:Mixture 1) were therefore 8:1, 1:1, 2:1, and 0.5:1. Here, the peptides were separated and analyzed using a nanoACQUITY UPLC System coupled to a Xevo G2-S QTof and operated in LC/MS^E acquisition mode. Processing, searching, and quantification were conducted with TransOmics for Proteomics (TOIP) using a species specific database to which sequence information of the spiked proteins was appended.

The TOIP procedure involves the following steps:

1. Importing the raw MS^E continuum data set (three technical replicates per sample)
2. Peak alignment to correct retention time drift between analytical runs
3. Chromatographic peak normalization to allow comparison across different sample runs
4. Chromatographic peak detection (peak picking)
5. Protein and peptide identification utilizing integrated database search algorithms
6. Multivariate statistical analysis
7. Absolute and relative quantitation

TOIP offers the same multivariate analysis tools as TOIML. Figure 4 illustrates an example of PCA of the detected features, i.e. charge state groups. Primary clustering at the technical replicate level can be readily observed. A qualitative peptide identification result for one of the spiked protein digest is shown in Figure 5, and the normalized expression profiles of all peptides identified to this protein are shown in Figure 6. The latter is demonstrative for the type of quantitation precision that can be obtained by means of label-free MS studies using and LC/MS^E- based acquisition strategy.

Figure 5 shows the qualitative results overview for an LC/MS^E acquisition of one of the analyses of the differentially spiked samples. In this particular instance, the on-column amount of highlighted BSA was 8 fmol and the amount of *E.coli* digest equal to 10 ng. The results, shown in Figure 6, demonstrate the corresponding relative quantification result.

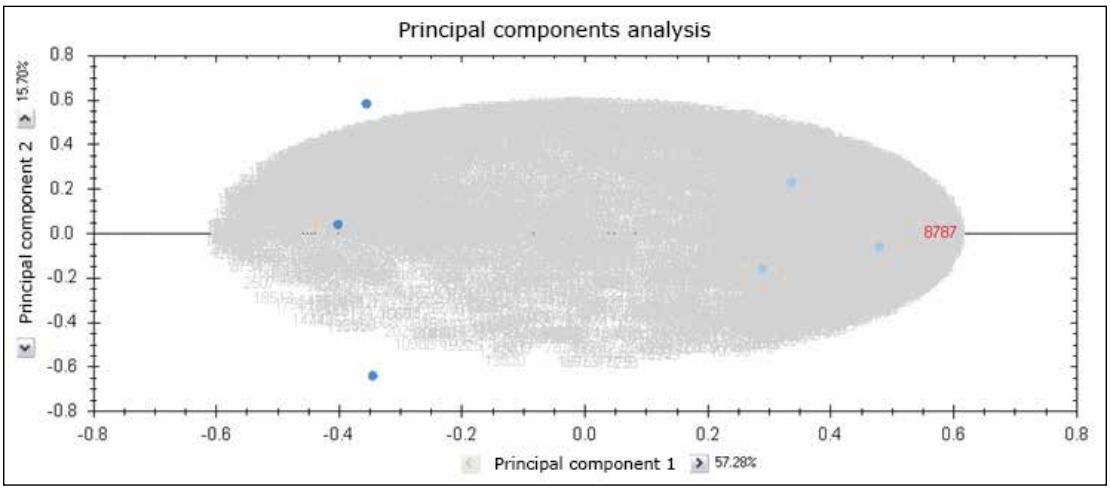

Figure 4. PCA of Mixture 1 spiked into E.coli (dark blue) and Mixture 2 spiked into E.coli (light blue) features (charge state groups).

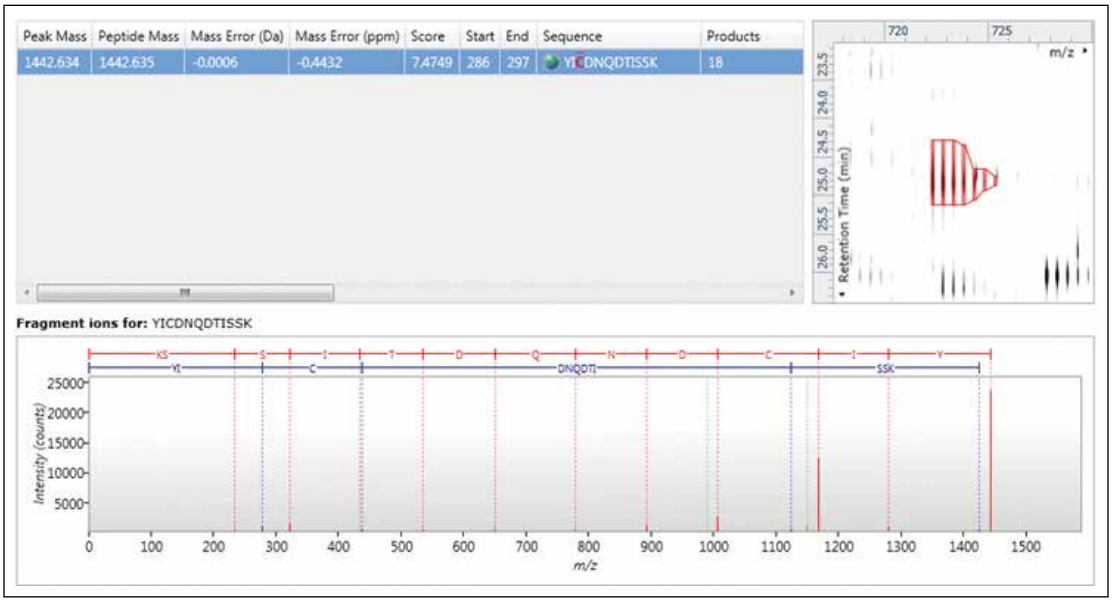

Figure 5. Qualitative LC/MS^E identification for a bovine serum albumin peptide that was differentially spiked into E.coli. Shown clock-wise are the identification associated metrics (score and error), a detail of the contour plot, and the annotated product ion spectrum.

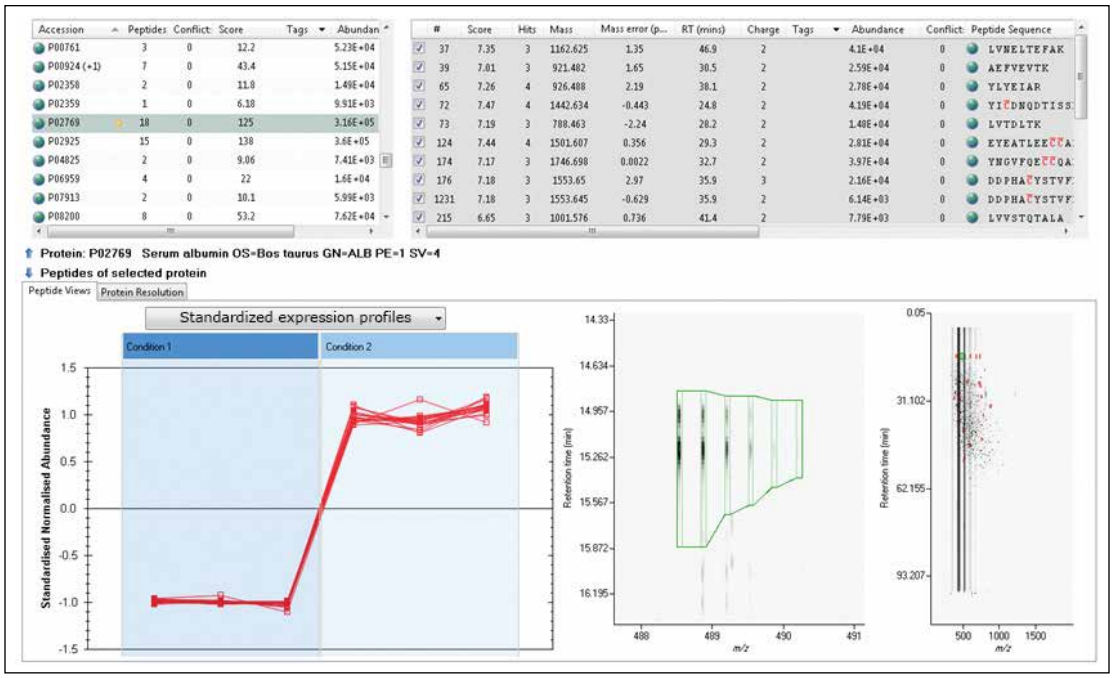

Figure 6. Quantitative profiling of the peptides identified to bovine serum albumin.

CONCLUSIONS

- TransOmics Informatics provides an easy-to-use, scalable system for multi-omics studies.
- LC/MS^E (LC with Data Independent Acquisition MS) provides a comprehensive qualitative and quantitative data set from a single experiment.
- Complementary information can be rapidly obtained and linked from metabolite, lipid, and protein analysis.

Waters

THE SCIENCE OF WHAT'S POSSIBLE.®

Waters Corporation
34 Maple Street
Milford, MA 01757 U.S.A.
T: 1 508 478 2000
F: 1 508 872 1990
www.waters.com

Waters
THE SCIENCE OF WHAT'S POSSIBLE.®

An Ion Mobility-Enabled Data Independent Multi-Omics Approach to Quantitatively Characterize Urine From Children Diagnosed With Idiopathic Nephrotic Syndrome

Lee Gethings[1]; Sandra Kraljević Pavelić[2]; Mirela Sedic[2]; John Shockcor[3]; Stephen McDonald[3]; Johannes Vissers[1]; Maja Lemac[4]; Danica Batinić[4]; James Langridge[1]

[1]Waters Corporation, Manchester, UK; [2]Department of Biotechnology, University of Rijeka, Rijeka, Croatia; [3]Waters Corporation, Milford, MA, USA; [4]Zagreb Univerisity Hospital Centre, Zagreb, Croatia

APPLICATION BENEFITS

A label-free multi-omics approach for the analysis of the urine of Idiopathic Nephrotic Syndrome (INS) patients that provides both qualitative and quantitative information in a single experiment. This enables possible diagnostic and therapeutic solutions for patients with INS.

WATERS SOLUTIONS

ACQUITY UPLC® System

nanoACQUITY® UPLC® System

SYNAPT® G2 Mass Spectrometer

Oasis® HLB Extraction Cartridges

ProteinLynx GlobalSERVER™

Markerlynx™ XS

TransOmics™ Platform and Informatics

MS^E/HDMS^E

TriWave™ technology

KEY WORDS

Idiopathic Nephrotic Syndrome (INS), metabolomics, clinical proteomics, multi-omics

INTRODUCTION

Idiopathic Nephrotic Syndrome (INS) results from the malfunction of the glomerular filter and it is the most prevalent glomerular disease in children. In spite of some progress, its pathogenesis is still unknown and therapy options are confined to gross immune modulation. A variety of methods for diagnostic and treatment purposes are available for patients; however, the lack of understanding regarding the pathogenic mechanisms underlying INS can lead to poor therapeutic response and adverse side-effects. In this application note, we describe a multi-omic approach to reveal new molecular factors involved in pathogenesis of INS with potential diagnostic and therapeutic significance.

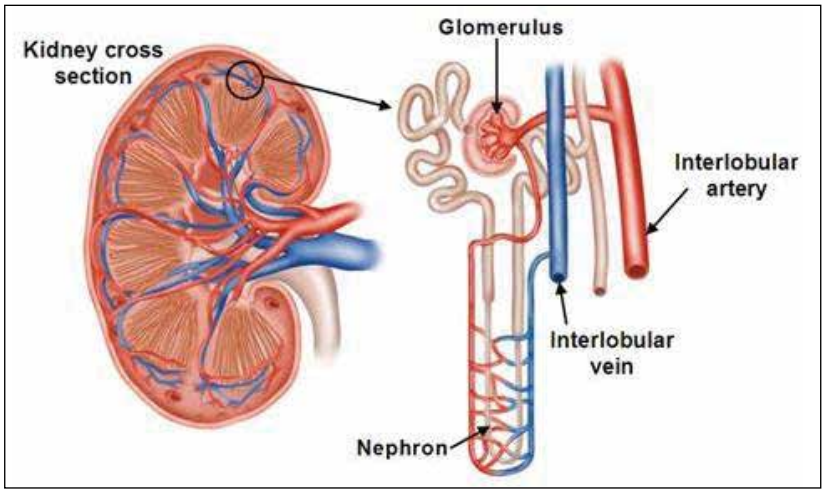

Figure 1. Kidney section highlighting a single nephron. A malfunctioning glomerulus is where INS occurs (courtesy of Wellcome Images).

EXPERIMENTAL

Sample preparation

Pediatric urine samples intended for peptide analysis were prepared for LC/MS analysis as previously described.[1] Samples were treated with 1% RapiGest™ SF prior to reduction and alkylation. Aliquots were incubated with anti-HSA resin and centrifuged using Vivaspin 5,000 MWCO filters. A series of washes using water were implemented to ensure adequate recovery. The resulting supernatant was digested using trypsin overnight as shown in Figure 2. Metabolite analysis samples were purified using Oasis HLB Extraction Cartridges. Water/methanol (90/10) washes were performed, followed by analyte elution using methanol. The resulting residue was reconstituted in 200 µL mobile phase and vortexed prior to LC/MS.

LC/MS conditions

Label-free LC/MS was used for qualitative and quantitative peptide analyses. Experiments were conducted using a 90 min gradient from 5% to 40% acetonitrile (0.1% formic acid) at 300 nL/min using a nanoACQUITY UPLC System and a BEH 1.7 µm C_{18} reversed phase 75 µm x 20 cm nanoscale LC Column.

For metabolite identification, the LC/MS experiments consisted of a 10 min gradient from 0% to 50% acetonitrile (0.1% formic acid) at 500 µL/min using an ACQUITY UPLC System. Here, a BEH 1.7 µm C_{18} reversed phase 2.1 x 10 cm LC column was used.

Data were acquired in data independent analysis (DIA) mode that utilized a nanoACQUITY UPLC or ACQUITY UPLC system directly interfaced to a hybrid IM-oaTof SYNAPT G2 Mass Spectrometer. Ion mobility (IM) was used in conjunction with both acquisition schemes, as illustrated in Figure 3.

Bioinformatics

The LC/MS peptide data were processed and searched with ProteinLynx GlobalSERVER. Normalized label-free quantification was achieved using TransOmics Software. The resulting metabolomic data were processed using MassLynx™ Software, and additional statistical analysis conducted with EZ Info.

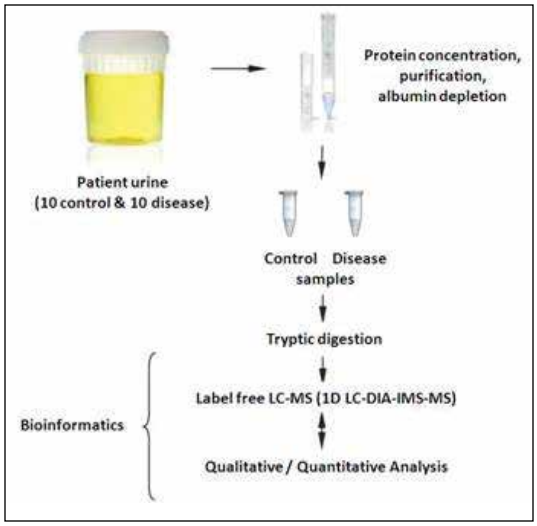

Figure 2. Experimental design study for urinary proteins.

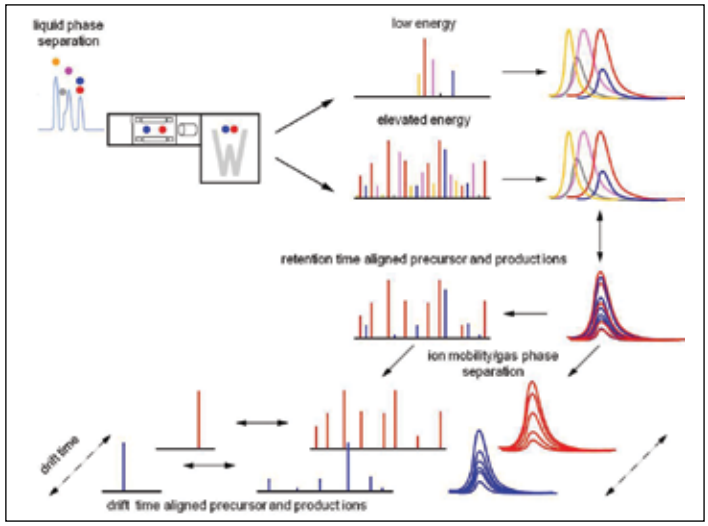

Figure 3. Retention and drift time principle ion mobility enabled data-independent analysis (IM-DIA-MS/HDMS^E).

RESULTS AND DISCUSSION

Small amounts of the purified urine were analyzed to identify, quantify, and investigate the proteomic and metabolomic variance between control and disease pre-treated subjects.

Principal Component Analysis (PCA) was used to identify and highlight significant changes between the control and disease pre-treated samples, as shown in Figure 4. Similar clustering patterns were observed for both the protein and metabolite datasets.

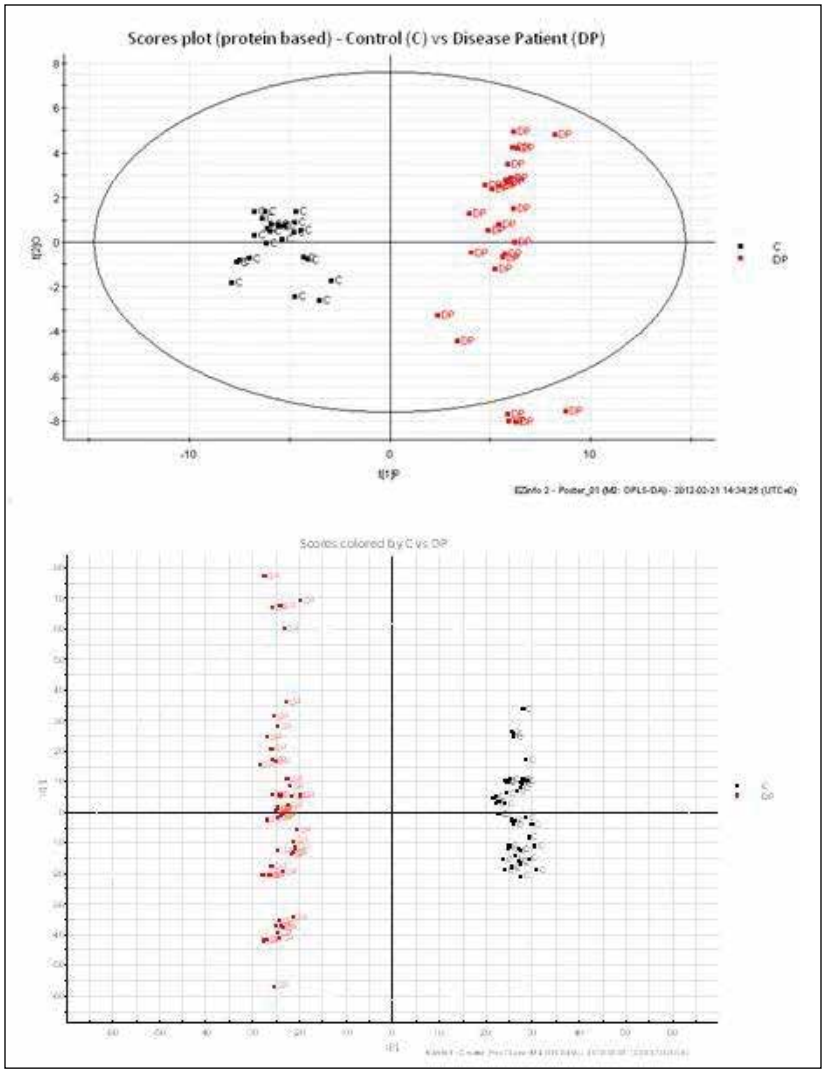

Figure 4. Scores plot from OPLS-DA analysis of disease pre-treated (red) vs. control (black).

Proteomic data were aligned, normalized, and quantified. A large proportion of the identified proteins are glycosylated and over 80% of the total number of proteins identified and exhibited a significant expression fold change. Figure 5 highlights the proteins, which have greater than a two-fold change between sample sets. The fold change at the peptide level can be visually displayed using 3D montage images. A charge state feature of one of the peptides of interest is shown in Figure 5.

The metabolomics workflow results are summarized in Figure 6. Using the metabolite contrasting loadings plot, significant metabolite identifications can be found at the extremes and are shaded in blue. Example compounds, which were found to contribute most significantly to the variance, are also shown.

A common pathway is shown in Figure 7, which illustrates a glutamate [NMDA] receptor subunit as one such example. NMDA belongs to the glutamate-gated ion channel family of proteins and is used in neuronal system pathways. Glutamate can also be located within the same pathway. Postsynaptic Ca(2+) is thought to increase through the NMDA receptors, which activate several signal transduction pathways including Erk/MAP kinase and cAMP regulatory pathways.

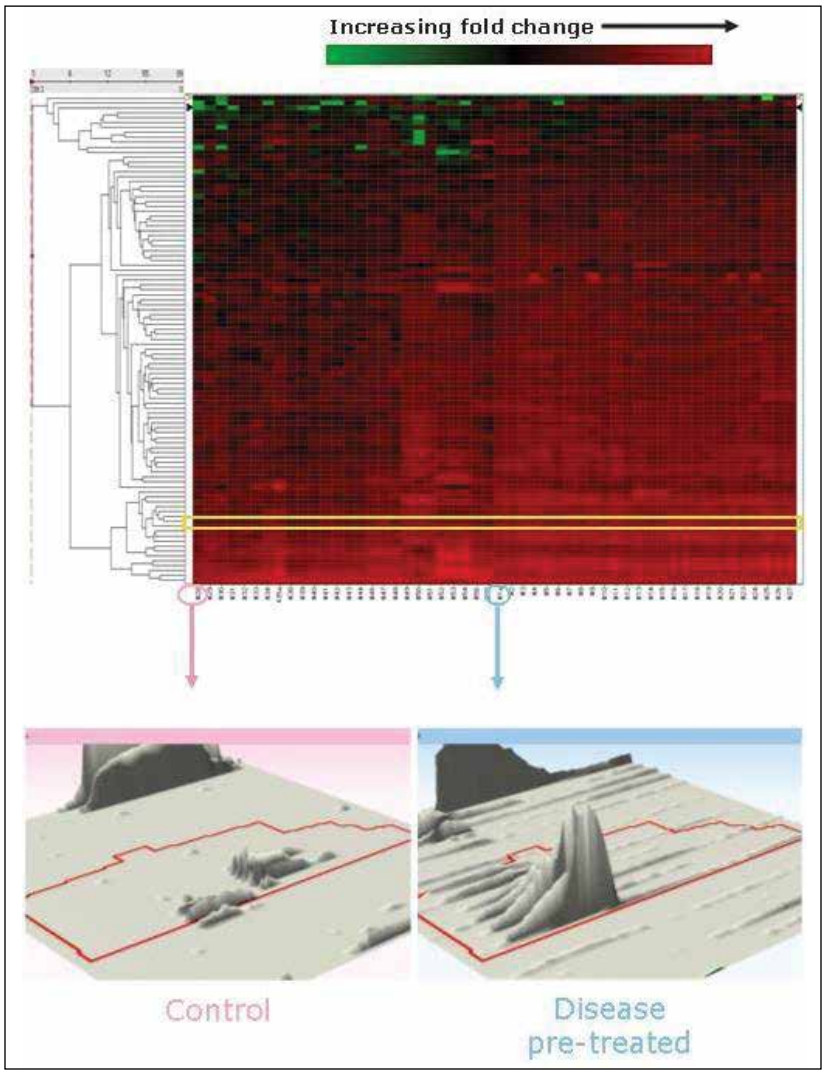

Figure 5. Hierarchal cluster analysis regulated proteins with a minimum of three identified peptides and a fold change greater than two. The highlighted region represents prostaglandin with associated 3D montage images for TMLLQPAGSLGSYSYR.

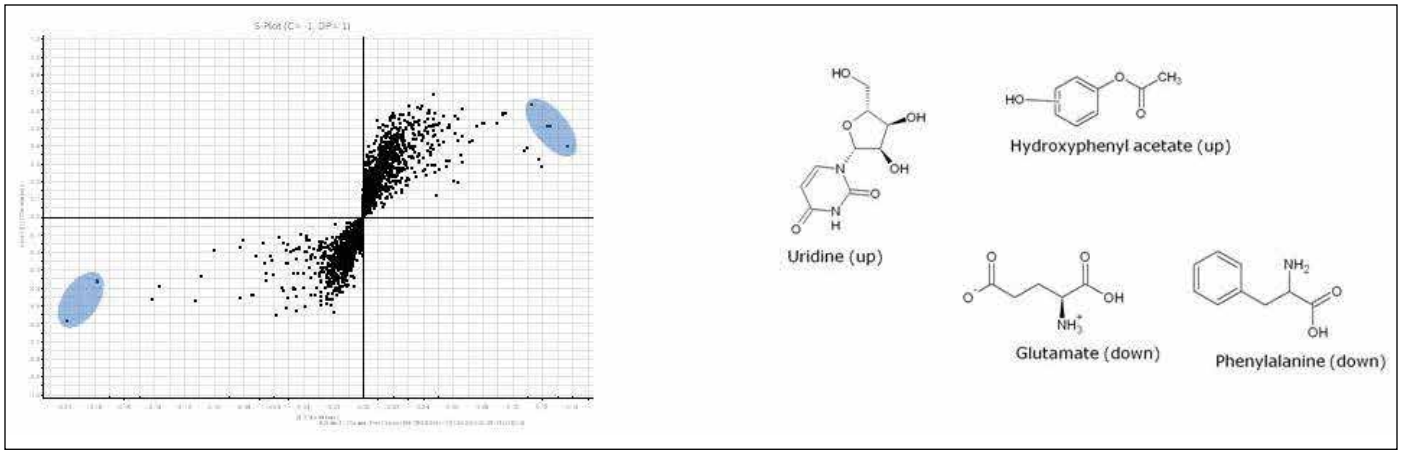

Figure 6. Metabolite loadings plot from OPLS-DA analysis of disease pre-treated versus control subjects based in positive ion mode. Metabolites contributing the greatest variance are represented within the blue shaded areas with examples provided.

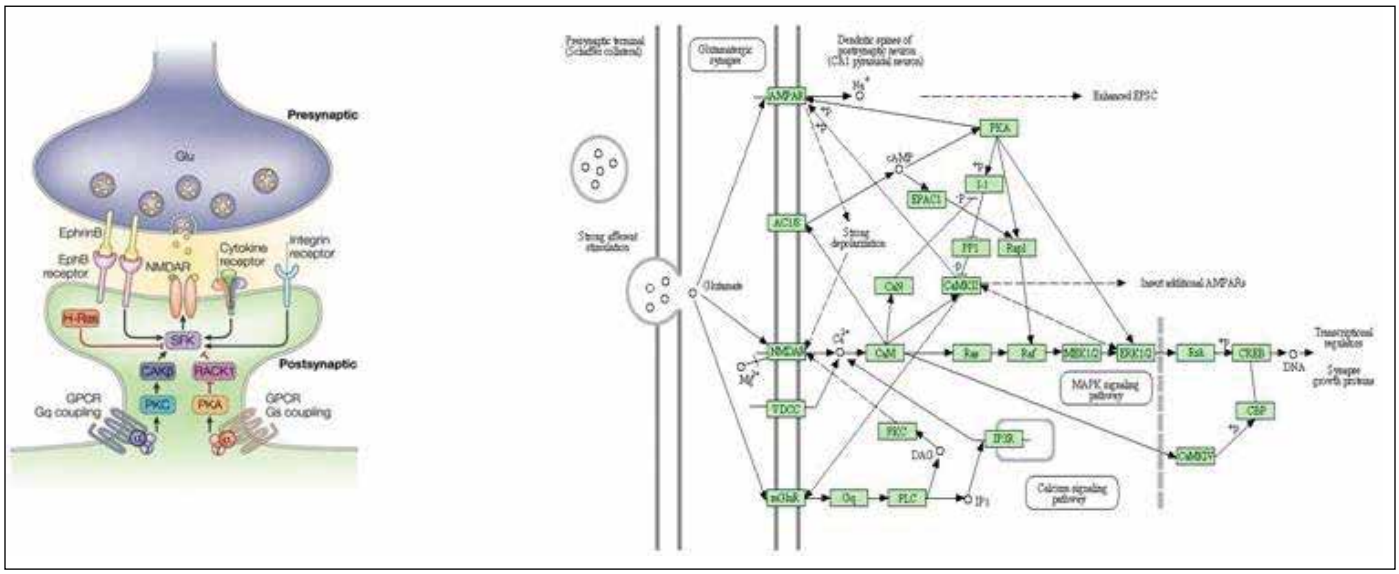

Figure 7. Neuronal system pathway, specifically highlighting the role of the glutamate [NMDA] receptor subunit and glutamate for downstream transmission in the postsynaptic cell.

CONCLUSIONS

- 80% of the proteins identified were expressed, with 30% of proteins having a maximum fold change ≥ 2 and ANOVA (p) value ≤ 0.05.
- The majority of identified proteins were glycosylated, of which many showed changes in relative abundance.
- PCA analysis shows both protein and metabolite data to be complimentary.
- A variety of analytes were identified as contributing towards the metabolite variance.
- Complementary information obtained from metabolite and protein analysis has been shown through the use of glutamate and NMDA within the neuronal system pathway.
- A label-free multi-omics approach has been applied for the analysis of the urine of INS patients by implementing HDMS^E, which provides both qualitative and quantitative information in a single experiment.

References

1. Vaezzadeh AR, Briscoe AC, Steen H, Lee RS. One-step sample concentration, purification and albumin depletion method for urinary proteomics. J Proteome Res. 2010;9(11):6082-89.
2. Li GZ, Vissers JP, Silva JC, Golick D, Gorenstein MV, Geromanos SJ. Database searching and accounting of multiplexed precursor and product ion spectra from the data independent analysis of simple and complex peptide mixtures. Proteomics. 2009 Mar;9(6):1696-719.
3. Han CL, Chien CW, Chen WC, Chen YR, Wu CP, Li H, Chen YJ. A multiplexed quantitative strategy for membrane proteomics: opportunities for mining therapeutic targets for autosomal dominant polycystic kidney disease. Mol Cell Proteomics. 2008 Oct;7(10):1983-97.
4. Salter MW, Kalia, LV. Src kinases: a hub for NMDA receptor regulation. Nature Reviews Neuroscience, 2004 April; 5: 317-328.

Waters

THE SCIENCE OF WHAT'S POSSIBLE.®

May 2012 720004329en AG-PDF

Waters Corporation
34 Maple Street
Milford, MA 01757 U.S.A.
T: 1 508 478 2000
F: 1 508 872 1990
www.waters.com

Waters
THE SCIENCE OF WHAT'S POSSIBLE.®

Metabolomics of Broccoli Sprouts Using UPLC with Ion Mobility Enabled LC/MS^E and TransOmics Informatics

Mariateresa Maldini[1], Simona Baima[1], Fausta Natella[1], Cristina Scaccini[1], James Langridge[2], and Giuseppe Astarita[2]
[1]National Research Institute on Food and Nutrition, Rome, Italy; [2]Waters Corporation, Milford, MA, USA

APPLICATION BENEFITS

Use of the Waters Omics Research Platform, which combines UPLC® with ion mobility LC/MS^E and TransOmics™ Informatics, allows for the rapid characterization of molecular phenotypes of plants that are exposed to different environmental stimuli.

WATERS SOLUTIONS

Omics Research Platform
with TransOmics Informatics

ACQUITY UPLC® System

SYNAPT® G2-S HDMS®

KEY WORDS

Lipid, metabolomics, lipidomics, natural products, food, nutrition, HDMS Compare

INTRODUCTION

Cruciferous vegetables, such as broccoli, cabbage, kale, and brussels sprouts, are known to be anti-carcinogenic and possess antioxidant effects. They are widely consumed in the world, and represent a rich source of bioactive metabolites.[1] Young broccoli plants are an especially good source of chemoprotective metabolites, with levels several times greater than mature plants. Growth conditions and environmental stresses exert a significant influence on the metabolism of broccoli sprouts.[2]

The aim of this work is to study how the complete set of small-molecule metabolites, the "metabolome," of broccoli sprouts is modulated under different growth conditions. As the metabolome reflects both genetic and environmental components (e.g., light conditions and nutrients), comprehensive metabolite profiles can describe a biological system in sufficient depth to closely reflect the ultimate phenotypes, as shown in Figure 1.

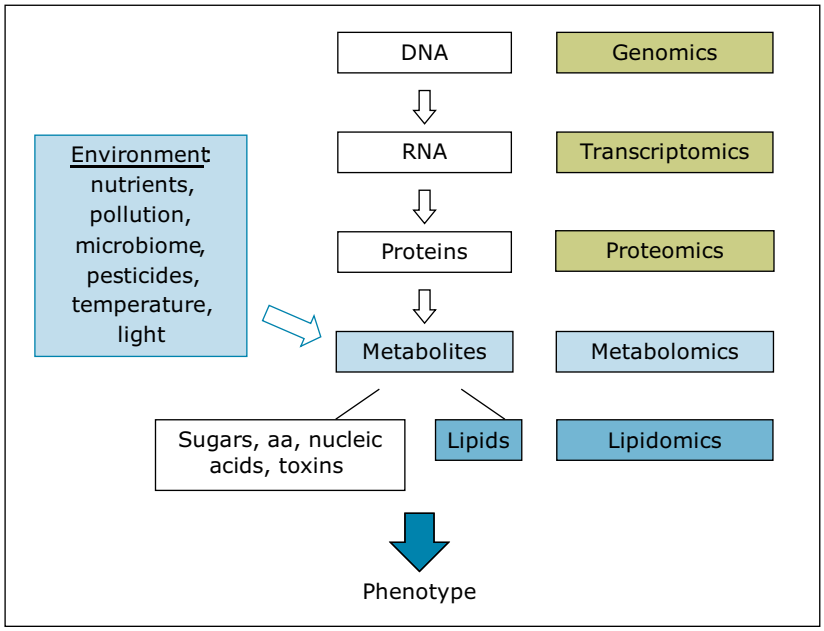

Figure 1. Metabolomics aims to screen all the metabolites present in biological samples. Metabolites can derive from both the generic imprint and from the environment (e.g., different growth conditions). Metabolites are counted in the order of thousands and have a wide range of chemical complexity and concentration. The profiling of the entire set of metabolites, or metabolome, characterizes the molecular phenotype of the biological system.

EXPERIMENTAL

Sample description

Broccoli seeds (*Brassica oleracea* L. var. *botrytis* subvar. *cymosa*) were germinated in the germination cylinder of Vitaseed sprouter, and grown hydroponically for five days at 21 °C in a plant growth chamber (Clf Plant Climatics, Wertingen, Germany) equipped with PHILIPS Master TL-D 36W/840 cool-white fluorescent tubes providing a photosynthetic photon flux density of 110 mmol m-2 s-1, under three different light regimes: a) dark (achieved by covering the sprouting device with a cardboard box), b) continuous light, and c) continuous light plus two days of treatment with sucrose 176 mM.

Sprout samples, collected from the germination cylinder, were immediately frozen in liquid nitrogen and stored at -80 °C. Frozen sprouts were ground to a fine powder in a Waring blendor cooled with liquid nitrogen. Each sample of broccoli sprouts was extracted with 100% methanol (sample to solvent ratio 1:25 w/v) at 70 °C for 30 minutes under vortex mixing to facilitate the extraction. The samples were successively centrifuged (4000 rpm, 30 minutes, 4 °C), the supernatants were collected, and the solvent was completely removed using a rotary evaporator under vacuum at 40 °C. The dried samples were dissolved in methanol with the same volume of extraction, and filtered through 0.20-µm syringe PVDF filters.[3]

UPLC conditions

System:	ACQUITY UPLC
Column:	ACQUITY CSH C_{18} 2.1 x 100 mm, 1.7 µm
Mobile phase A:	60:40 10 mM NH_4HCO_2 in ACN/H_2O
Mobile phase B:	90:10 10 mM NH_4HCO_2 in IPA/ACN
Flow rate:	0.4 mL/min
Column temp.:	55 °C
Injection volume:	5.0 µL

Elution gradient:

Min	A%	B%	Curve
Initial	60.0	40.0	Initial
2.0	57.0	43.0	6
2.1	50.0	50.0	1
12.0	46.0	54.0	6
12.1	30.0	70.0	1
18.0	1.0	99.0	6
18.1	60.0	40.0	6
20.0	60.0	40.0	1

MS conditions

UPLC analytical column was connected to the ESI probe using PEEK Tubing, 1/16 inch, (1.6 mm) O.D. x 0.004 inch. (0.100 mm) I.D. x 5 ft (1.5 m) length, cut to 400 mm in length.

Mass spectrometer:	SYNAPT G2-S HDMS
Mode of operation:	Tof HDMS^E
Ionization:	ESI +ve and -ve
Capillary voltage:	2.0 KV (+ve) and 1.0 KV (-ve)
Cone voltage:	30.0 V
Transfer CE:	Ramp 20 to 50 V
Source temp.:	120 °C
Desolvation temp.:	550 °C
Cone gas:	50 L/h
MS gas:	Nitrogen
IMS T-Wave™ velocity:	900 m/s
IMS T-Wave height:	40 V
Acquisition range:	50 to 1200

Data acquisition and processing:

TransOmics Informatics and HDMS Compare for SYNAPT Systems

RESULTS AND DISCUSSION

We applied an untargeted metabolomics approach (Figure 1) to identify molecular alterations induced by different growth conditions in broccoli sprouts (Figure 2). Metabolites were extracted from the sprouts, and analyzed using UltraPerformance LC® (UPLC) coupled with an ion mobility enabled QTof mass spectrometer, the SYNAPT G2-S HDMS (Figure 3), as reported in the Experimental conditions.

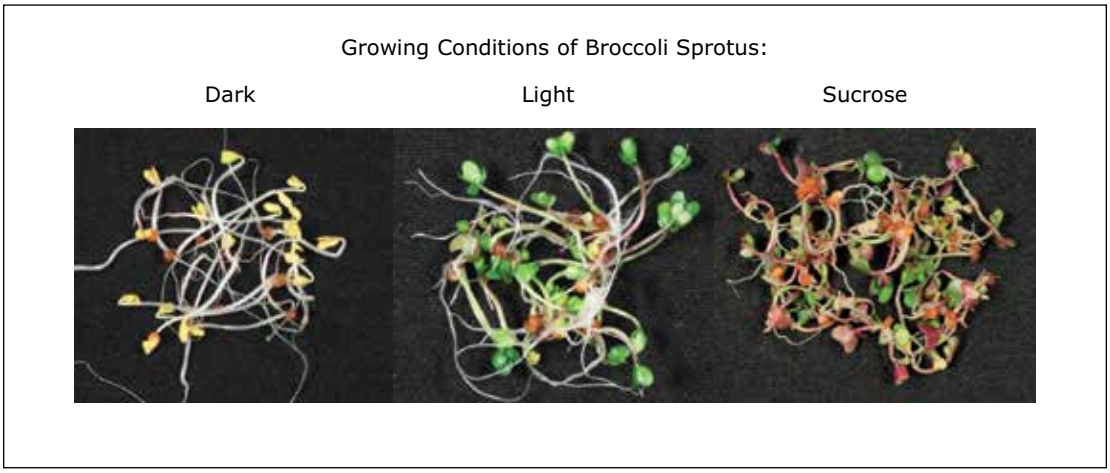

Figure 2. Broccoli sprout samples grown under different conditions.

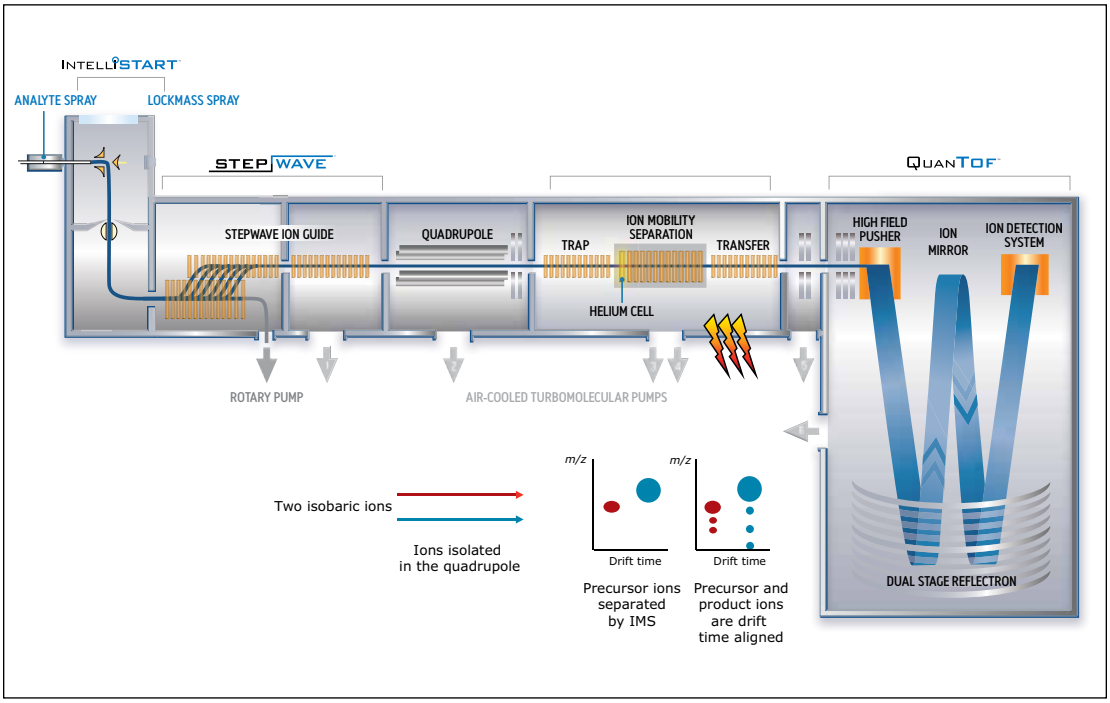

Figure 3. Schematic of the SYNAPT G2-S HDMS System configuration showing the ion mobility cell and the collision cell used to fragment the metabolites in HDMS^E mode.

UPLC maximized the separation of a wide range of chemical complexity present in the broccoli sprouts (Figure 4). Metabolites were ionized using ESI and, subsequently entered into the vacuum region of the MS system where they passed through the tri-wave ion mobility separation (IMS) cell (Figures 3, 4, and 5).

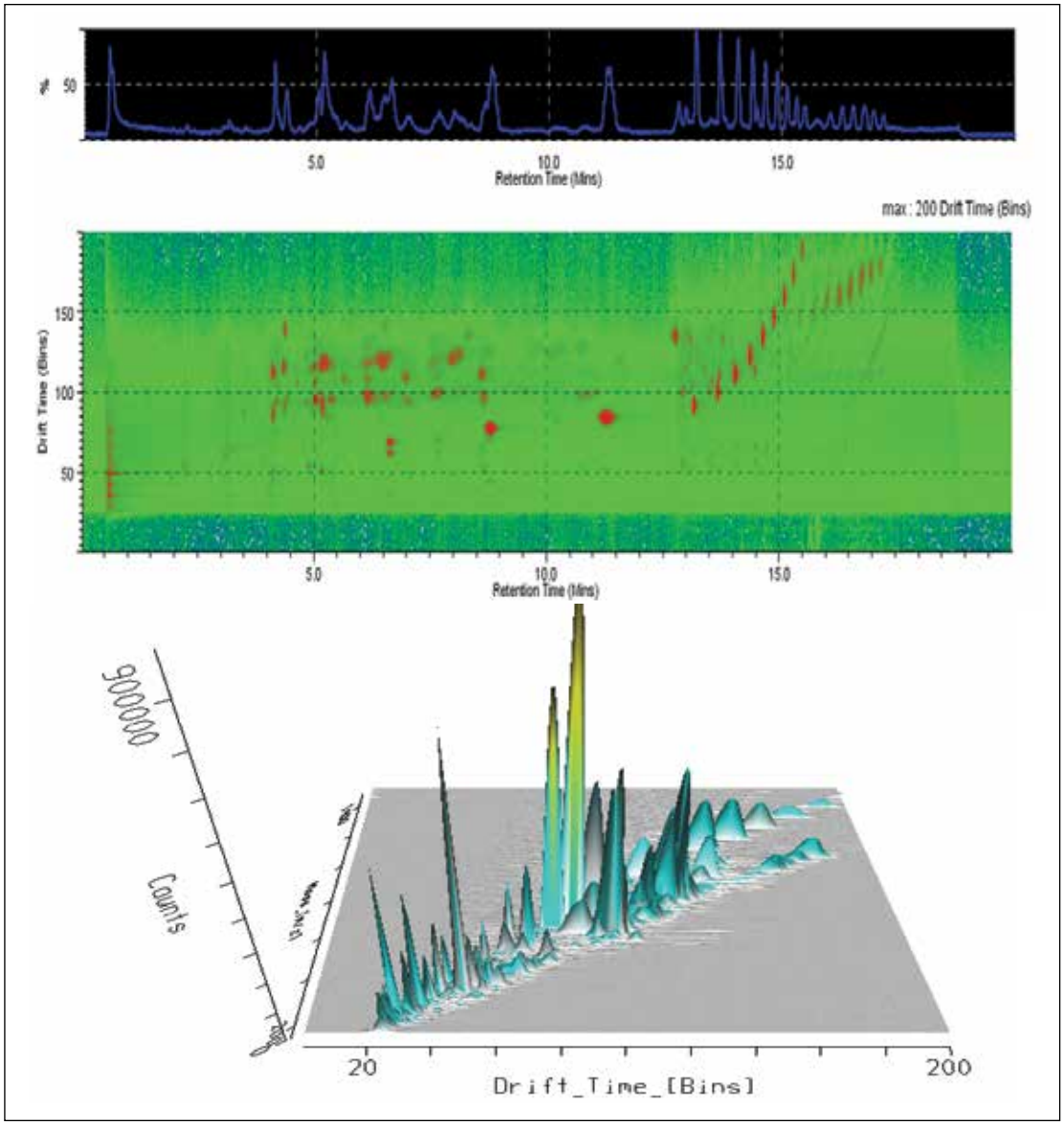

Figure 4. After UPLC separation, metabolites can be further separated in another dimension using ion mobility cell before MS detection This mode of acquisition is named High Definition Mass Spectrometry® (HDMS). Metabolites show characteristic drift times according to their size, shape and charge. The combination of UPLC and ion mobility increase peak capacity and specificity in the quantification and identification process.

The T-Wave IMS device uses RF-confining fields to constrain the ions in the radial direction, while a super-imposed repeating DC voltage wave propels ions in the axial direction through the dense gas-filled cell. The height and speed of the wave can be used to separate ions by their ion mobility[1]. As such, metabolites migrate with characteristic mobility times (drift times) according to their size and shape (Figures 3, 4, and 5). Therefore, IMS provides an additional degree of separation to chromatography, improving peak capacity over conventional UPLC/MS techniques (Figure 5).

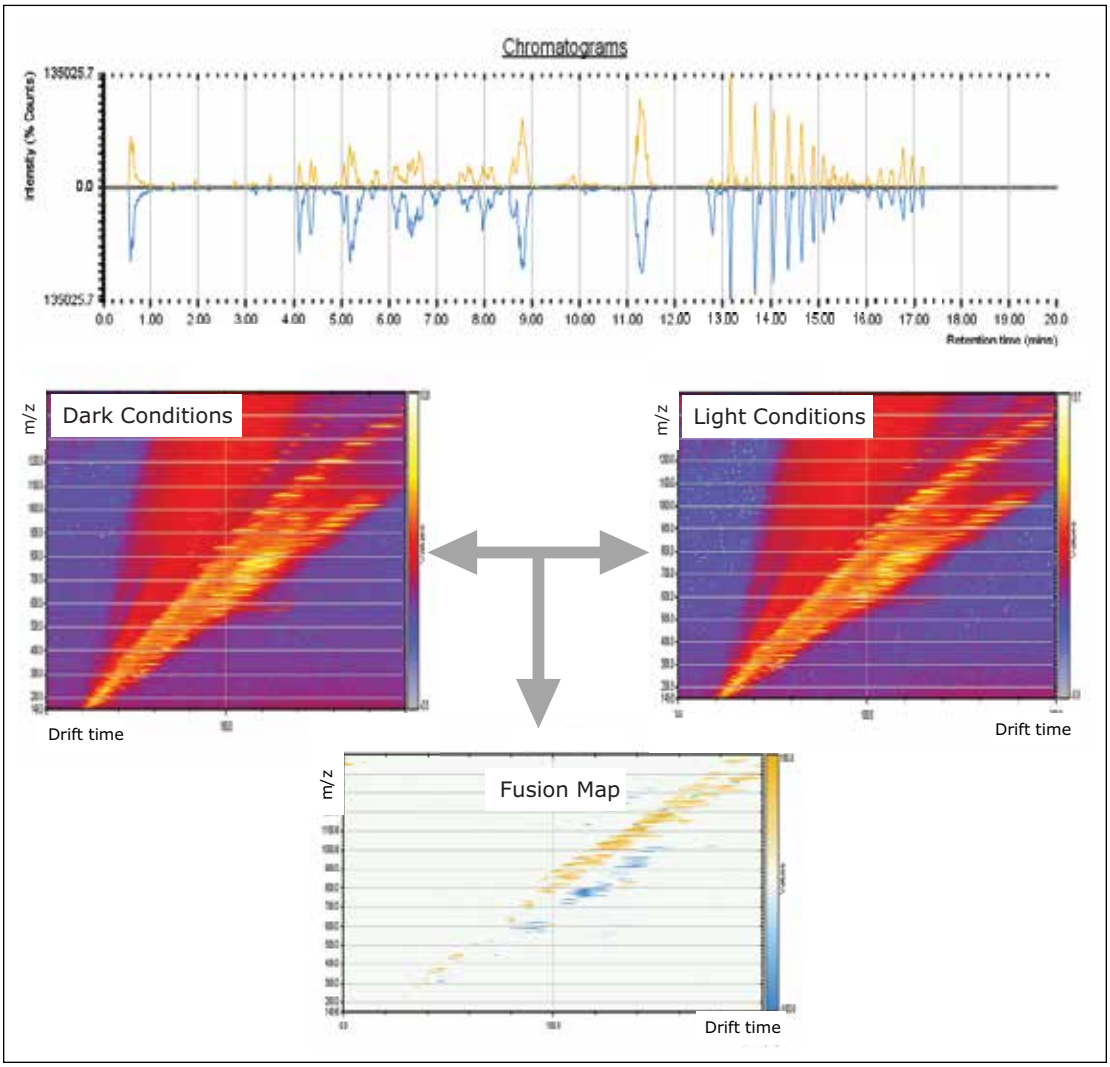

Figure 5. Representative UPLC/UPLC/MS chromatograms showing qualitative differences between broccoli sprout samples grown under light or dark conditions (upper panel). HDMS Compare Software was used to compare condition-specific molecular maps, highlighting key areas of significant differences between two samples with two different colors (bottom panel).

To aid in the identification and structural elucidation of metabolites, collision induced dissociation (CID) of metabolite precursor ions after IMS separation is performed using a particular mode of operation named HDMS^E. This approach utilizes alternating low and elevated collision energy in the transfer cell, thus recording all of the precursor and fragment ions in a parallel and continuous manner (Figure 6). The alternating scans acquire low collision energy data, generating information about the intact precursor ions, and elevated collision energy data, that provides information about associated fragment ions (Figure 6). The incorporation of ion mobility separation of coeluting precursor ions before CID fragmentation produces a cleaner MS/MS product ion spectra, facilitating easier metabolite identification, as shown in the bottom panel of Figure 6.

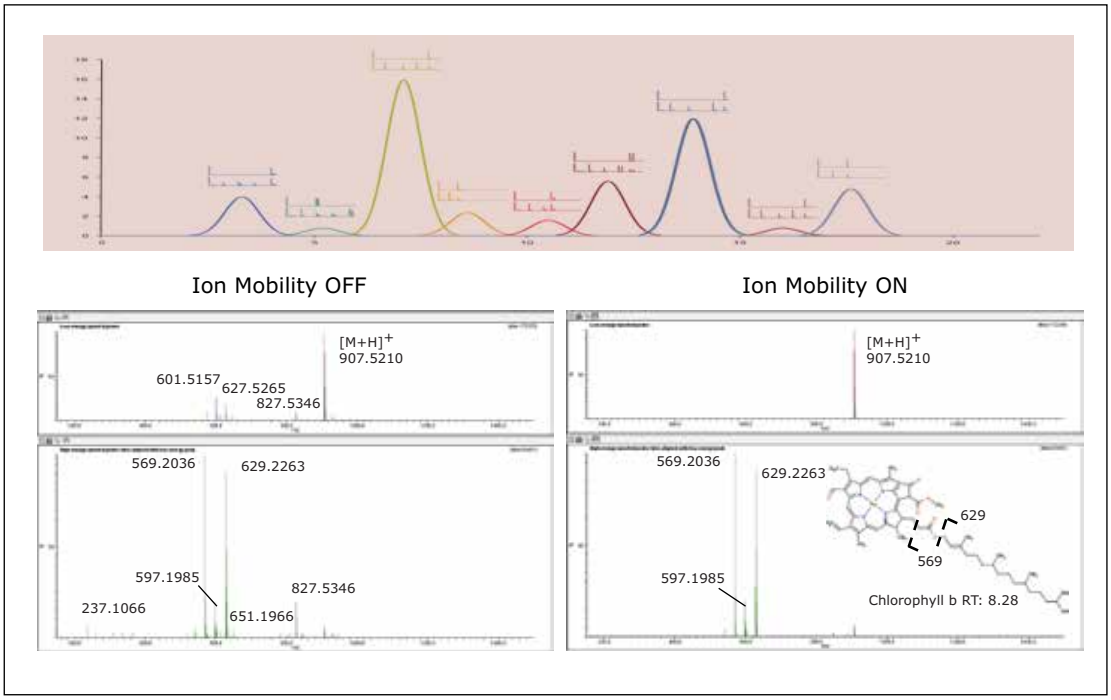

Figure 6. Representative UPLC/HDMS^E chromatogram showing the acquisition of both precursors and fragment spectra information along one single chromatographic run (upper panel). Applying high collision energy in the transfer collision cell, precursor molecules can be broken down into constituent parts, to deduce the original structure (bottom panel). In this example, the identification of the chlorophyll structure is based on the observation of characteristic fragments generated with high energy, using MS^E which matched with a compound search (Figure 8) and previously published results.[4]

The analysis provided a metabolite profile, which represents a biochemical snapshot of the metabolite inventory for each sample analyzed. Differences at the metabolite level between groups were analyzed using TransOmics Informatics which provided multivariate statistical analyses tools, including principal component analysis (PCA) (Figure 7A), correlation analysis (Figure 7B), review compound (Figure 8A), and database search functionalities (Figure 8B) for metabolite identification.

Preliminary results suggest that growth conditions induce specific alterations in the "metabolome" of broccoli sprouts, some of which are strictly related to photosynthetic processes.

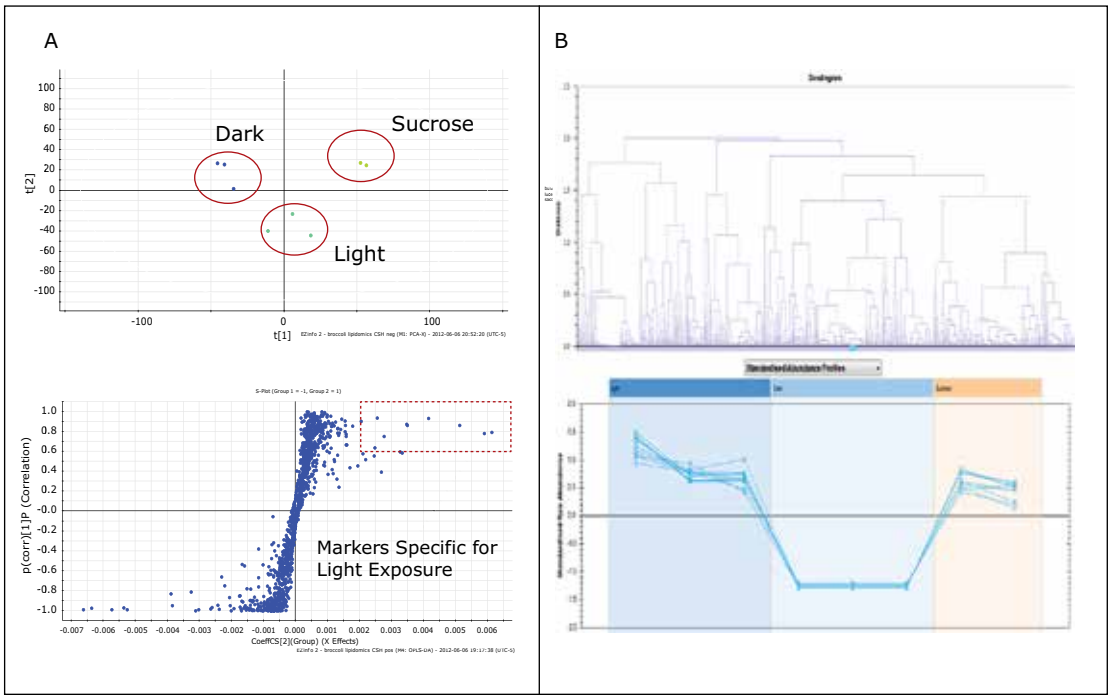

Figure 7. TransOmics multivariate statistical analysis of the UPLC/HDMS^E runs (A) allowed to separate samples into clusters, isolating the metabolites that contributed most to the variance among groups. Correlation analysis (B) helped to identify similar patterns of alterations among metabolites.

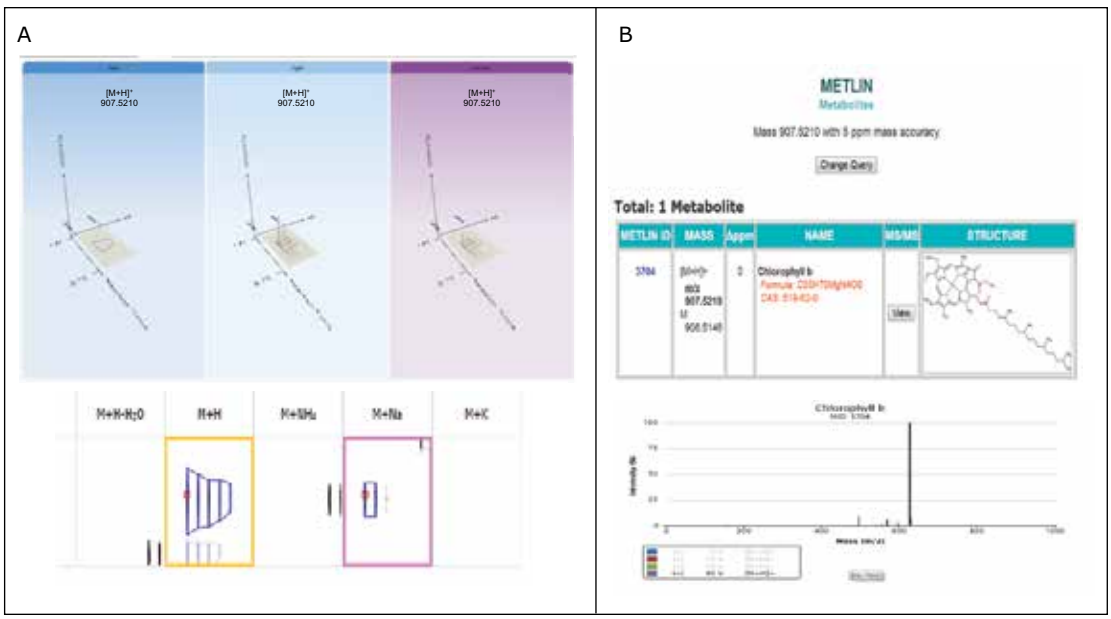

Figure 8. The statistical identification of metabolic alterations was followed by a review of the measurements (e.g., 3D montage and adducts deconvolution, (A) and a search on local or online databases (e.g., METLIN, (B)) for structural identification. In this example, a database search lead to a putative structure of a chlorophyll metabolite, which was only detected in broccoli sprouts grown in light conditions (A).

CONCLUSIONS

The Waters Omics Research Platform with TransOmics Informatics, featuring UPLC and HDMS^E technologies, enables researchers to improve how they screen and differentiate molecular phenotypes of plants exposed to different environmental stimuli. This high-throughput approach has applications in agricultural, food, and nutritional, as well as natural product research.

References

1. Jahangir M, Abdel-Farid IB, Kim HK, Choi YH, Verpoorte R. Metal ion-inducing metabolite accumulation in *Brassica rapa*. *Environmental and Experimental Botany*. 2009; 67: 23-33.
2. Pérez-Balibrea S, Moreno D, Garcìa-Viguera C. Glucosinolates in broccoli sprouts (*Brassica oleracea var. italica*) as conditioned by sulphate supply during germination. *Journal of the Science of Food and Agriculture*. 2008; 88: 904-910.
3. Maldini M, Baima S, Morelli G, Scaccini C, Natella F. A liquid chromatography-mass spectrometry approach to study "glucosinoloma" in broccoli sprouts. *Journal of Mass Spectrometry*. 2012; 47: 1198-1206.
4. Fu W, Magnúsdóttir M, Brynjólfson S, Palsson BØ, Paglia G. UPLC-UV MS(E) analysis for quantification and identification of major carotenoid and chlorophyll species in algae. *Anal Bioanal Chem*. 2012 Dec; 404(10): 3145-54.

Waters

THE SCIENCE OF WHAT'S POSSIBLE.®

June 2013 720004703EN LL-PDF

Waters Corporation
34 Maple Street
Milford, MA 01757 U.S.A.
T: 1 508 478 2000
F: 1 508 872 1990
www.waters.com

Waters
THE SCIENCE OF WHAT'S POSSIBLE.®

Qualitative and Quantitative Characterization of the Metabolome, Lipidome, and Proteome of Human Hepatocytes Stably Transfected with Cytochrome P450 2E1 Using Data Independent LC/MS

Suzanne Geenen,[1] Cristian Cojocariu,[2] Lee Gethings,[2] Janet Hammond,[2] Giorgis Isaac,[3] Lucy Fernandes,[2] Robert Tonge,[2] Johannes Vissers,[2] James Langrige,[2] Ian Wilson[1]

[1] AstraZeneca, Macclesfield, UK; [2] Waters Corporation, Manchester, UK; [3] Waters Corporation, Milford, MA, US

APPLICATION BENEFITS

A label-free multi-omics approach has been applied for the analysis of the transfected human hepatocyte cells by implementing LC/HDMS^E (LC-DIA-IM-MS), providing both qualitative and quantitative information within a single experiment.

WATERS SOLUTIONS

ACQUITY UPLC® System

nanoACQUITY® UPLC® System

SYNAPT® G2 HDMS™

CSH™ Technology

ProteinLynx GlobalSERVER™

MarkerLynx™ Application Manager

TransOmics™ Informatics Software

MS^E/HDMS^E

Triwave® Technology

KEY WORDS

Omics, metabolomics, lipidomics, proteomics, THLE cells

INTRODUCTION

Drug toxicity is a major reason for the failure of candidate pharmaceuticals during their development. Therefore, it is important to realize the potential for toxicity in a timely fashion. Many xenobiotics are bioactivated into toxic metabolites by cytochromes P450 (CYP), as shown in Figure 1. However, the activity of these enzymes typically falls in *in vitro* systems. Recently, a transformed human hepatocyte cell line (THLE) became available, where the metabolic activity of specific CYP isoforms is maintained. THLE cells could be an ideal system to examine the potential toxicity of candidate pharmaceuticals. The baseline effect of the addition of CYP2E1 gene, which encodes a member of the cytochrome P450 superfamily of enzymes into THLE hepatocytes, has been characterized to better understand the biochemistry of this model system. In this application note, a label-free multi-omics approach has been applied for the analysis of the transfected human hepatocyte cell by implementing LC/HDMS^E (LC-DIA-IM-MS), providing both qualitative and quantitative information within a single experiment.

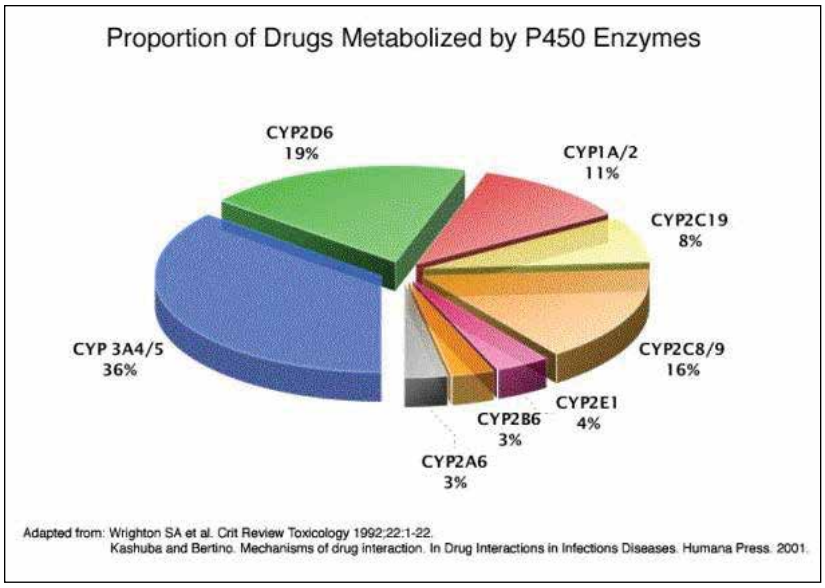

Figure 1. CYPs are the major enzymes involved in drug metabolism, accounting for about 75% of the total metabolism. Most drugs undergo deactivation by CYPs, either directly, or by facilitated excretion from the body.

EXPERIMENTAL

Sample preparation

Dedicated and independent sample preparation protocols were applied in order to isolate metabolites, lipids, or proteins, as shown in Figure 2. Three independent replicates of THLE null or THLE+2E1 cells were investigated for all analyte classes. Proteins were recovered and digested with trypsin overnight.

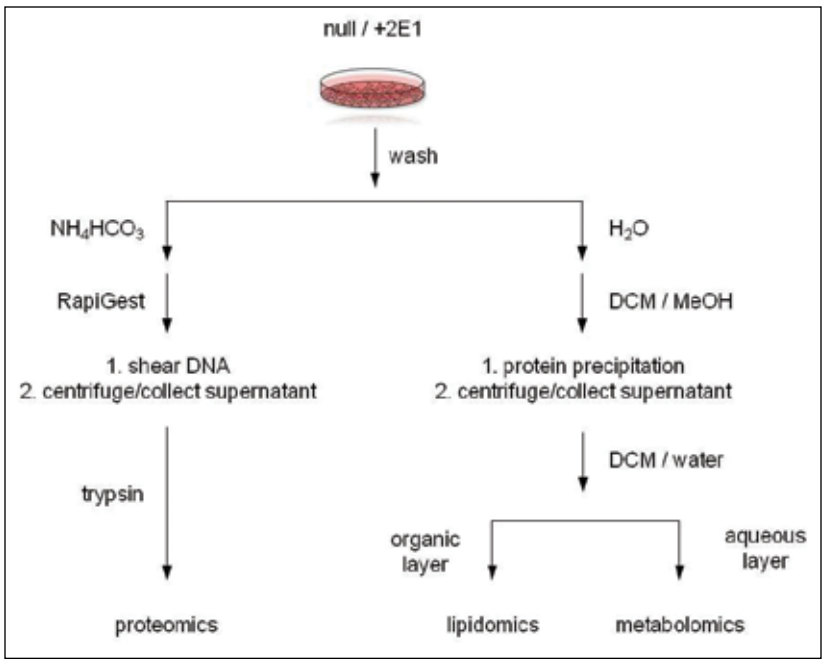

Figure 2. Sample preparation protocol cytochrome P450 2E1 THLE cells for integrated proteomics, lipidomics, and metabolomics LC/MS experiments/studies.

LC/MS conditions

Waters® Omics Research Platform Solution with TransOmics Informatics powered by Nonlinear Dynamics was used for all experiments; generic application-dependent LC conditions were applied throughout. In all instances, MS data were acquired using a data independent analysis (DIA) approach, MS^E, where the energy applied to the collision cell was switched between a low and elevated energy state during alternate scans. For the proteomics experiments, ion mobility separation (IM) was incorporated into the analytical schema (IM-DIA), $HDMS^E$. The principle of an $HDMS^E$ acquisition is shown in Figure 3. Precursor and product ions were associated using dedicated algorithms by retention and/or drift time alignment. For structural elucidation, supplementary MS/MS experiments were conducted for the metabolomics and lipidomics studies.

Label-free LC/MS was used for qualitative and quantitative peptide/protein analyses. Experiments were conducted using a 90 min gradient from 5% to 40% acetonitrile (0.1% formic acid) at 300 nL/min, using a nanoACQUITY UPLC System and an ACQUITY UPLC BEH 1.7 µm C_{18} reversed phase 75 µm x 20 cm nanoscale LC Column.

For metabolite identification, the LC/MS experiments consisted of a 10 min gradient from 0% to 50% acetonitrile (0.1% formic acid) at 500 µL/min, using an ACQUITY UPLC System. Here, an ACQUITY UPLC BEH 1.7 µm C_{18} reversed phase 2.1 x 10 cm LC Column was used.

The lipid separations were conducted with a CSH (Charged Surface Hybrid) C_{18}, 1.7 µm, 2.1 x 100 mm Column, also connected to an ACQUITY UPLC System. Mobile phase A consisted of 10 mM NH_4HCO_2 in ACN/H_2O (60/40); and mobile phase B of 10 mM NH_4HCO_2 in IPA/ACN (90/10). The initial composition of the gradient was 40% B, which was stepped from 43% to 54% B from 2 to 12 min, followed by an additional gradient step from 70% to 99% from 12.1 to 18.0 min. The column flow rate was 400 µL/min and the column temperature maintained at 55 °C.

Data acquisition

Data were acquired through data independent analysis (DIA) that utilized a nanoACQUITY UPLC or ACQUITY UPLC System directly interfaced to a hybrid IM-oaToF SYNAPT G2 Mass Spectrometer.

Bioinformatics

The LC/MS peptide data were processed and searched with ProteinLynx GlobalSERVER v.3.0. Normalized label-free quantification was achieved using TransOmics Informatics Software and additional statistical analysis conducted with Spotfire and EZinfo. The resulting metabolomic and lipidomic data were processed using either MarkerLynx Application Manager or TransOmics Informatics Software, and complementary statistical analysis was conducted with EZinfo.

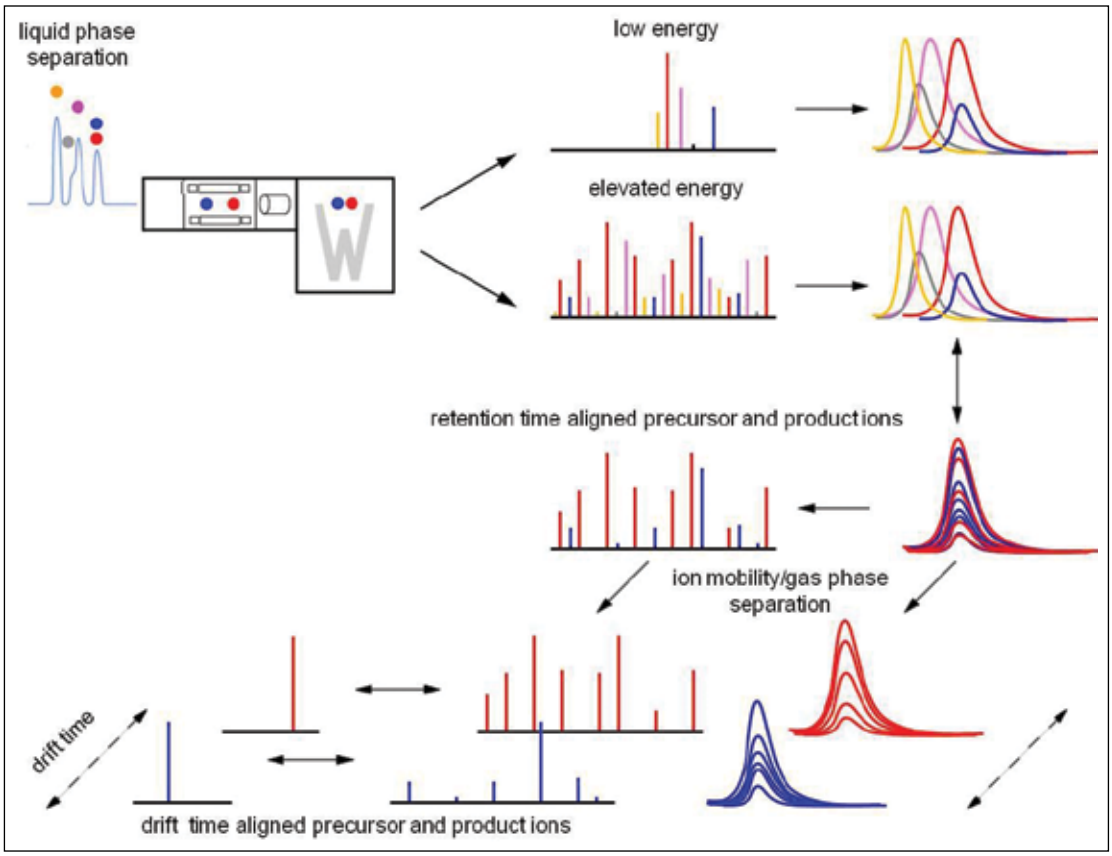

Figure 3. Retention and drift time principle ion mobility enabled data-independent LC/HDMSE analysis (LC-DIA-IM-MS).

RESULTS AND DISCUSSION

Small amounts of the isolated and purified samples were LC/MS analyzed to identify, quantify, and investigate the metabolomic, lipidomic, and proteomic variances between THLE null (CYP2E1 gene absent) and THLE+2E1 cells. Figure 4 shows the type of chromatographic profiles that were typically obtained for the samples, providing chromatographic definition for downstream analysis of the various data streams. In a similar fashion, spectral profiles were obtained for all sample types and in the instance of the proteomics datasets, ion mobility profiles were obtained as well.

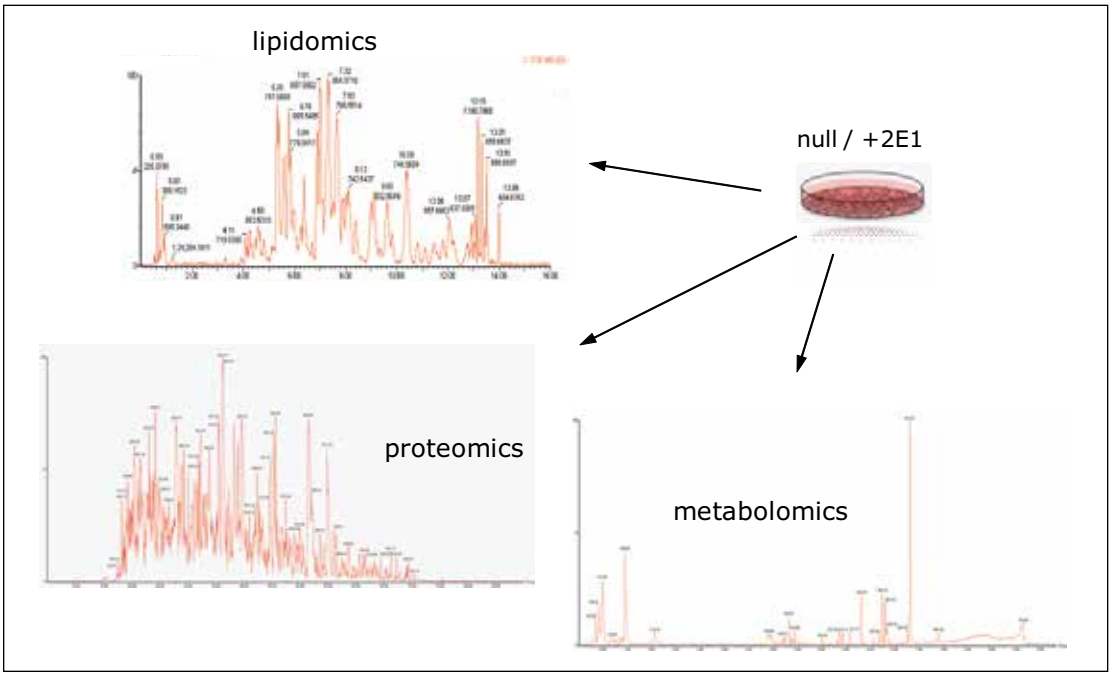

Figure 4. Chromatographic example profiles THLE+2E1 cells. The lipidomics experiments were conducted in ESI(-) mode, whereas the metabolomics and proteomics experiments were carried out in ESI(+) mode.

Principal component analysis (PCA) was used in the first instance to identify and highlight significant differences between THLE null and THLE+2E1 cells; an example is shown in Figure 4. For all experiments, good technical LC/MS measurement replication was observed, with slightly greater biological and/or sample preparation variation. The top pane of Figure 4 illustrates group level analysis of the metabolomics data using TransOmics Informatics Software, whereas the bottom pane of Figure 4 demonstrates analysis at the sample level using EZinfo. Further analysis of the data using MarkerLynx Application Manager indicates significant variance in the metabolic expression of guanine and heteropyrithiamine (data not shown). Similar clustering patterns were observed for the lipid, metabolite, and protein datasets.

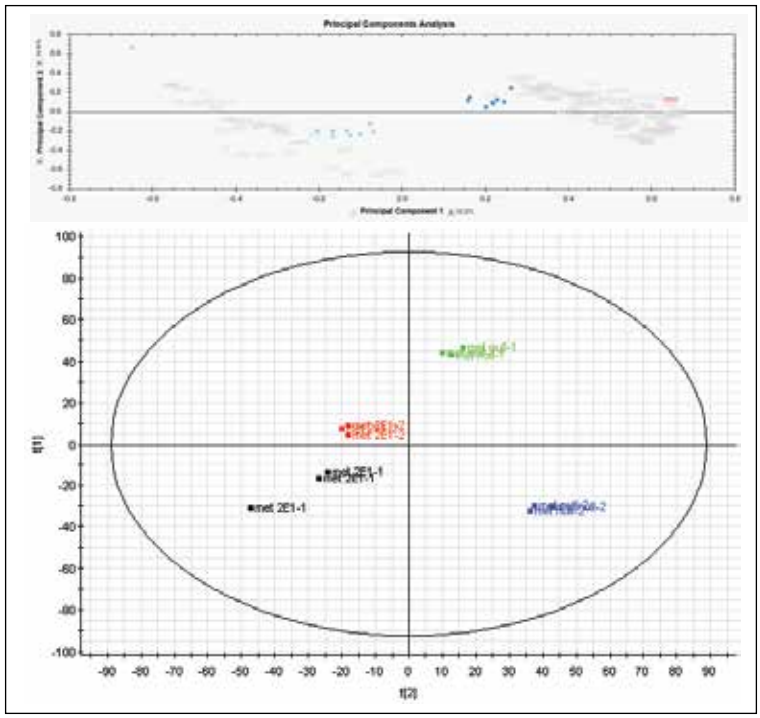

Figure 5. TransOmics Informatics Software (top) and EZinfo (bottom) principal component analysis of the metabolism data, illustrating THLE null versus THLE+2E1 group and sample level differences, respectively.

The estimated protein amounts were normalized and exported to facilitate additional statistical analysis at the protein level. First, hierarchical clustering was conducted, which revealed primary grouping at the technical level and secondary grouping at the sample level, as shown in Figure 6. Next, protein regulation values were calculated as a function of sample group level regulation probability. Only the proteins that were identified for which a regulation probability value could be expressed and found to be common to both samples; *i.e.* THLE null and THLE+2E1 were considered for protein/gene pathway analysis using Ingenuity IPA. The most significantly enriched canonical signalling pathways were EIF2, regulation of EIF4 and p70S6K, mTOR, Actin cytoskeleton, and ILK.

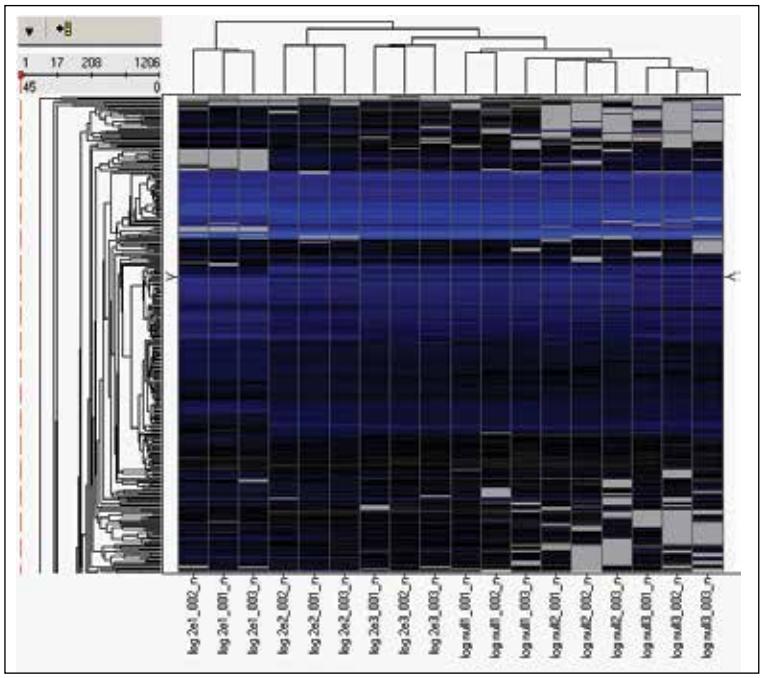

Figure 6. Unsupervised hierarchical clustering protein data using TransOmics Informatics Software normalized, log-scaled estimated protein amounts as input values.

The previously mentioned metabolites interplay with the proteins/genes in the EIF2 (eukaryotic initiation factor 2) signalling pathway, as shown in Figure 7. For example, EIF2B is a guanine nucleotide releasing factor required to release Guanosine diphosphate (GDP), so that a new Guanosine-5'-triphosphate (GTP) molecule can bind and activate EIF2. Moreover, the presence of thiamines is known to inhibit the synthesis of 40S ribosomal subunits. These observations are not unexpected since CYPS readily induce oxidative stress when no substrate is available. Moreover, the EIF2 signalling pathway is one of the primary responders to cellular stress.

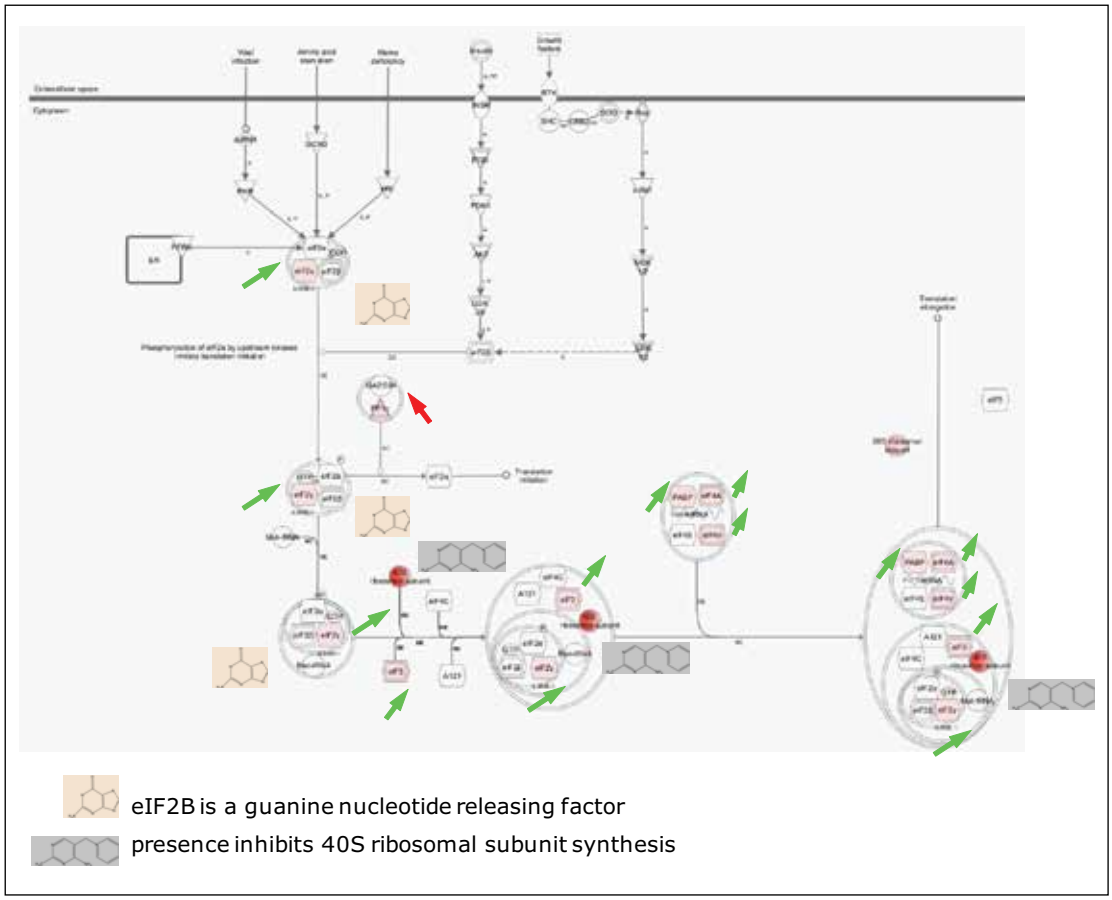

Figure 7. EIF2 signalling pathway, which illustrates up-regulated genes/protein (groups) in green and down-regulated components in red. The size and direction (angle) of the arrows is a measure of the regulation value. The pathway is annotated with two components that were identified as part of the metabolomics track of the experiment/analysis.

CONCLUSIONS

- A label-free multi-omics approach has been applied for the analysis of the transfected human hepatocyte cells by implementing LC/HDMS^E (LC-DIA-IM-MS), providing both qualitative and quantitative information within a single experiment.
- Various clustering, statistical, and data analysis approaches show protein, lipid, and metabolite data to be complimentary.
- A variety of compounds were identified as contributing towards the metabolite and lipid variance.
- Approximately 20% of the proteins identified were significantly expressed with 10% of the proteins illustrating a p value ≤0.05 when common to both samples.
- Complementary information obtained from metabolite/lipid and protein analysis has been shown through the use of guanine and heteropyrithiamine within the EIF2 signaling pathway.

References

1. Liu H, Jones BE, Bradham C, Czaja MJ. Increased cytochrome P-450 2E1 expression sensitizes hepatocytes to c-Jun-mediated cell death from TNF-alpha. Am J Physiol Gastrointest Liver Physiol. 2002 Feb;282(2):G257-66.
2. Pavitt GD, Ron D. New Insights into Translational Regulation in the Endoplasmic Reticulum Unfolded Protein Response. Cold Spring Harb Perspect Biol. 2012 Apr 25; doi: 10.1101/cshperspect.a012278. [Epub ahead of print]
3. Silva JC, Gorenstein MV, Li GZ, Vissers JP, Geromanos SJ. Absolute quantification of proteins by LCMS^E: a virtue of parallel MS acquisition. Mol Cell Proteomics. 2006 Jan;5(1):144-56.
4. Rodríguez-Suárez E, Hughes C, Gethings L, Giles K, Wildgoose J, Stapels M, Fadgen KE, Geromanos SJ, Vissers JP, Elortza F, Langridge JI. An Ion Mobility Assisted Data Independent LC-MS Strategy for the Analysis of Complex Biological Samples. Current. Anal. Chem. special issue: Ion Mobility Spectrometry: Using Size and Shape to Understand Real-World Systems at the Molecular Level, HT-SBJ-CAC-0005.

Waters

THE SCIENCE OF WHAT'S POSSIBLE.®

Waters Corporation
34 Maple Street
Milford, MA 01757 U.S.A.
T: 1 508 478 2000
F: 1 508 872 1990
www.waters.com

Waters
THE SCIENCE OF WHAT'S POSSIBLE.®

Metabolic Phenotyping Using Atmospheric Pressure Gas Chromatography-MS

Vladimir Shulaev,[2] Ghaste Manoj,[2,3] Steven Lai,[1] Carolina Salazar,[2] Nobuhiro Suzuki,[2] Janna Crossley,[2] Feroza Kaneez Coudhury,[2] Khadiza Zaman,[2] Ron Mittler,[2] James Langridge,[1] Robert Plumb,[1] Fulvio Mattivi,[3] Giuseppe Astarita[1]

[1] Waters Corporation, Milford, MA, USA
[2] Department of Biological Sciences, College of Arts and Sciences, University of North Texas, Denton, TX, USA
[3] Department of Food Quality and Nutrition, Research and Innovation Centre, Fondazione Edmund Mach, San Michele all'Adige, Italy

APPLICATION BENEFITS

Atmospheric pressure gas chromatography mass spectrometry (APGC-MS) provides molecular ion information, which is typically absent when traditional vacuum source (i.e., electron ionization) gas chromatography mass spectrometry (GC-MS) is employed. This application note highlights the use of APGC-MS^E for analysis in metabolomics.

WATERS SOLUTIONS

SYNAPT® G2-S HDMS®
Mass Spectrometer

APGC System

Progenesis® QI Software

MassLynx® Software v4.1 SCN870

KEY WORDS

Metabolomics, GC, atmospheric pressure gas chromatography

INTRODUCTION

Gas chromatography coupled with mass spectrometry is a well established analytical approach to metabolomics. The most widely used ionization technique is electron ionization (EI), which produces highly fragmented spectra that are library searchable. The molecular ion in an EI spectrum is often absent or of very low abundance. The lack of molecular ion information, especially for derivatized compounds in complex mixtures, can lead to incorrect identification when using spectral matching alone.

Atmospheric pressure GC (APGC) is a soft chemical ionization technique that generates a mass spectrum in which there is minimal fragmentation and conservation of the molecular ion (Figure 1). Additionally, when APGC is combined with a time of flight mass spectrometer (TOF-MS) for exact mass MS^E analysis, comprehensive precursor and fragment ion spectral data is obtained for every detectable component in a complex sample. GC-MS^E offers a simple route to providing high selectivity and confidence for simultaneous identification and quantitation in a single analysis.

Here we report an APGC-TOF MS^E profiling approach and its application to metabolic fingerprinting of Arabidopsis.

EXPERIMENTAL

GC conditions

GC system:	7890A GC
Column:	HP-5MS column, 30 m length, 0.25 mm I.D., and 0.25 µm film thickness (Agilent Technologies)
Carrier gas:	Helium 1 mL/min
Temp. gradient:	Initial 70 °C, 5 °C/min to 310 °C, hold 1 min
Injection type:	split mode (split 4:1)
Injector temp.:	230 °C
Injection vol.:	1 µL
Make-up gas:	Nitrogen 400 mL/min
Transfer line temp.:	310 °C

MS conditions

MS system:	SYNAPT G2-S HDMS
Mode of operation:	TOF-MS^{E}
Ionization:	APGC
Corona current:	3 µA
Cone voltage:	20 V
Source temp.:	150 °C
Cone gas:	10 L/h
Auxiliary gas flow:	500 L/h
MS gas:	Nitrogen
Acquisition range:	50 to 1200
Transfer CE:	Ramp 20 to 40 V

Data management

Progenesis QI Software v1.0

MassLynx Software v4.1 SCN870

Sample preparation

Arabidopsis thaliana seeds were grown under controlled conditions. Seedlings were harvested and polar metabolites were extracted and derivatized. The dried polar phase was methoximated for 90 minutes at 45 °C and trimethylsilylated for 30 minutes at 37 °C.

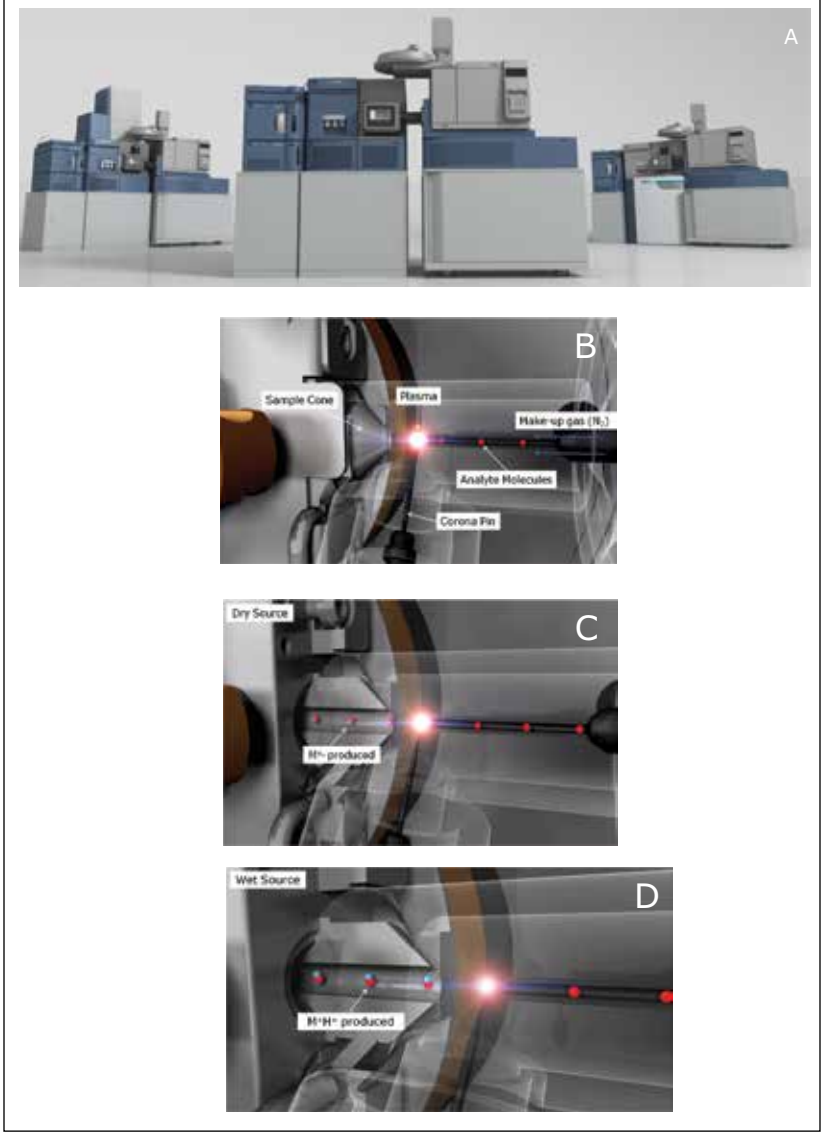

Figure 1. A) An APGC System can be coupled to various Waters MS instruments, including the Xevo® TQ-S and the SYNAPT G2-S. The changeover from UPLC® to APGC takes less than five minutes. B) The APGC source consists of an ion chamber with a corona pin inside. The GC column enters the source via a heated transfer line. Corona discharge creates nitrogen plasma within this region. Radical cations generated in this plasma interact and ionize the analyte molecules. The ions created are then transferred to the mass analyzer. C) Under dry source conditions the predominant method of ionization is charge transfer, generating molecular radical cations [$M^{+\bullet}$]. This method favours relatively non-polar molecules. D) When a protic solvent, such as water or methanol, is added to the source, the predominant ionisation is proton transfer, generating [$M^{+}H]^{+}$ ions. This method favors relatively polar molecules.

RESULTS AND DISCUSSION

APGC-MS analysis of commercially available pure reference compounds of known plant metabolites was performed. Following the analysis, an in-house APGC reference database was created containing retention times, and accurate mass-to-charge ratio (*m/z*) for precursor and fragment ions (Figure 2). APGC provided abundant molecular ions with minimal fragmentation at low collision energy (Figure 2A). To add confidence to compound identification, collision energy was ramped from 20 to 40 eV in the high energy function to generate maximum information from fragment ions (Figure 2A). Due to the use of charge exchange chemical ionization, elevated collision energy data resulted in a spectrum similar to the traditional EI data (Figure 2B).

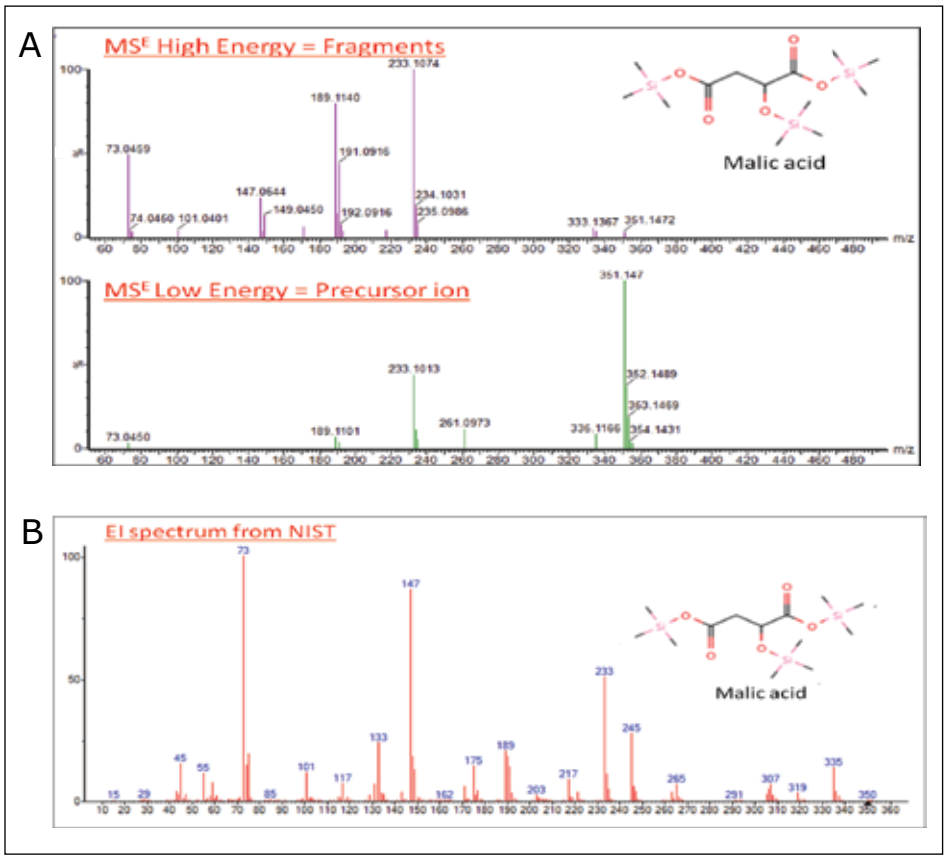

Figure 2. A) Synthetic reference standards were derivatized and analyzed by APGC-SYNAPT HDMS using MS^E acquisition mode. This mode alternates between low and elevated collision energy to acquire both precursor and product ion information in a single analytical run. Advanced software algorithms align precursor and fragment spectra according to retention time and links them together. An in-house database of derivatized precursors and fragments, and retention times was created. B) EI spectrum of derivatized malic acid, obtained from the NIST library, was comparable with the MS^E spectrum obtained by ramping up the collision energy from 20 to 40 eV in the high energy function.

Plant extracts were analyzed using APGC-TOF MS^E and raw data were imported to Progenesis QI Software for processing and analysis (Figure 3A and B). Multivariate statistical analysis highlighted the molecular differences between groups of samples (Figure 4A and B). The Progenesis QI search engine Metascope allowed us to query experimentally-derived or in-house databases. We were able to customize the search parameters for the metabolite identification according to multiple orthogonal measures such as mass accuracy, retention time and fragmentation matching (Figure 4C). Additionally, if ion mobility is activated, collision cross-section (CCS) data, which reflect the ionic shape of the metabolites in the gas phase, can also be mined for identification.

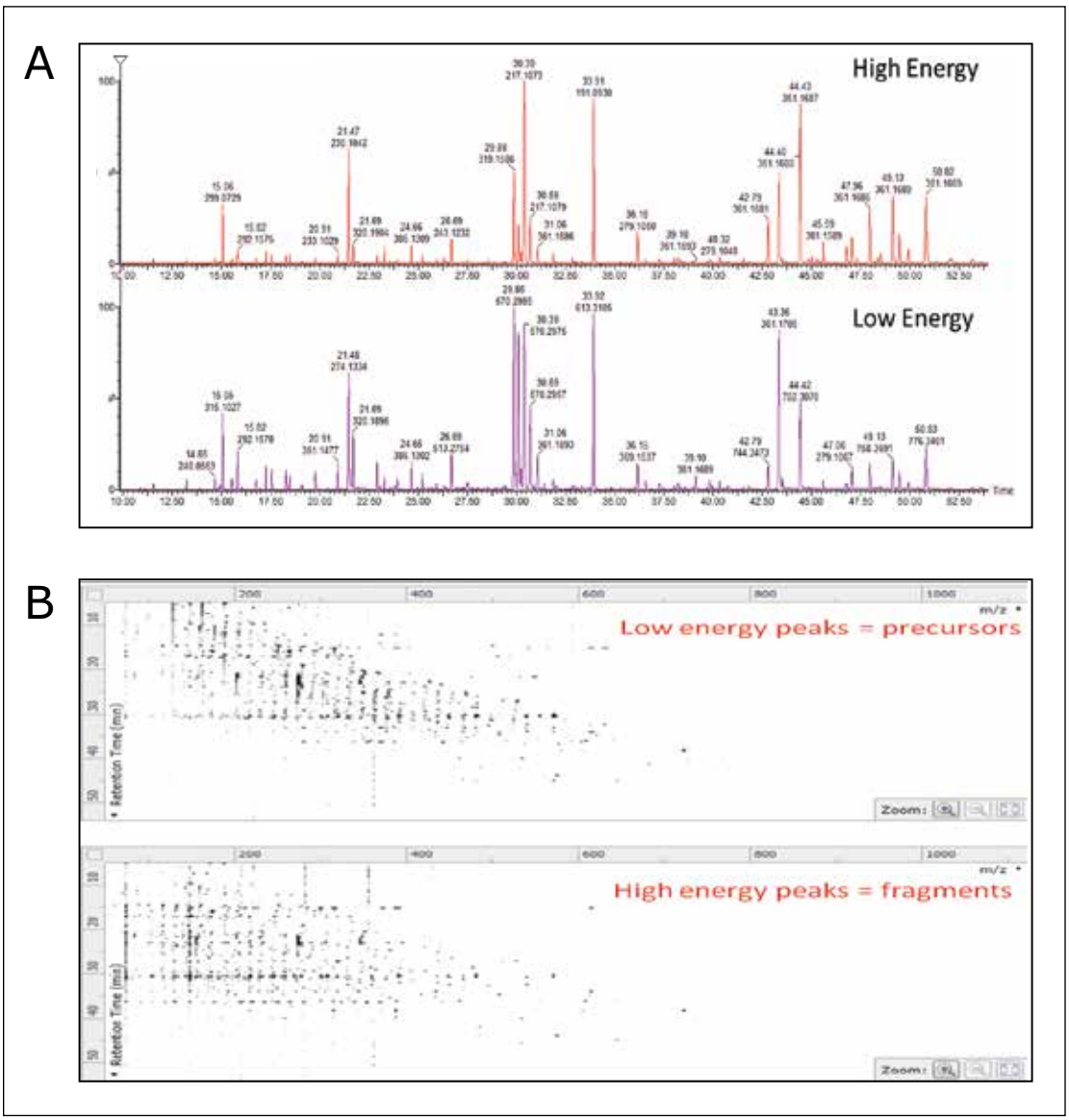

Figure 3. Biological samples were analyzed using APGC-MS^E which provided information for both the intact precursor ions (at low collision energy) and the fragment ions (high collision energy). A) APGC-MS^E chromatogram of the Col-0 Arabidopsis leaf extract. B) Data were imported as bidimentional maps (retention times versus m/z) and processed using Progenesis QI.

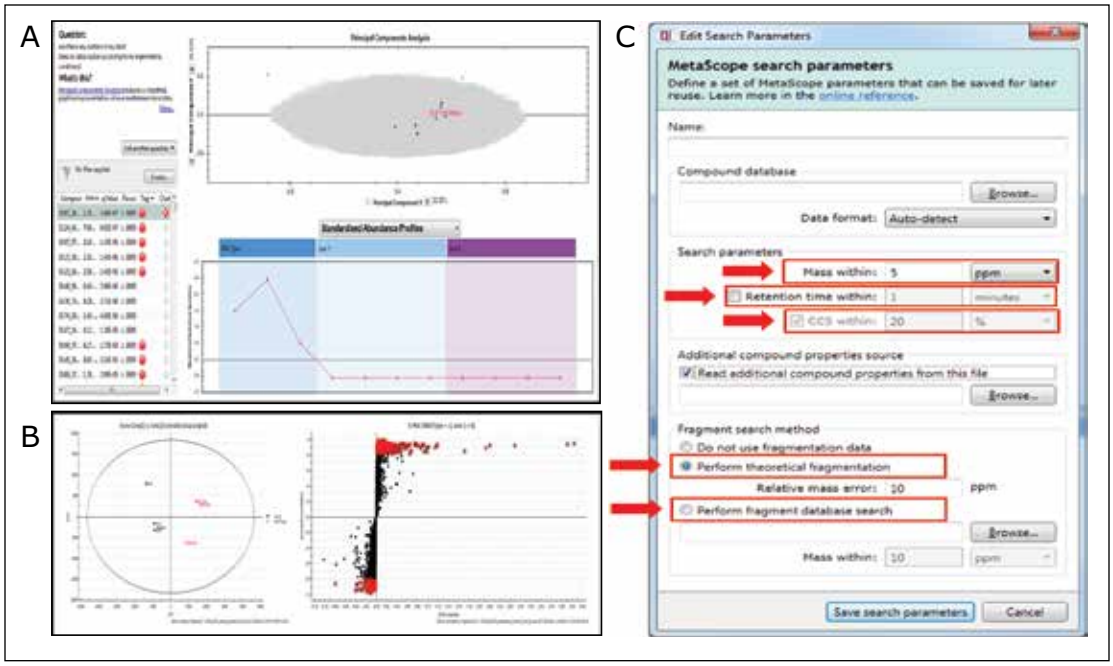

Figure 4. A) PCA model for wild type and mutant lines. B) OPLS-DA model for Arabidopsis Col-O wild type plants and mutant line. C) The Progenesis QI search engine allowed us to query experimentally-derived or in-house databases.

Sample data, generated with the low energy (precursor ion) spectrum and high energy (fragment ion) spectrum of each component, was searched against both the in-house and commercial mass spectrum libraries (Figure 5A and B). The identification score described the level of confidence obtained for each library hit based on accurate mass for precursor and fragment matching, retention time, and isotope ratios (Figure 5A and B).

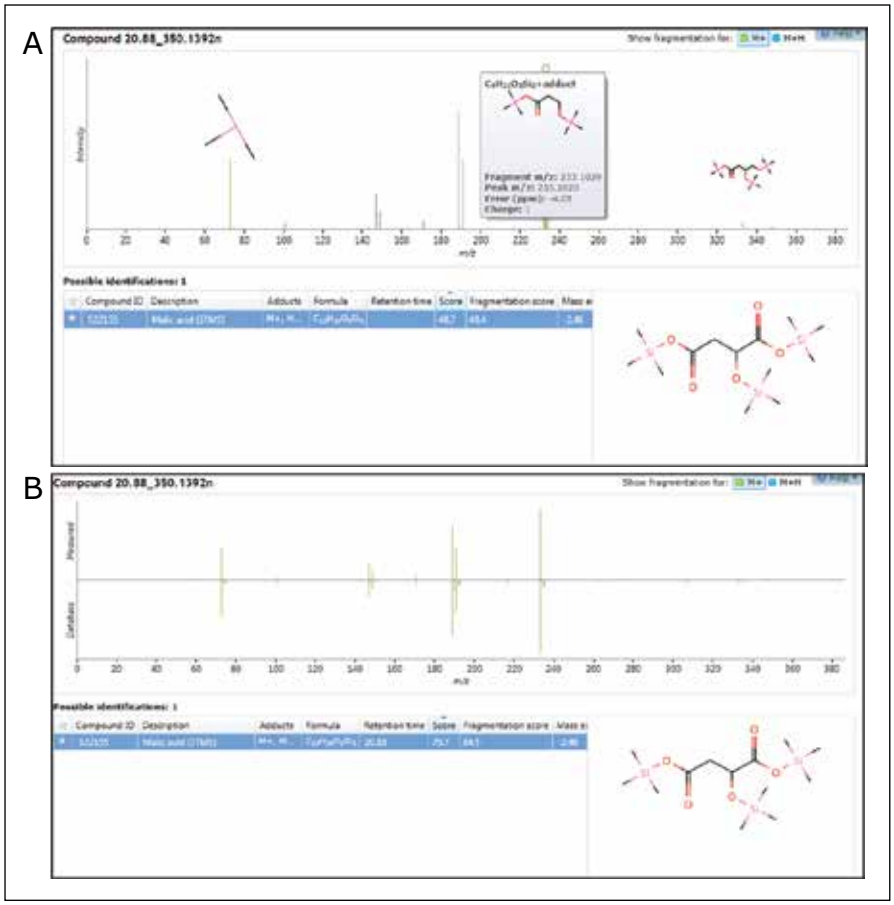

Figure 5. A) APGC-MS^E allowed the identification of malic acid extracted from a biological matrix, using theoretical fragmentation within Progenesis QI. The spectra of fragment ions were aligned with co-eluting precursor ions and matched against theoretically generated spectra (green signals). B) The identification score improved when identification of malic acid was conducted using an in-house database within Progenesis QI. The spectra of fragment ions were aligned with co-eluting precursor ions and matched against experimentally generated spectra (green signals).

As structurally similar metabolites often co-elute, the concurrent acquisition of an intact molecular ion, along with fragmentation data for sub-structural determination, was particularly useful. In combination with accurate mass measurement, the molecular ion helps determine the limits of chemical composition, which can subsequently be used along with the fragmentation data for more detailed and specific structural elucidation of both known and unknown metabolites.

A summary workflow for the APGC-TOF-MS^E approach:

1. An in-house database of derivatized metabolites was generated using APGC-MS.^{E}
2. APGC provided abundant molecular ions with minimal fragmentation at low collision energy, which are typically missing when traditional vacuum source GC-MS is employed.
3. Due to the use of charge exchange chemical ionization, the elevated collision energy data resulted in a spectrum similar to the traditional EI data.
4. APGC-MS approach was used for metabolic fingerprinting of a set of Arabidopsis mutants.
5. Sample data generated with the low and high energy function (MS^E) were searched against the in-house database using the search engine within Progenesis QI.

CONCLUSIONS

APGC-TOF MS^E with Progenesis QI is a valuable solution for metabolomics applications. The use of orthogonal information for the metabolite identification, including accurate mass, retention time, and theoretical or measured fragmentation, increased the confidence of metabolite identification while decreasing the number of false positive identifications.

Waters

THE SCIENCE OF WHAT'S POSSIBLE.®

Waters Corporation
34 Maple Street
Milford, MA 01757 U.S.A.
T: 1 508 478 2000
F: 1 508 872 1990
www.waters.com

Waters
THE SCIENCE OF WHAT'S POSSIBLE.®

The Use of HRMS and Statistical Analysis in the Investigation of Basmati Rice Authenticity and Potential Food Fraud

Gareth Cleland,[1] Adam Ladak,[2] Steven Lai,[2] and Jennifer Burgess[1]
[1]Waters Corporation, Milford, MA, USA
[2]Waters Corporation, Beverly, MA, USA

APPLICATION BENEFITS

- Authenticity of food
- Detecting food fraud
- Metabolomics

WATERS SOLUTIONS

MassLynx® Software

Atmospheric Pressure Gas Chromatography (APGC)

SYNAPT® G2-S*i* High Definition Mass Spectrometry® (HDMS®)

Progenesis® QI Software

KEY WORDS

HDMS^E, APGC, Multivariate Analysis, MVA, spectral cleanup, ion mobility, data alignment, CCS, food fraud, food authenticity, food safety, food research

INTRODUCTION

There is increased concern regarding the authenticity of basmati rice throughout the world. For years, traders have been passing off a lesser quality rice as the world's finest long-grained, aromatic rice, basmati, in key markets like the US, Canada, and the EU. A DNA rice authenticity verification service in India has concluded that more than 30% of the basmati rice sold in the retail markets of the US and Canada is adulterated with inferior quality grains.[1] In Britain, the Food Standard Agency found in 2005 that about half of all basmati rice sold was adulterated with other strains of long-grain rice.[2]

Genuine basmati rice is grown in the foothills of the Himalayas. What external factors play a part in the growth of the rice? Can a basmati strain grown elsewhere in the world can be classed as basmati rice?

A proof of principle method has been established to assess the authenticity of basmati rice using off the shelf supermarket samples with the latest advancements in high resolution GC-MS hardware and informatics. Volatile compounds of interest were extracted from heated dry rice via SPME and headspace. Following a generic GC separation, detection was performed using a Waters® SYNAPT G2-S*i* MS run in HDMS^E mode.[3] Collection of an HDMS^E dataset offers a high level of specificity as a result of an ion mobility separation of compounds based on size, shape, and charge, performed after and orthogonal to a GC or UPLC separation.

Progenesis QI, the latest OMICS informatics package from Waters, is designed to utilize the 4-dimensional data produced during a SYNAPT G2-S*i* HDMS^E acquisition. Initially, alignment of all injections is performed followed by the unique peak co-detection process resulting in the same number of analyte measurements in every sample and no missing values. Data from all isotopes and adducts of a parent compound are then deconvoluted giving a single robust and accurate measurement for that parent compound. Compounds of interest were highlighted using various Multi Variate Analysis (MVA) techniques and identified using elucidation tools and relevant database searches within the software platform.

EXPERIMENTAL

Autosampler conditions

System:	CTC PAL
Incubation temp.:	120 °C
Extraction time:	300 s
Desorption time:	600 s
SPME Fiber:	Supelco SPME fiber assembly (DVB/CAR/PDMS) 50/30 µm coating

GC conditions

GC system:	7890A GC
Column:	DB5-MS 30 m x 0.25 mm x 0.25 µm film
Carrier gas:	He 2 mL/min
Temp. gradient:	Initial 40 °C for 2 minutes, 30 °C/min to 130 °C, 10 °C to 270 °C, 30 °C to 320 °C, hold 2 min
Injection type:	Pulsed splitless
Injector temp.:	250 °C
Pulse time:	2.00 min
Pulse pressure:	550 KPa
Injection volume:	2 mL
Make up gas:	N_2 at 200 mL/min
Transfer line temp.:	330 °C

Data processing

Principle Component Analysis (PCA), Orthogonal Projections to Latent Structures Discriminent Analysis (OPLS-DA), and Correlation Analysis were statistical analysis algorithms utilized within EZ Info and Progenesis QI.

MS conditions

MS system:	SYNAPT G2-S*i*
Mode:	API
Corona:	2.2 µA
Cone gas:	220 L/h
Aux gas:	200 L/h
Source temp.:	150 °C
Low energy CE:	4 V
High energy CE ramp:	10 to 45 V

Sample preparation

Several varieties of rice from different producers, shown in Table 1, were obtained from local supermarkets. Sample IDs were given to avoid brand disclosure. 10 g of dried rice was weighed out in a 20 mL amber headspace vial. Rice samples were prepared in triplicate as to provide three replicate injections for each sample without returning to the same vial. A pooled, composite sample was prepared by mixing 100 g of each rice sample together prior to weighing out 10 g vials. All samples were placed in the autosampler tray and data collected with a randomized sample list.

Sample	Description	Sample ID
1	Basmati Manufacturer 1	BAS M1
2	Basmati Manufacturer 2	BAS M2
3	Long Grain Manufacturer 3	LG M3
4	Basmati Manufacturer 4	BAS M4
5	Jasmine Manufacturer 5	JAS M5
6	Basmati Manufacturer 3	BAS M3
7	Jasmine Manufacturer 4	JAS M4
8	Composite Sample	Pool

Sample preparation

Several varieties of rice from different producers, shown in Table 1, were obtained from local supermarkets. Sample IDs were given to avoid brand disclosure. 10 g of dried rice was weighed out in a 20 mL amber headspace vial. Rice samples were prepared in triplicate as to provide three replicate injections for each sample without returning to the same vial. A pooled, composite sample was prepared by mixing 100 g of each rice sample together prior to weighing out 10 g vials. All samples were placed in the autosampler tray and data collected with a randomized sample list.

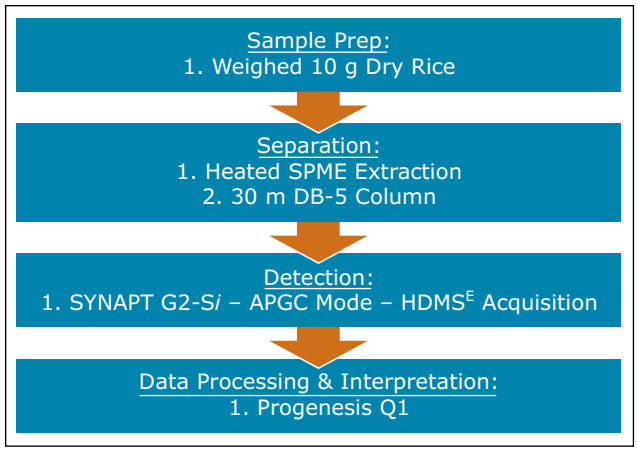

Figure 1. Analysis workflow for rice samples in this study.

RESULTS AND DISCUSSION

Collection and interrogation of a comprehensive APGC/HDMS^E non-targeted dataset was performed following the analysis workflow shown in Figure 1. Atmospheric Pressure Gas Chromatography (APGC) is a 'soft' ionization technique resulting in less compound fragmentation when compared to conventional electron ionization (EI).[4]

Increased abundance of precursor ion enhances sensitivity for
Data processing was performed using Progenesis QI, the latest Omics software package from Waters fully able to utilize the information afforded in HDMS^E datasets. Progenesis QI is a novel software platform that is able to perform alignment, peak picking and mining of data to quantify then identify significant molecular differences between groups of samples.

Following alignment, peak detection and deconvolution, 3885 compound ions were investigated. Initially, Principle Component Analysis (PCA) was performed yielding the scores plot in Figure 2. Tight pooling of injections from replicate samples and a centralized composite/pool sample indicated a statistically relevant dataset. Some of the basmati rice samples fell in the upper left quadrant, jasmine rice samples fell in the lower right quadrant and a long grain rice in the upper right quadrant. Exceptions to the pooling of the rice types were observed for two basmati rice samples. One originated from the same producer as a jasmine rice and pooled with other jasmine rice samples (BAS M4). The second basmati outlier (BAS M3) came from the same producer as the long grain rice and pooled alongside this long grain rice sample (LGM3).

Since the origin of these stored purchased samples is essentially unknown, it is not possible to draw conclusions about the origin or purity of the samples. The aim of this work was to devise a proof-of-principle method for the investigation of basmati rice authenticity and potential food fraud. A study with a larger number of well characterized samples, including both authentic and non-authentic basmati rice samples, is required. Finding unique markers of interest in this new study may then make it possible for a pass/fail method to be established on a more routinely used instrument in a quality control laboratory, such as a single or tandem quadrupole.

Further investigation into the data was performed using a supervised Orthogonal Projections to Latent Structures Discriminant Analysis (OPLS-DA) model. For this, the markers comprising the injections for the basmati rice samples (BAS M1 and BAS M2), highlighted with blue squares in Figure 2, were compared to the markers comprising the long grain rice sample (LG M3), highlighted with red squares in Figure 2. The S-plot from this analysis is shown in Figure 3 where the x-axis shows the measure of the magnitude of change in a particular analyte, and the y-axis shows a measure of analyte significance in the two-group comparison. Significant markers or ions of interest, highlighted with red squares in Figure 3, are the ions representing the significant markers with the biggest difference between the two rice types. Once highlighted, a set of markers can be tagged with a simple right mouse click. This subset of analytes can then be assigned a 'tag' within Progenesis QI for further consideration.

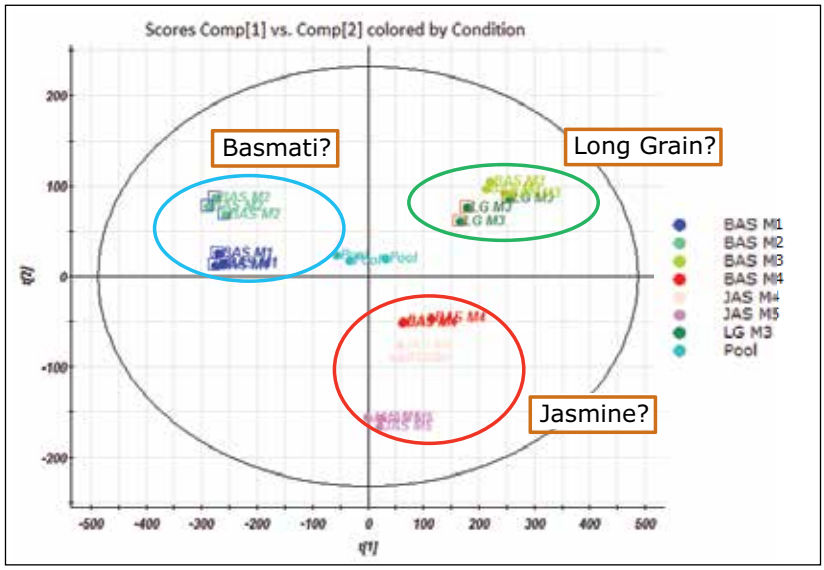

Figure 2. Scores plot from the PCA performed on rice samples.

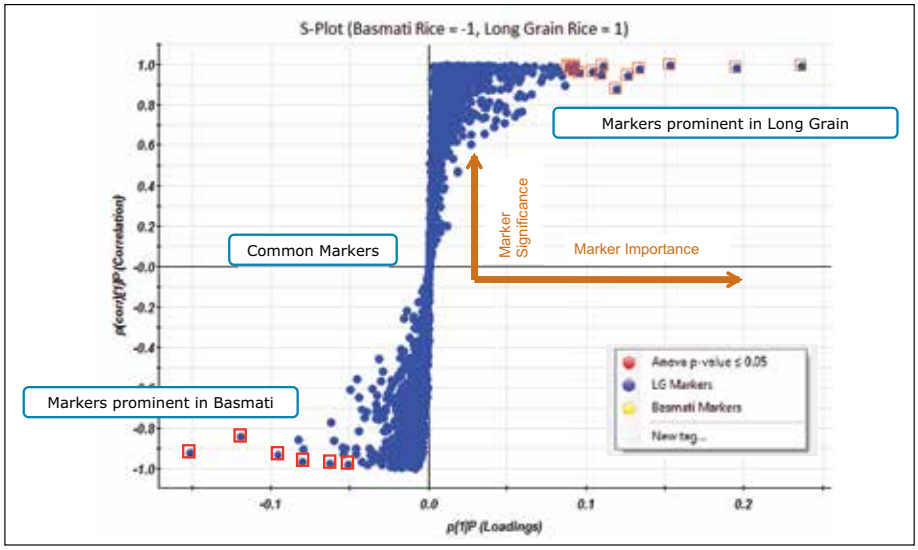

Figure 3. OPLS-DA model showing differences between basmati rice and long grain rice samples.

Figure 4 shows the standardized abundance profile for the six markers tagged in basmati rice. The standardized abundance profile (also known as a trend plot) shows the normalized intensity of the six markers of interest that were highest in basmati M1 and M2 samples compared to all other injections. Their presence in the composite sample (pool) is expected owing to the contribution of the M1 and M2 samples.

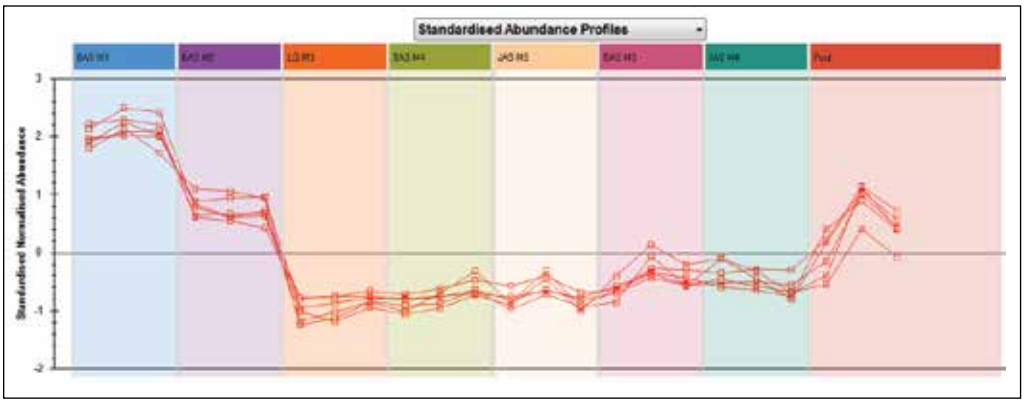

Figure 4. Standardized abundance profiles for six basmati rice-related markers.

Further interrogation of the 3885 compounds ions was performed using default quick tag filters and the Correlation Analysis, available within Progenesis QI. Applying the quick tag filter for ANOVA P value ($p<0.05$), resulted in a focus on 2907 statistically significant ions from the 3885 originally generated. Figure 5 shows the table of markers satisfying the ANOVA P value filter (A). The standardized abundance profile for a marker of interest previously obtained from the S-Plot in Figure 3, is also displayed (B). Selecting Correlation Analysis from the highlighted dropdown menu (C) results in a Dendrogram of markers. The correlation analysis groups compounds according to how similar their abundance profiles are across all samples. Our marker of interest is shown as the red line highlighted by the circle (D). Markers showing a similar abundance profile are found within the same Dendrogram branch.

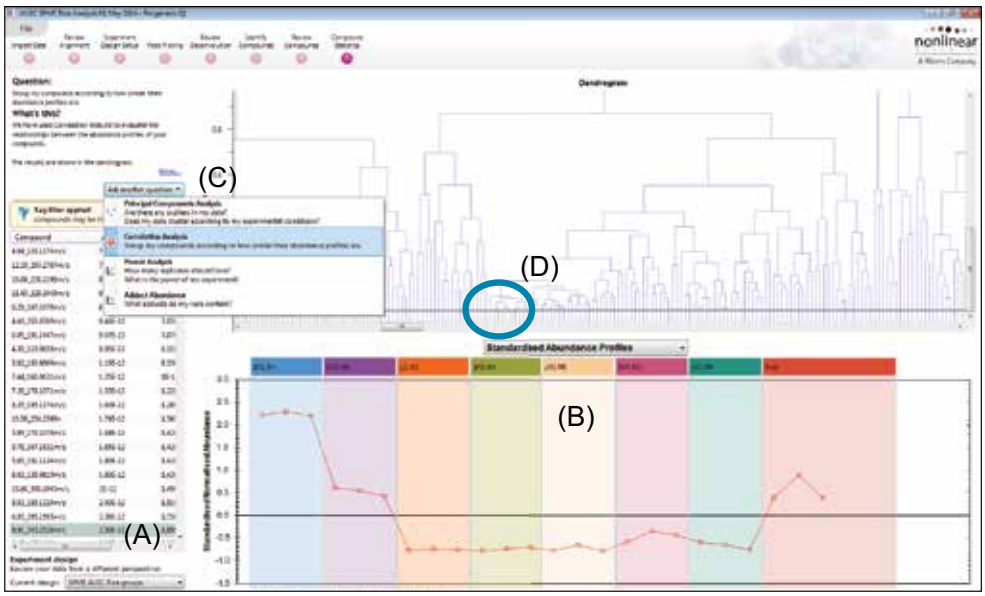

Figure 5. Accessing and using the correlation analysis within Progenesis QI (C) enables the user to extract further ions of interest that follow a similar profile to a selected marker (B).

These markers of a similar profile to the one highlighted are easily isolated, viewed and tagged using the Dendrogram within the Correlation Analysis, as shown in Figure 6. Over 50 markers of interest in basmati rice, showing a similar trend across all injections, have now been isolated and tagged.

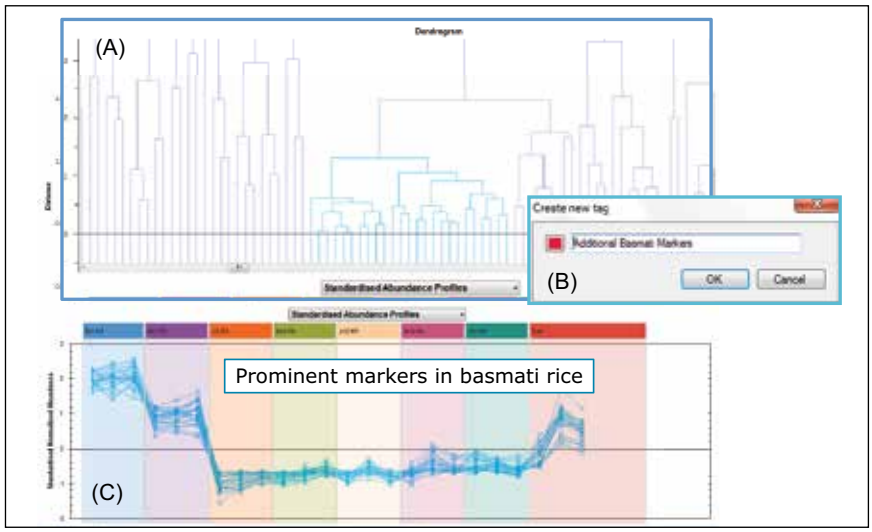

Figure 6. (A) Further markers of interest in basmati rice, isolated using the Correlation Analysis in Progenesis QI. (B) A right click allows easy tagging of these markers for elucidation. (C) Standardized abundance profiles of all 57 isolated markers are shown across all injections.

The same steps were followed for selection of the key markers in the long grain rice sample (LGM3). The standardized abundance profile of 26 markers of interest, extracted using the correlation analysis within Progenesis QI, in long grain rice are displayed in Figure 7. As can be seen from Figure 7, the basmati rice from the same producer as the long grain rice showed very similar abundance profiles on the same markers of interest; yet none of these markers were observed in other basmati rice samples. This could imply that is very little difference between the basmati rice and the long grain rice samples from this producer. This could also imply that packaging material is having an impact on our profiling.

A study with a larger number of well characterized samples, including both authentic and non-authentic basmati rice samples, is required to test this proof-of-principle method, as previously mentioned.

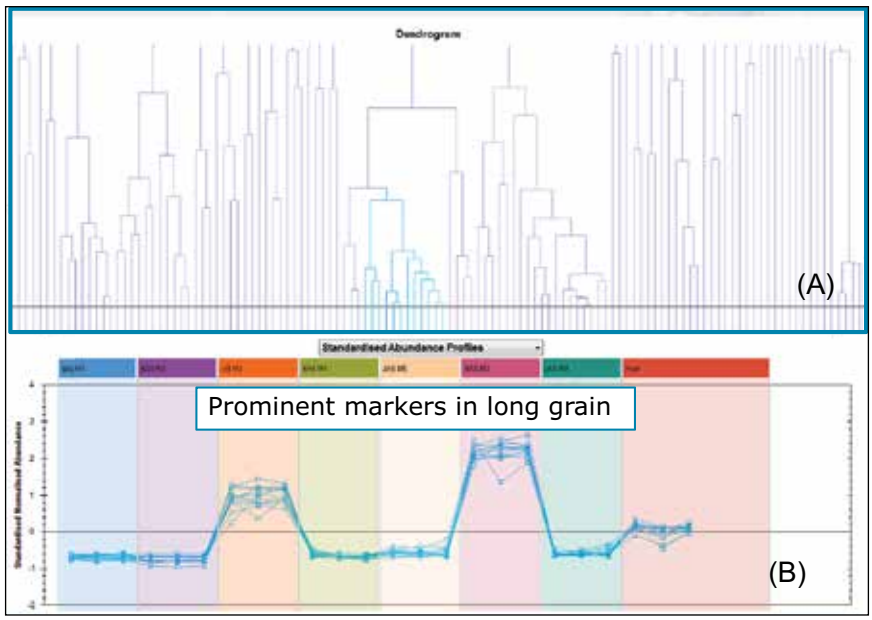

Figure 7. (A) Markers of interest in long grain rice isolated using Correlation Analysis. (B) Standardized abundance profiles of all 26 isolated markers across all injections.

Once markers of interest have been isolated there are several options for elucidation and identification:

1. Structural elucidation within MassLynx Software.
2. Batch database searching within Progenesis QI.
3. Batch database searching outside of Progenesis QI.

Structural elucidation

To determine the structure of an ion of interest the mass, or formula (from elemental composition calculation) is submitted to a chemical structure database, such as ChemSpider. A selected structure resulting from the search is checked for matching high energy accurate mass fragment ions using the MassFragment™ tool. Figure 8 summarizes the steps involved in structural elucidation for the marker 271.2644 Da at 10.79 minutes (10.79_271.2644) obtained from the OPLS-DA analysis. To confirm the proposed structure, a purchased or synthesized standard would have to be analyzed using GC-MS/MS.

Note: Progenesis QI V2.0, available end 2014, will have Elemental Composition and ChemSpider search functionality embedded within the software. These functions were not available for use when this project was completed.

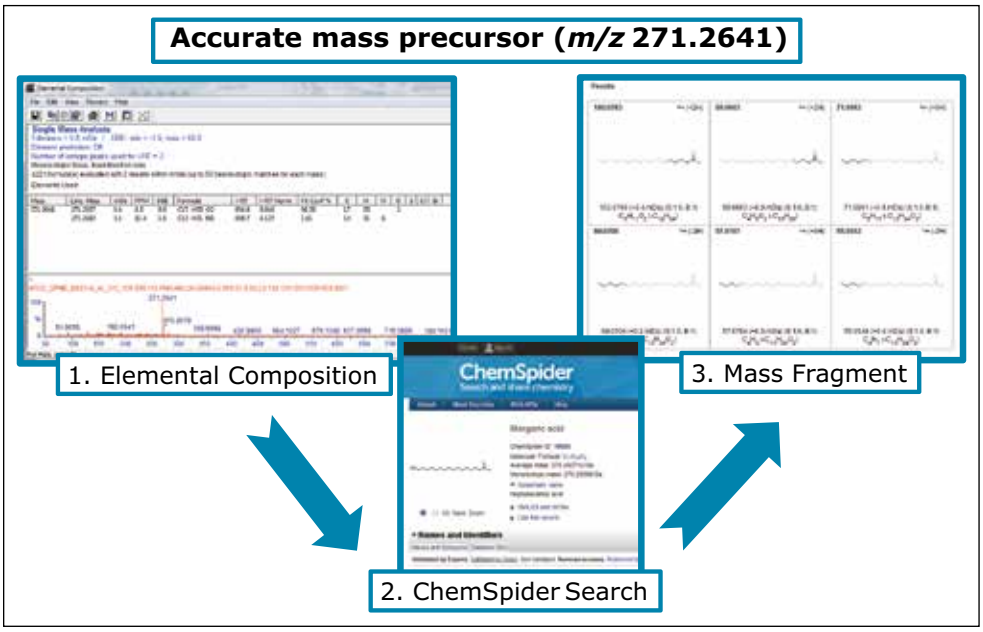

Figure 8. MassLynx Software's structural elucidation workflow for isolated markers of interest.

Database searching within Progenesis QI

Progenesis QI's search engine (Progenesis Metascope) allows users to query in-house and publicly available databases. Search parameters can be customized to maximize all aspects of the data acquired to the database being searched. A list of potential identifications is generated and scored using criteria such as mass accuracy, isotope distribution, retention time, drift time, and fragment matching. If the chosen database contains structures, theoretical fragmentation of the molecule is performed and a fragmentation score is used to rank potential identifications of high energy accurate mass fragment ions to the theoretical dissociation of the molecule.

Figure 9 highlights these customizable database searching parameters in Progenesis QI software (A). An example identification of the marker elucidated earlier is shown (B) when searching several downloaded publically available databases (NIST, ChEBI, and HMDB), and the search settings used in Figure 9A. High spectral specificity (spectral cleanup) is observed due to the ability of the software to time align and drift align spectra from the four-dimensional HDMS^E acquisition. All fragments in the high energy spectrum of Figure 9 (B) have been assigned to the theoretical dissociation of the molecule proposed in the database search, which increases confidence in the identification made. Identification of the same molecule via elucidation within MassLynx and via database searching within Progenesis QI also increases confidence in the identifications made.

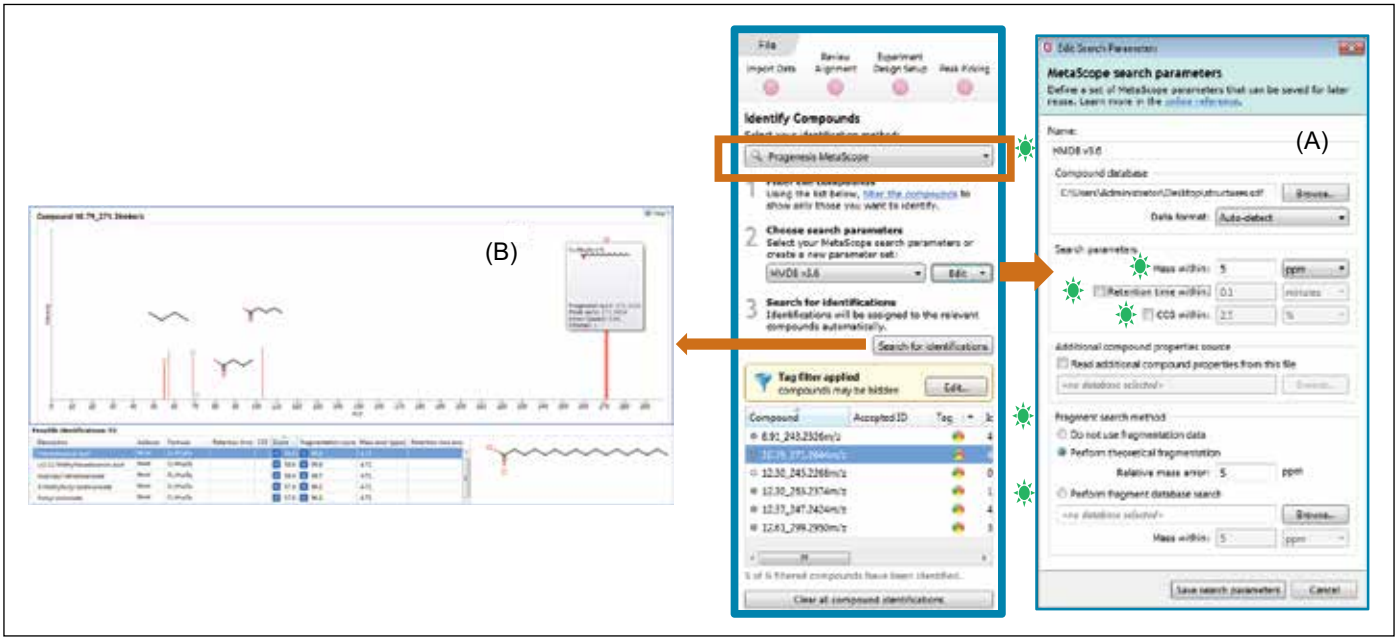

Figure 9. Database and search settings available in Progenesis QI (A). An example of a typical identification is also shown (B).

Database searching outside of Progenesis QI

Batch submission to the METLIN (Metabolite and Tandem MS Database) is also possible using a clipboard copied list of masses from Progenesis QI, Figure 10. The Scripts Center for Metabolomics web page is automatically launched when the user copies a list of tag filtered markers of interest to the clipboard. MS/MS spectra within the METLIN database can be used to compare to the drift and time aligned high energy spectra obtained from a HDMS^E acquisition.

Figure 10. Screen capture of the compound identification page in Progenesis QI. Highlighted areas show the ease of batch submission for markers of interest to an external (METLIN) database.

CONCLUSIONS

- Data independent, information rich, HDMS^E acquisitions enable accurate mass precursor and accurate mass product ion information to be captured in a single chromatographic run.
- APGC is a soft ionization technique which results in an increased abundance of the parent ion and therefore enhances sensitivity and specificity.
- The combination of a GC separation, an HDMS^E acquisition, and informatics that is able to process and review four dimensional data results in a unprecedented level of specificity for all compounds the chromatographic run.
- Alignment algorithms within Progenesis QI enable features across injections to be properly aligned prior to peak picking. This improves the ability to track ions of interest across all injections in an analysis.
- Progenesis QI effectively streamlines and simplifies complicated non targeted, unknown screening workflows and makes compound isolation and identification faster, easier, and more robust.
- Statistical analysis models within the software such as PCA, OPLS-DA, and Correlation Analysis allow ions of interest in complex matrices to be isolated with ease.
- Easy-to-use database searching allows ions of interest to be identified from several publically available databases.
- The combined use of APGC, SYNAPT G2-S*i* and Progenesis QI Software allow a flexible configuration that can be used for food fraud and food authenticity applications.

References

1. The Economic Times, "Basmati Export Adulteration Leaves Bad Taste in Mouth", Prabha Jagannathan, Jul 6, 2007. http://articles.economictimes.indiatimes.com/2007-07-06/news/28467196_1_basmati-rice-india-s-basmati-basmati-export
2. Contamination concerns force new Basmati regulations, Fletcher A, August 2005. http://www.foodnavigator.com/Legislation/Contamination-concerns-force-new-Basmati-regulations
3. Waters SYNAPT G2-Si product brochure, Part. No. 720004681EN.
4. Waters APGC White Paper, Part No. 720004771EN.

Waters

THE SCIENCE OF WHAT'S POSSIBLE.®

Waters Corporation
34 Maple Street
Milford, MA 01757 U.S.A.
T: 1 508 478 2000
F: 1 508 872 1990
www.waters.com

www.waters.com/metabolomics

Waters

THE SCIENCE OF WHAT'S POSSIBLE.®

Waters Corporation
34 Maple Street
Milford, MA 01757 U.S.A.
T: 1 508 478 2000
F: 1 508 872 1990
www.waters.com